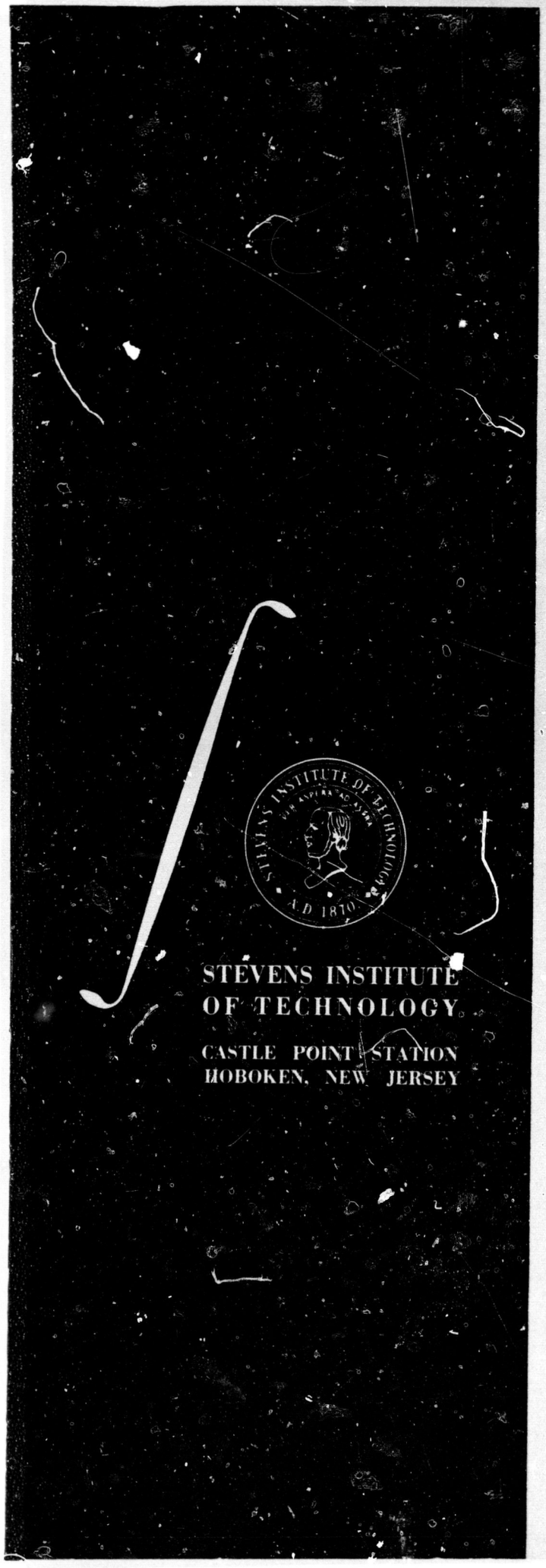

DDC
RECEIVED
AUG 17 1971
B

DEPARTMENT OF MECHANICAL ENGINEERING

THE LINEAR PYROLYSIS OF AMMONIUM PERCHLORATE BY CONVECTIVE HEATING

TECHNICAL REPORT ME-RT 71005

by

Richard B. Cole

Robert F. McAlevy, III

Reproduced by
NATIONAL TECHNICAL
INFORMATION SERVICE
Springfield, Va. 22151

June 1971

208

UNCLASSIFIED

Security Classification

DOCUMENT CONTROL DATA - R & D

Security classification of title, body of abstract and indexing annotation must be entered when the overall report is classified

1. ORIGINATING ACTIVITY (Corporate author)	2a. REPORT SECURITY CLASSIFICATION
Stevens Institute of Technology Department of Mechanical Engineering Hoboken, New Jersey	Unclassified
	2b. GROUP

3. REPORT TITLE

The Linear Pyrolysis of Ammonium Perchlorate by Convective Heating

4. DESCRIPTIVE NOTES (Type of report and, inclusive dates)

Technical Report, June 1971

5. AUTHOR(S) (First name, middle initial, last name)

Richard B. Cole and Robert F. McAlevy, III

6. REPORT DATE	7a. TOTAL NO. OF PAGES	7b. NO. OF REFS
June 1971	187 + xviii	81

8a. CONTRACT OR GRANT NO.	9a. ORIGINATOR'S REPORT NUMBER(S)
N00014-67-A-0202-0023	ME-RT 71005
b. PROJECT NO.	
c.	9b. OTHER REPORT NO(S) (Any other numbers that may be assigned this report)
d.	

10. DISTRIBUTION STATEMENT

The distribution of this document is unlimited and qualified requesters may obtain copies from D.D.C.

11. SUPPLEMENTARY NOTES	12. SPONSORING MILITARY ACTIVITY
	Office of Naval Research Power Branch Washington, D.C. 20360

13. ABSTRACT A new technique for investigating the linear, surface pyrolysis of ammonium perchlorate (AP) is reported along with the results of extensive testing of pressed AP at 1 atm. ambient pressure. The technique involves both convective heating by an impinging jet from a gas rocket and also surface-temperature measurement by infrared spectra-radiometry.

An apparent activation energy of 22 kcal/mole is reported for AP with surface temperatures between 425 and 575°C and with regression rates between 0.002 and 0.04 cm/sec. The overall pyrolysis mechanism is proposed to be rate-controlled, dissociative sublimation. The reported results are consistent with some earlier experimental results obtained by other methods and with some theoretical models of AP pyrolysis which are discussed.

A different pyrolysis regime is reported for rates exceeding 0.04 cm/sec. and this is speculated to involve surface-structure changes.

The technique used and the results reported are the first such for AP which allow for consideration of partial pressures and heat fluxes at the pyrolyzing surface in addition to measurements of regression rates and surface temperatures during pyrolysis.

14 KEY WORDS	LINK A		LINK B		LINK C	
	ROLE	WT	ROLE	WT	ROLE	WT
Ablation						
Ammonium perchlorate						
Combustion						
Composite propellant						
Convective heating						
High-temperature test						
Impinging Jet						
Kinetics						
Linear pyrolysis						
Oxidizer						
Pyrolysis						
Rapid-heating experiment						
Rocket propellant						
Solid propellant						
Sublimation						
Surface pyrolysis						
Surface-temperature measurement						

DEPARTMENT OF THE NAVY
OFFICE OF NAVAL RESEARCH
POWER BRANCH
Contract N0014-67-A-0202-0023

THE LINEAR PYROLYSIS OF AMMONIUM PERCHLORATE BY CONVECTIVE HEATING

Technical Report ME-RT 71005

by

Richard B. Cole and Robert F. McAlevy, III

June 1971

Stevens Institute of Technology
Department of Mechanical Engineering
Hoboken, New Jersey

Reproduction, translations, publication, use and disposal in whole or in part by or for the United States Government is permitted.

The contents of this report have been submitted in partial fulfillment of the requirements for the degree of Doctor of Philosophy from Stevens Institute of Technology, May 1971.

ABSTRACT

The work reported arises from two needs: (1) a general need for further development of techniques for investigating the linear, surface-pyrolysis of solid materials, (2) a specific need for resolving current disagreements concerning ammonium perchlorate (AP) pyrolysis at elevated temperatures and heating rates. New linear-pyrolysis data and interpretations for AP are especially necessary because of the central position of this pyrolysis process in models of composite-solid-propellant deflagration.

A new technique for investigating the linear, surface pyrolysis of AP is reported along with the results of extensive pyrolysis testing. The technique involves both convective heating of AP specimens by an impinging jet and also infrared spectraradiometry for surface-temperature measurement.

The test method is shown to have notable advantages over earlier linear-pyrolysis techniques for AP. The convective-heating method provides for optical pyrometry. Beyond this, the convective-heating technique allows, for the first time in linear-pyrolysis experiments, estimates of surface partial pressures and heat flux. Such estimates have been impractical with prior pyrolysis techniques, and prior linear-pyrolysis data have been limited to regression rate (r) vs. surface temperature (T_S) relations.

General agreement with the results of earlier linear-pyrolysis experiments is reported, though these experiments have involved completely different ("hot-plate") techniques; specific discrepancies

are, however, noted and rationalized. An apparent activation energy of about 22 kcal/mole is reported for AP with $425^{o}C \leq T_S \leq 575^{o}C$ and with 0.002 cm/sec $\leq r \leq$ 0.04 cm/sec. The observed activation energy (E_S) agrees better with that of earlier linear-pyrolysis data than with that of lower-temperature, isothermal pyrolysis (sublimation) data.

The overall mechanism behind the observed data is proposed to be nearly-unopposed ("rate-controlled") dissociative sublimation of AP into gaseous NH_3 and $HClO_4$. The present results and the proposed overall mechanism explain apparently anomalous discontinuities both in the present data and in earlier hot-plate pyrolysis data. However, it is recognized that the details of the mechanism of AP pyrolysis (such as identification of the reaction step which apparently controls pyrolysis rates) probably can not be deduced from pyrolysis results alone.

The present results favor interpretation of recent isothermal sublimation data for AP as deriving from a diffusion-controlled situation rather than from the rate-controlled process suggested by Jacobs and Russell-Jones (1968). Guirao and Williams (1969) have offered such a diffusion-controlled interpretation based on the isothermal data per se, but the relation between these data and the new linear pyrolysis data strongly reinforces such an interpretation.

Evidence of a new pyrolysis regime is reported for r > 0.04 cm/sec, though more intensive study is proposed for this regime. Data in this regime involve increasing pyrolysis rates with little or no change in surface brightness temperature. This regime is speculated to involve

surface structure changes which are related to the structures observed for AP deflagration. The nearly-constant surface temperatures deduced radiometrically for this regime are close to the temperatures measured as the surface of deflagrating single crystals of AP and to those estimated for the melting point of pure AP.

NOMENCLATURE

A	pre-exponential factors in Arrhenius expression
a	radial velocity gradient in axisymmetric, potential, stagnation-point flow; also measured, experimental radial velocity gradient
B	driving force for heat or mass transport (Spalding (1963))
$B_\lambda(T)$	Planck's specific-intensity function (on a wavelength basis) evaluated at λ and T ($= C_1/n^2_{\lambda,b}\lambda^5 \exp(C_2/\lambda T) - 1$)
C_1, C_2	Planck's first and second radiation constants, respectively
c	specific heat in gas phase (assumed constant)
$\bar{c}$	mean specific heat of pyrolyzate between T_S and T_0
D	binary diffusion coefficient
E_S	apparent activation energy of surface process
F	view factor for radiant energy transport
f_S, f_w	transpiration or "blowing" parameters (dimensionless stream functions evaluated at surface) for axisymmetric and wedge flows, respectively
g	conductance or Reynolds flux (Spalding (1963))
ΔH_{sub}	molar heat of sublimation at surface conditions
h	enthalpy
Δh^0_{sub}	specific heat-of-sublimation at conditioning temperature
J_{λ,L_F}	specific intensity of radiation at wavelength λ from gas-phase surface layer of thickness L_F
$\mathcal{J}_\lambda$	fractional radiometric error due to gas-phase emission at wavelength λ
k	gas-phase thermal conductivity

$\bar{k}$	mean gas-phase thermal conductivity between T_S and T_F
L	characteristic distance for diffusion
L_F	effective flame stand-off distance (from surface); also thickness of emitting gas-phase layer
M	molecular weight (without subscript: AP)
$\bar{M}_J$	molar-average molecular weight of all species j ($j \neq i$)
m	mass fraction
$\dot{m}$	mass flux from pyrolyzing surface
N	number of data points
Nu	Nusselt number based on radial distance from centerline (axisymmetric flow) and surface conditions
n	molar concentration of emitting species
n_λ	index of refraction of AP at wavelength λ
$n_{\lambda,b}$	index of refraction at wavelength λ of space adjacent to emitting blackbody
P	pressure
$\hat{p}$	non-dimensional parameter ($= P_{i,S}/P_{i,eq}$)
q	total surface heat flux
q_R	net radiant heat flux to surface
R	universal gas constant
Re	Reynolds number $= \rho_S u_E x/\mu_S$ (axisymmetric) $= \rho_w u_E x/\mu_w$ (wedge flow)
r	surface regression (pyrolysis) rate
$S_{\Delta\lambda}(\lambda,T)$	recorded spectrometer-signal level for spectral slit width $\Delta\lambda$, central wavelength λ, and source brightness temperature T

s_e	standard error of estimate
s_X	standard deviation of X
s_{Ye}	standard error of estimated Y
T	temperature
T_B	brightness temperature
ΔT_B	(T_B) corrected for gas-phase emission $- T_B$
T_0	conditioning temperature of pyrolyzing specimen
T_{REF}	blackbody (reference) temperature
T_{vp}	temperature corresponding with given vapor pressure
u	velocity component in x-direction
V_{jet}	centerline velocity of impinging jet
v	velocity component in y-direction
v_S, v_w	transpiration velocities (at surface); axisymmetric flow and wedge flow, respectively
X	independent variable in linear regression
$\bar{X}$	average of N values of X
x	distance from centerline parallel to surface in axisymmetric, stagnation-point flow
Y	dependent variable in linear regression
y	outward-normal distance from surface
y*	characteristic boundary-layer thickness = $(\mu_S/\rho_S a)^{\frac{1}{2}}$
y_N	distance between surface and exit plane of jet exhaust-duct

Greek Symbols

α	exponent for empirical temperature-dependence of Arrhenius expression pre-factor
β	evaporation or accomodation coefficient

γ	heat-transfer coefficient
δ	non-dimensional parameter ($= \rho_S D_S / L \dot{m}_{vac}$)
ε	surface emittance
η	non-dimensional distance normal to pyrolyzing surface; boundary-layer similarity parameter ($= y / y^*$)
Θ	non-dimensional temperature $= (T - T_S)/(T_E - T_S)$
θ	angle of emitted radiation with surface normal
κ	spectral absorption coefficient
λ	wavelength
μ	dynamic viscosity
ν	kinematic viscosity
χ	mass fraction
Π	"conserved" property (Spalding (1963))
ρ	density (without subscript: density of crystalline AP at T_0)
$\hat{\rho}$	non-dimensional parameter ($= \rho_S/\rho_{1,eq}$)
σ	Stefan-Boltzmann constant
τ	quasi-optical-thickness

Subscripts

$(\frac{1}{2})$	value for regression using $\ln r/(T_S)^{\frac{1}{2}}$ as independent variable
(1)	value for regression using $\ln r/T_S$ as independent variable
1	pyrolyzate
2	ambient species
E	local condition at outer edge of boundary layer

eq	condition of thermodynamic solid-vapor equilibrium at surface
F	flame condition
i,j	for species i , j , respectively
NH_3	for gaseous NH_3
ref	reference condition (1 atm, 27°C.)
S	condition at pyrolyzing surface
STD	common standard condition (1 atm., 25°C)
std	arbitrary "standard" condition
T	condition of "transferred" substance (Spalding (1963))
vac	in vacuo
w	condition at wall (wedge flow only)

TABLE OF CONTENTS

Acknowledgement i

Abstract ii

Nomenclature v

Table of Contents x

List of Figures xv

List of Tables xvii

CHAPTER I - INTRODUCTION

I.A GENERAL BACKGROUND 1

I.B PYROLYSIS PROCESSES AND MODELS IN GENERAL 5

I.B.1 Alternative Pyrolysis Processes 5

I.B.2 Models 6

I.B.2a Sublimation Models 7

I.B.2a(1) Single-Step, Unimolecular Sublimation 7

I.B.2a(2) Multi-Step Sublimation 9

I.B.2b Surface Decomposition Models 11

I.B.2c "In-Depth" Decomposition Models 12

I.B.2d Insufficiency of r vs. T_S Data for Diagnosing Pyrolysis Mechanisms 12

I.C LINEAR PYROLYSIS OF AP 13

I.C.1 Experimental Linear-Pyrolysis Studies 13

I.C.2 Models of the Linear-Pyrolysis of AP 15

I.C.3 Summary 17

CHAPTER II - PRIOR INVESTIGATIONS OF THE LINEAR PYROLYSIS OF AMMONIUM PERCHLORATE AND RELATED INVESTIGATIONS

II.A EXPERIMENTAL LINEAR-PYROLYSIS STUDIES 19

CHAPTER II (Continued)

II.A.1 General Comments 19

II.A.1a "Hot-Plate and Heated-Wire-Mesh Techniques 20

II.A.1b Diffusion-Flame Technique 22

II.A.2 Experimental Results from Combustion in Porous AP Beds and in AP-Fuel Mixtures 22

II.A.3 Hot-Plate and Hot-Mesh Data 23

II.A.3a Solid-Hot-Plate Data 23

II.A.3b Porous-Hot-Plate Data 26

II.A.3c Heated-Wire-Mesh Data 29

II.A.4 Diffusion-Flame Pyrolysis Data 31

II.A.5 Summary of Prior Linear-Pyrolysis Data 32

II.B RELATED EXPERIMENTAL STUDIES 35

II.B.1 Low-Temperature Decomposition Studies 35

II.B.2 Isothermal Sublimation Studies 35

II.B.2a Vapor-Pressure Measurements 35

II.B.2b Sublimation Kinetics 37

II.B.2b(1) Thermogravimetry 37

II.B.2b(2) Surface-Regression Measurements 40

II.C SUMMARY 42

CHAPTER III - EXPERIMENTAL APPROACH

III.A MEASUREMENT OF LINEAR-PYROLYSIS CHARACTERISTICS OF AP 45

III.A.1 AP Specimens 48

III.A.2 Apparatus 49

III.A.2a Gas Rocket 49

CHAPTER III - (Continued)

III.A.2b AP Specimen Holder 50

III.A.2c Infrared Spectraradiometer 50

III.A.2d Auxiliary Equipment 53

III.A.3 Test Procedure 53

III.A.4 Data Reduction 54

III.A.4a Regression Rate 54

III.A.4b Surface Brightness Temperature 57

III.B SUPPORTING EXPERIMENTS AND CALCULATIONS 58

III.B.1 Influence of Source of AP and Preparation of Samples 58

III.B.2 Influence of Monitoring Wavelength 59

III.B.3 Influence of Gas-Rocket Operating Conditions 61

III.B.4 Influence of Gas-Phase Emission 61

III.B.5 Scanning-Electron Micrographs 64

CHAPTER IV - EXPERIMENTAL AND ANALYTICAL RESULTS

IV.A AP PYROLYSIS CHARACTERISTICS 65

IV.B SUPPORTING EXPERIMENTAL RESULTS 68

IV.B.1 Photographs of the Surfaces of Specimens Quenched During Pyrolysis 68

IV.C SUPPORTING ANALYTICAL RESULTS 71

IV.C.1 Estimates of Convective Surface Heat-Fluxes 71

IV.C.2 Estimates of Pyrolyzate Partial Pressures at the Surface and Corresponding Vacuum Sublimation Rates 71

CHAPTER V - INTERPRETATION OF RESULTS

V.A SURFACE TEMPERATURES 76

CHAPTER V - (Continued)

V.B IMPLICATIONS OF THE PRESENT RESULTS 79

V.B.1 Regime B 79

V.B.1a Heat-Flux and Partial-Pressure Estimates 82

V.B.1b Discontinuity in Trend of Regression Rate vs. Surface Temperature (Onset of Gas-Phase Reaction) 82

V.B.1c Pyrolysis Mechanism 84

V.B.1d Summary 86

V.B.2 Regime C 87

V.B.2a Validity of Data in Regime C 87

V.B.2b Speculations Regarding Regime C 88

V.B.2c Obstacles to Speculations 89

V.B.2c(1) Vapor-Pressure Discrepancies 89

V.B.2c(2) Lack of Physical Evidence for a Liquid Phase 90

V.B.2d Summary 91

V.C. RELATION OF PRESENT RESULTS TO PRIOR PYROLYSIS RESULTS OF OTHERS 92

V.C.1 Pyrolysis in AP-Gaseous-Fuel Diffusion Flames 92

V.C.2 Porous Hot-Plate Pyrolysis Data 94

V.C.2a Data of Lieberherr 94

V.C.2b Data of Coates 98

V.C.3 Solid-Hot-Plate Pyrolysis Data 99

V.C.4 High-Temperatures Isothermal Sublimation Data 100

CHAPTER VI - CONCLUSIONS

VI.A THE PRESENT PYROLYSIS TECHNIQUE 101

VI.A.1 Convective Heating 101

CHAPTER VI - (Continued)

VI.A.2 Surface Temperature Measurement by Infrared Spectraradiometry 103

VI.A.3 Summary 103

VI.B PYROLYSIS CHARACTERISTICS OF AP 104

VI.B.1 Regimes A and B 104

VI.B.2 Regime C 106

VI.C RECOMMENDATIONS FOR FUTURE RESEARCH 106

REFERENCES 108

APPENDICES

A. AP SPECIMENS 118

B. GAS-ROCKET OPERATING CHARACTERISTICS 127

C. EXPERIMENTAL AND ANALYTICAL CHECKS ON VALIDITY OF THE EXPERIMENTAL TECHNIQUE 140

D. PARTIAL-PRESSURES OF PYROLYZATE AT THE SURFACE AND CORRESPONDING VACUUM SUBLIMATION RATES 161

E. STATISTICAL ANALYSIS OF PYROLYSIS DATA 164

F. ESTIMATES OF CONVECTIVE HEAT FLUX DURING PYROLYSIS 171

G. SURFACE PARTIAL-PRESSURE ESTIMATES FOR POROUS HOT-PLATE PYROLYSIS 176

H. AMBIENT PRESSURE EFFECTS ON SOLID-HOT-PLATE PYROLYSIS EXPERIMENTS 180

J. LINEAR-PYROLYSIS DATA 184

LIST OF FIGURES

Fig. No.	Title	Page
II-1	Envelopes of Prior Linear-Pyrolysis Data for AP	24
II-2	Selected Recent AP Pyrolysis Data from Heated-Wire-Mesh Experiments (after Lieberherr(1969))	30
II-3	Ambient Pressures for Linear-Pyrolysis Experiments Compared with AP Vapor Pressures	34
II-4	Reaction Scheme for AP Decomposition (after Jacobs and Whitehead (1968))	36
II-5	Recent Isothermal Linear-Pyrolysis Data for AP (after Krauetle (1969))	41
III-1	Schematic of Experimental Apparatus for Linear-Pyrolysis of AP via Convective Heating with Infrared Spectraradiometry	46
III-2	Detail of Specimen Holder for AP Linear-Pyrolysis Apparatus	47
III-3	Photograph of AP Specimen Holder	51
III-4	Example Record of Measured Infrared Radiation Levels (at 3.05 μm)	55
III-5	Example Record of Specimen Displacement History During Linear-Pyrolysis Test	56
IV-1	Pyrolysis Rate (r) vs. Inverse Surface Brightness Temperature ($10^3/T_B$) from Convective Heating of Pressed AP (with Least-Squares Fits)	66
IV-2	Low-Magnification Scanning-Electron Micrograph of Quenched Pyrolysis Surfaces	69
IV-3	High-Magnification Scanning-Electron Micrographs of Quenched Pyrolysis Surfaces	70
IV-4	Estimated Surface Heat-Flux vs. Pyrolysis Rate for AP Pyrolysis via Convective Heating	72
IV-5	AP Pyrolysis (Sublimation) Rate vs. Surface Temperature for $\varepsilon = 0.72$ with Correction for Recondensation	75

LIST OF FIGURES (Continued)

V-1	AP Pyrolysis Rate (r) vs. Surface Temperature (T_S)	78
V-2	AP (Vacuum) Pyrolysis Rates (r) vs. Surface Temperatures (T_S) for ε = 0.72 to 0.83 with Regimes Deduced in this Study	80

APPENDICES

A-1	Die for Pressing AP	119
A-2	Photograph of Jig for Forming AP Specimens	122
B-1	Schematic of Gas-Rocket System	128
B-2	Measured Gas-Rocket Exhaust-Jet Temperatures vs. Fuel Supply Pressure	131
B-3	Radial Static-Pressure Distributions on Flat Plate Normal to Impinging Jet Axis	138
C-1	Spectral Scan (Fast) of Surface Emission During Pyrolysis	141
C-2	Spectral Scan (Slow) of Surface Emission During Pyrolysis	142
C-3	Spectral Scans of Gas-Rocket Exhaust-Jet Emission (S_J) Relative to Emission from 500°C Blackbody ($S_{500°C}$)	144
C-4	Emitting Gas Layer Near Pyrolyzing Surface	150
E-1	Standard Errors of Estimate (s_e) in ln r for Sub-Sets of Data with Successively Increasing (and Decreasing) Maximum (and Minimum) Surface Temperatures (with One-Sided 80% Confidence Limits)	167
E-2	Least-Squares Fits to Different Sets of Pyrolysis-Rate vs. Surface Brightness Temperature Data Showing Error-Bands for "Standard Errors of Estimated Y"	170
H-1	Comparison of Measured Pyrolysis Characteristics of NH_4Cl with Prediction Based on Vapor Pressure of NH_4Cl	181

LIST OF TABLES

Table No.	Title	Page
II-1	Ambient, Loading, and Vapor Pressures in Hot-Plate Pyrolysis Experiments	25
II-2	Summary of Kinetic Parameters from Least-Squares Fits to Prior Linear-Pyrolysis Data ($r=A\exp(-E_S/RT_S)$)	33
IV-1	Summary of Kinetic Parameters from Least-Squares Fits to Present Linear-Pyrolysis Data (Several Functional Forms)	67
IV-2	Results of Surface Partial-Pressure and (Vacuum) Sublimation-Rate Estimates	74
V-1	Summary of AP Pyrolysis Regimes	81

APPENDICES

A-1	Dimensions of Test Specimens Used to Determine Density of AP Pressings	123
A-2	Specifications of AP Comparison Specimens	125
A-3	Regression Rates of Comparison Specimens	126
B-1	Gas-Rocket Exhaust-Jet Velocities, (V_{jet}), Mach No's. (M_{jet}), Reynolds No's. (Re_{jet}) and Stagnation-Point Velocity Gradients (a) for Typical Operating Conditions	134
C-1	Estimated Corrections to Measured Surface Brightness Temperatures due to Gas-Rocket Exhaust-Jet Emissions	146
C-2	Boundary-Layer Thicknesses (after Howe and Mersman (1959))	160
J-1	Summary of Prior AP Linear-Pyrolysis Data	185
J-2	Summary of Prior AP Linear-Pyrolysis Data	186
J-3	Summary of Present AP Linear-Pyrolysis Data	187

CHAPTER I - INTRODUCTION

The purpose of this chapter is to suggest the reasons for the investigation reported here and the context in which it was carried out.

I. A GENERAL BACKGROUND

The combustion of a great variety of solid materials involves the gasification of the solid material and its consequent reaction in the gas or vapor phase. Steady-state solid propellant combustion has been demonstrated to include solid gasification as a precursor to gas-phase reaction. Similarly ignition, flame-spreading, extinguishment, and unstable burning of solid propellants all involve intimately a conversion of condensed-phase reactants into gas-phase ones. A host of other practically important situations, both reactive and otherwise, also include the gasification of solid materials, for example, fires involving wood and wood products, the burning of natural and synthetic textiles, ablation of reentry vehicle nose cones, etc. In all such situations, solid gasification appears as a central elemental process in the chain of phenomena which constitute the overall process from unreacting solid to gaseous (and possibly solid) products of reaction.

It is useful to abstract the process of solid gasification from the variety of situations in which it occurs and to investigate it as a single, component process independent of co-existing flames and other coupled processes. Such isolation of gasification from more complex

combustion situations not only makes its investigation more practical, it appears to be a necessity. Attempts at modeling combustion situations typically require explicit accounting for the nature of solid gasification per se. Furthermore, parametric variations are more subject to control in pyrolysis tests than in combustion situations.

When a solid gasifies under the action of applied heat, the process is commonly termed "pyrolysis"*, i.e., change caused by heating. Thermal decomposition or pyrolsis of solids has classically been studied chemically by measuring the evolution of gas or the weight loss of solids over relatively long time periods (e.g., minutes or hours) with the solid at essentially constant, low temperatures. In such "bulk pyrolysis" studies (including the modern techniques of differential thermal analysis (DTA) and differential scanning calorimetry (DSC)), the decomposing specimen, being isothermal, may react throughout the bulk of the specimen, and reaction products may then diffuse to the surface. The temperatures at which a solid may be studied are limited to those for which the specimen reacts slowly enough to remain essentially isothermal and to allow pressure rise, weight loss, etc. to be followed quasi-steadily. In contrast, under intense heating, a solid specimen may react in a thin surface layer. In this layer elevated temperatures (and reaction rates) exist but most of the solid is at much lower temperature and may not be reacting. This type of thermal decomposition due to intense surface heating often manifests itself

---

*From the Greek: "pyr" = fire; "lyein" = to loosen, to destroy.

as a macroscopically regular regression of the exposed surface in the direction of the surface normal. Hence, it has come to be termed "linear pyrolysis" and to be characterized by the rate of surface regression during pyrolysis.

A well-developed example of linear pyrolysis and the subject of the present study is the pyrolysis of ammonium perchlorate, NH_4ClO_4, often termed "AP". AP is an ionic, crystalline solid produced in large quantities commercially by reacting NH_3, HCl, and $NaClO_4$ (Schumaker (1960)). It is capable of reacting exothermally into gaseous species which are useful oxidizing agents, e.g., $HClO_4$, Cl_2, HCl and O_2. It is also known to sublime dissociatively into NH_3 and $HClO_4$ with a heat of sublimation of about 58 kcal/mole (Inami, Rosser, and Wise (1963)). The pyrolysis of AP, the most commonly used composite-solid-propellant oxidizer, serves the vital function in propellant combustion of providing for exothermic oxidation of the various types of fuel-reactants with which it is mixed in the solid propellant, e.g., thermoplastics, elastomers, various metals, etc. For example, two of the most common types of solid propellants are heterogeneous mixtures of a polymerized matrix of polyurethane or polybutadiene containing small (e.g., 0.1 mm-dia.) particles of AP and metallic additives.

During the deflagration of heterogeneous (or "composite") solid propellants, the regressing propellant surface may be in the neighborhood of 500°C or more with a subsurface temperature gradient of 10^3 to 10^5 °K /cm and a regression rate of 0.1 to more than 1.0 cm /sec (for ambient pressures between 1 and 100 atm). Under these conditions

the gas formation processes at the solid propellant surface are boundary conditions which must necessarily be embedded in any realistic model of the deflagration mechanism.

The surface conditions cited for propellants are much more extreme than those which can be sustained in classical bulk pyrolysis experiments; it has never been clear how satisfactorily the results of such experiments can be applied to describing the behavior of AP (or fuels) during combustion. Therefore, starting in the early 1950's propellant researchers in the U.S. began studies of the linear pyrolysis of AP (Andersen et al. (1952)). These studies were attempts to measure the relationship between the linear pyrolysis rate, r, and the surface temperature, T_S, of AP during pyrolysis. These results have always been reported in terms of an Arrhenius expression:

$$r = A \exp(-E_S/RT_S) \text{ or } BT_S \exp(-E_S/RT_S)$$

and the activation energy, E_S, deduced by fitting such an equation to the data.

The use of linear pyrolysis experiments to characterizing pyrolysis has continued to the present. The investigation reported here is a continuation of these efforts. However, the experimental and interpretive methods described here represent a distinct departure from previous approaches.

I. B PYROLYSIS PROCESSES AND MODELS IN GENERAL

As part of the task of characterizing the linear pyrolysis of a solid material like AP, it is useful to consider first the sorts of processes which may comprise the macroscopic linear-regression of a pyrolyzing surface. Such consideration has rarely been reported along with experimental pyrolysis data though it is essential to an evaluation of these data. Several sorts of processes are evident as alternatives and their implications relative to combustion situations are different.

The following sections serves as a framework for later, critical views both of the results of the present work and of the pyrolysis data of others. The general aim of the following sections is to relate mechanisms for pyrolysis to the mathematical forms which might describe experimental pyrolysis characteristics (e.g., r vs. T_S).

I. B. 1 Alternative Pyrolysis Processes

Two alternative types of fundamental chemical processes may be suggested as distinguishable mechanisms for pyrolysis: sublimation and chemical decomposition. These processes might be considered the ends of a broad spectrum of possibilities. At one extreme is simple, unimolecular sublimation and, at the other, full-fledged, irreversible chemical reaction involving products quite unlike the original reactants. Intermediately, one might consider a range from complex (e.g.,dissociative) sublimation to various chemical reactions involving only modest structural changes.

On the one extreme, sublimation may be considered. As a physical phase-transition, this is a reversible process in the classical sense. Some cases of sublimation apparently involve the direct process of desorption into the gas phase (e.g., rhombic sulfur and benzene, Schultz and Dekker (1955)). In other cases, intermediate steps such as dissociation or charge transfer and surface diffusion may precede desorption (e.g., NH_4Cl; Schultz and Dekker (1956)). Changes in molecular structure are typically very modest (e.g., dissociation) or nonexistent, but a variety of detailed mechanisms have been established (Somorjai (1968)).

On the other hand, substantial chemical decomposition may be involved in pyrolysis, either as a surface process or as an in-depth process in a surface-"layer" which decomposes macroscopically as if by a surface process. In this sort of pyrolysis process, some of the reaction steps are typically highly irreversible chemically. Indicative of multiple bond-breaking and extensive chemical rearrangement, the gaseous products of pyrolysis bear little semblence to the original reactants (e.g., "low-temperature" decomposition of NH_4ClO_4; Jacobs and Whitehead (1969); vaporization of condensation polymers; Madorsky (1964)). Heterogeneous reactions may also be involved (e.g., graphite; Scala and Gilbert (1965)).

I. B. 2 Models

The diversity of vaporization processes obviously involves a wide variety of detailed mechanisms. However, the various models of these

processes which have been aimed at explaining vaporization rates show few or relatively minor conceptual differences. In the context of reaction-rate ("rate-process") theory, there are not major qualitative distinctions made between reactions comprising sublimation and those involved in surface decomposition reactions* (Somorjai (1968), Laidler (1950)).

I. B. 2a Sublimation Models

I. B. 2a(1) Single-Step, Unimolecular Sublimation

In models of sublimation, repeated reference is made to the Knudsen relation which describes sublimation into a vacuum ("free" or "unopposed" vaporization) in terms of the surface mass flux ($\dot{m}_{vac}$), an accomodation or evaporation coefficient (β), molecular weight (M), surface temperature (T_S), and the corresponding equilibrium vapor-pressure of the subliming, "i"th species ($P_{i,eq}$) (Kennard (1938)):

$$\dot{m}_{vac} = \beta P_{i,eq}(T_S) \sqrt{M/2\pi RT_S} \qquad (I\text{-}1)$$

Very similar relations may be derived from absolute reaction-rate theory if a single-step, unimolecular sublimation is considered (Penner (1948)). The vacuum evaporation rate, $\dot{m}_{vac}$, is the maximum theoretical rate of vaporization. Eq.(1-1) has been applied with reasonable success to a variety of materials (benzene, Schultz and Dekker (1955); NaCl, metals, Somorjai (1968)).

---

*Quantitatively, however, the complexity of the latter type of pyrolysis is certainly much more troublesome.

From the Clausius-Clapeyron relation, $P_{i,eq}$ is exponentially temperature dependent, and, at least over limited temperature ranges:

$$P_{i,eq} \sim \exp\left(-\Delta H_{sub}/RT_S\right) \qquad \text{(I-2)}$$

If β is only weakly temperature dependent (as would be the case with a single-step, unimolecular process), Eq.(I-1) is dominated by the temperature dependence of $P_{i,eq}$, the equilibrium vapor-pressure, i.e., from Eq's. (I-1) and (I-2):

$$\dot{m}_{vac} \sim \beta \sqrt{M/2\pi RT_S}\ \exp\left(-\Delta H_{sub}/RT_S\right) \qquad \text{(I-3)}$$

Data for linear-pyrolysis rates as a function of surface temperature might be expected, therefore, to vary exponentially in the extreme of simple vacuum sublimation (<u>via</u> Eq.(I-1)):

$$r_{vac} = \frac{\dot{m}_{vac}}{\rho} \sim \beta \sqrt{M/2\pi RT_S}\ \exp\left(-\Delta H_{sub}/RT_S\right) \qquad \text{(I-4)}$$

That is, pyrolysis data would evidence an apparent activation energy equal to the heat of sublimation, ΔH_{sub}.

If, in the other extreme, a subliming material is <u>not</u> maintained in a vacuum, linear-pyrolysis (sublimation) rates may be expected to be decreased by recondensation, and therefore to vary not only with surface temperature, as in Eq. (I-4), but also with whatever (partial) vapor-pressure, P_i, is sustained at the surface. Thus, for <u>non-vacuum</u> environments (Williams (1965)):

$$r = r_{vac}\left(T_S\right)\left[1 - P_i/P_{i,eq}\left(T_S\right)\right] \qquad \text{(I-5)}$$

In this case, the temperature dependence of r apparent in pyrolysis tests depends on changes in experimental conditions not only *via* changes in T_S but also *via* any coupled changes in partial pressure at the surface. Such experimental variables as total pressure, environmental composition, and mode of heating may, therefore, influence the relations observed between r and T_S during pyrolysis testing. In the limit of P_i approaching $P_{i,eq}$, the sublimation rate is governed by mass diffusion from the surface and:

$$r = \frac{\dot{m}}{\rho} = \frac{DM}{\rho L} \frac{P_{i,eq}}{RT_S} \sim \frac{DM}{\rho LRT_S} \exp\left(-\Delta H_{sub}/RT_S\right) \quad (I\text{-}6)$$

where D is the diffusion coefficient of the subliming species and L is a characteristic diffusion length at which $P_i/P_{i,eq}$ is essentially zero (determined by the physical situation). Again, an apparent activation energy of ΔH_{sub} is notable.

I. B. 2a(2) Multi-Step Sublimation

The one-step, unimolecular sublimation model described above contains implicit in it the concept of a single evaporation step which occurs whenever a molecule has sufficient energy to change phase. In contrast, multi-step models typically consider desorption from the surface as the last in a set of component steps some of which may occur in parallel and some in series.

As an example of the kinetics of such a multiple-step process, consider a situation in which desorption is the slowest of these steps

(and, therefore, "rate-controlling")*. In this case, the sublimation rate depends not only on the kinetic rate constant of the desorption process but also on the surface concentration(s) of desorbing species. Such surface concentrations are determined by the temperature-dependent equilibrium constants of preceding sublimation steps, e.g., charge-transfer between ions in an ionic solid. Thus, the temperature-dependence of the overall sublimation rate ("apparent" activation energy) reflects not only the temperature-dependence (activation energy) of the desorption kinetics but also the temperature-dependence of the equilibrium constants of the sublimation steps which are in (dynamic) equilibrium. Furthermore, the functional forms of such relations typically imply apparent activation energies which change with temperature (Guirao and Williams (1969) derive a variety of these forms). It is quite possible, of course, that apparent activation energies for overall sublimation show a dependence on gas-phase compositions; adsorption may perturb surface-process equilibria.

In consideration of these facts, it might be expected that only exceptional sublimation cases could be well-described by the empirical Arrhenius expression (Williams (1965), p.373):

$$r = AT_S^{\alpha} \exp(-E_S/RT_S) \qquad \text{(I-7)}$$

where the empirical constant $\alpha < 1$ and E_S is the apparent acti-

---

* This situation will be termed "equilibrium" sublimation for the remainder of this work. Other "non-equilibrium" cases may be dealt with via rate-process theory in similar fashion.

vation energy*. Such cases might involve, for example,:

(i) vacuum sublimation with relatively high surface concentrations of adsorbed species or, in the other extreme (cp., Eq.(I-6)),

(ii) diffusion-controlled, multi-step sublimation ($E_s = \Delta H_{sub}$)+

or

(iii) rate-control by the first step in the sublimation process.

I. B. 2b Surface-Decomposition Models

The features of vaporization-rate models of pyrolysis with irreversible surface reactions differ little in the context of rate-process theory from those models just mentioned for multi-step sublimation. In the event of rate-control by a single surface-reaction step, the same Arrhenius expression as described above (Eq.(I-7)) for sublimation may, in special cases, relate r and T_S :

$$r = A\, T_S^{\alpha} \exp\left(-E_S/RT_S\right) \qquad \text{(I-8)}$$

Such an expression was proposed, for example, in early attempts to model the combustion of double-base (homogeneous) solid propellants in terms of a single-step surface process (Wilfong et al. (1950)).

As in multi-step sublimation, however, either competing or

---

*The activation energy of the desorption step may be less than, greater than, or equal to ΔH_{sub}. Examples of each such possibility have been observed for different materials (Somorjai (1968)).

+The nature of the sublimation may affect the definition of this activation energy in terms of ΔH_{sub}. The sublimation of NH_4ClO_4, for example, is known to be dissociative (Inami et al. (1963)). In this case, it may be shown that ΔH_{sub} / 2 should appear in place of ΔH_{sub} in Eq's. (I-2,3,and 5) and at appropriate locations in Section I.B.2a(1).

sequential rate-processes may lead to temperature-dependence of the apparent activation energy, E_s, for irreversible surface decomposition. Further in parallel with multi-step sublimation, the overall rate of irreversible surface decomposition may or may not be sensitive to adsorption of species from the gas phase.

I. B. 2c "In-Depth" Decomposition Models

Beyond the range of surface processes which might comprise linear pyrolysis is the possibility of chemical reaction "in depth", i.e., in an appreciable volume beneath the pyrolyzing "surface". Again, the variety of detailed mechanisms is wide, but the conceptual approach is similar to that outlined immediately above. A major complication is introduced, however, in the fact that sub-surface temperature profiles may couple with chemical kinetics requiring spatial integration of the temperature-dependent rate-process equations (like Eq.I-8) in order to describe overall pyrolysis rates. For example, such attempts have been made for the linear pyrolysis of polymers (Palinovitch (1965)) and of AP (Laverdo (1967)).

I. B. 2d Insufficiency of r vs. T_s Data for Diagnosing Pyrolysis Mechanisms

In light of the previous outline of pyrolysis models, it is clear that experimental relations between r and T_s are an insufficient basis for establishing what sort of pyrolysis process gives rise to a given set of experimental data; the same apparent activation energy

may arise in different ways. Even if the process is known to be sublimation, r vs. T_S data cannot necessarily distinguish between equilibrium and non-equilibrium sublimation as described above. Efforts to distinguish among alternative sublimation mechanisms can be seen to depend experimentally on more information than r vs. T_S data. Similarly distinguishing sublimation from irreversible surface reactions cannot necessarily be accomplished simply from r vs. T_S data: again, at least some of the typical r vs. T_S relations are very similar in both cases. Additional data, for example, surface partial pressures, are required to distinguish among different pyrolysis mechanisms.

I. C LINEAR PYROLYSIS OF AP

I. C. 1 Experimental Linear-Pyrolysis Studies

The results of linear pyrolysis experiments with AP have typically been reported and interpreted in terms of vacuum sublimation or surface decomposition models of pyrolysis, i.e., as representative of rate-controlled processes. Consistent with this view (though not necessarily with the actual mechanism), Arrhenius expressions have been used to characterize the relationship between r and T_S *:

$$r = A \exp(-E_S/RT_S) \text{ or } A\, T_s \exp(-E_S/RT_S)$$

---

*Such an expression has been incorporated, almost without exception, as a surface boundary condition, in a variety of models of both steady-state propellant deflagration and of transient propellant processes such as acoustic and non-acoustic instability, extinguishment, ignition, and flame-spreading.

Results have been reported from "hot-plate" experiments using AP pressed against both solid (Andersen and Chaiken (1961)) and porous hot-plates (Coates (1965), Guinet (1965), Lieberherr (1967)); recently, results from pressing AP against hot wire-meshes have also been reported (Lieberherr (1969)).

Relations between r and T_s for AP have also been measured during the burning of particulate mixtures and porous beds of AP burning with either volatile solid fuels (notably paraformaldehyde, Powling and Smith (1962, 1963)) or gaseous fuels (e.g., methane, Powling (1967)).

Such results were found (Powling (1965)) to correlate moderately well with a relation of the form of Eq.(I-2) if ambient pressures (P_{amb}) were considered rather than the (unknown) partial pressures of "AP vapor" at the surface:

$$P_{amb} \sim \exp(-\Delta H_{sub}/RT_s) \qquad (I-9)$$

Though partial pressures of the subliming species at the surface are of fundamental significance rather than total, ambient pressures, these partial pressures were not estimated, probably because of the difficulty in doing so in the face of the largely unknown gas-phase reactions which are inherent in the test methods used.

In 1966, Powling reviewed all such linear pyrolysis data (Powling (1967)). These data included all of the results from both the burning of particulate AP-fuel mixtures and also from new diffusion-flame experiments involving pressed AP burning in combustible-gas

environments. The conclusion was that the collected data (excepting those from hot-plate experiments) might be fitted by either Eq's. (I-8) or (I-9), though somewhat better by the former (using $E_S \cong 30$kcal/mole $\cong \Delta H_{sub}/2$)*. Thus, the set of data from combustion experiments might have been considered representative of either unopposed, dissociative sublimation+ (Eq.(I-7)), diffusion-controlled sublimation+ (Eq.(I-6), if $P_{i,eq} \cong P_{ambient}$), or even irreversible surface decomposition (Eq.(I-8)).

Powling noted further that the collected hot-plate data, though all considerably scattered, indicated a substantially lower apparent activation energy, i.e., $E_S \cong 20$ kcal/mole via Eq.(I-8). Thus, the set of data for linear pyrolysis might have been considered representative of rate-controlled sublimation (Eq.(I-7)) or irreversible surface decomposition (Eq.(I-8)); equilibrium sublimation does not seem a likely alternative in these experiments (excepting erroneous data) since $E_S < \Delta H_{sub}/2$. It was suggested that the differences in apparent E_S in the two cases might arise from differences in surface geometry (particulate in the case of the combustion experiments with granular mixtures and porous beds; continuous in the case of solid, linear-pyrolysis specimens) (Powling (1967)).

I. C. 2 Models of the Linear Pyrolysis of AP

In addition to the experimental studies cited above, two different

---

*See footnote, p. 11.

+with surface-reaction steps at equilibrium

mechanistic views of the linear pyrolysis of AP have recently been postulated and discussed (see Jacobs and Powling (1969), Guirao and Williams (1969)). Both of these views of linear pyrolysis rest on extrapolations of different, alternative interpretations of data from recent isothermal pyrolysis studies by Jacobs and Russell-Jones (1968). Both see linear pyrolysis as comprised of dissociative sublimation of AP into NH_3 and $HClO_4$. However, Jacobs and Powling propose an unopposed equilibrium sublimation mechanism, while Guirao and Williams consider a diffusion-controlled equilibrium sublimation as likely during both isothermal and linear pyrolysis. Both approaches allow for the experimentally observed pressure-dependence of pyrolysis rate as observed by Russell-Jones (1964); Jacobs and Powling attribute pressure-dependence to adsorption of inert gases on the subliming AP surface while Guirao and Williams emphasize the pressure-dependence of mass diffusion coefficients (which are central in their diffusion-controlled model).

Only Jacobs and Powling have, however, actually extrapolated isothermal results to describe the linear pyrolysis situation. Their approach yields an apparent activation energy for linear pyrolysis of about 30 kcal/mole which is appreciably greater than that observed in linear pyrolysis experiments. The regression rates predicted are of the observed order-of-magnitude. The predicted activation energies are moderately consistent (within scatter) with AP pyrolysis results inferred from AP combustion experiments (porous-plug and diffusion flame; (Powling (1967)) if the previously-mentioned pressure-depend-

ence is accounted for. Jacobs and Powling suggest, then, that their approach accounts reasonably for the observed pyrolysis data. However, there are several significant obstacles to accepting this judgem as Guirao and Williams (1969) have pointed out.

I. C. 3 Summary

The diversity of possible pyrolysis processes makes typical linear-pyrolysis data (r vs. T_s) an insufficient basis for distinguishing which of this variety of processes may be dominant in any particular experiment. Additional, more detailed experimental results must be brought to bear in making such a distinction. The only substantial attempt to delineate AP pyrolysis mechanistically appears to be that of Powling who used a variety of AP-combustion experiments rather than pyrolysis experiments per se. This attempt was, unfortunately, subject to the limitation of approximating unknown partial-pressures at the surface by the total, ambient pressure; the results were understandably inconclusive. While clarifying the situation, Powling's attempt failed to distinguish between two possible mechanisms of AP pyrolysis: (i) rate-controlled, unopposed sublimation and (ii), diffusion-controlled sublimation. A further unresolved complication to mechanistic interpretation of pyrolysis data is the apparent contradiction between the activation energies deduced from the r vs. T_s trends of linear pyrolysis (ca. 20 kcal/mole) and the higher activation energies deduced from a variety of AP-combustion experiments (ca. 30 kcal/mole).

The present investigation is in response to the situation just described. This study deals with a new linear-pyrolysis technique which, unlike previous ones, provides the potential for characterizing pyrolysis experiments by more than r *vs.* T_S relations, i.e., in terms of heat fluxes, partial pressures, etc. Even in terms of simple r *vs.* T_S data, the technique throws light on the discrepancy between 20 and 30 kcal/mole activation energies (as described above) by providing r *vs.* T_S data from a type of experiment completely different from that used in previous linear-pyrolysis studies. To provide a context for the present work, these prior linear-pyrolysis experiments and related studies are reviewed in the next chapter with particular regard for information other than r *vs.* T_S data.

CHAPTER II - PRIOR INVESTIGATIONS OF THE LINEAR PYROLYSIS OF AMMONIUM PERCHLORATE AND RELATED INVESTIGATIONS

The purpose of this chapter is to review prior experimental efforts which relate directly to the linear pyrolysis of AP with particular emphasis on those data relevant to determining pyrolyzate partial-pressures at the pyrolyzing surface.

II. A EXPERIMENTAL LINEAR PYROLYSIS STUDIES

II. A. 1 General Comments

As cited above (Section I. C.1), Powling has summarized a considerable body of linear pyrolysis data (Powling (1967)). The more recent work of Lieberherr (1967, 1969) has also been cited and described briefly. All of these prior efforts to characterize experimentally the linear pyrolysis of AP deal with pyrolysis driven by either:

(1) heated metallic surfaces pressed into intimate contact with the pyrolyzing AP surface [solid and porous "hot-plates" (Andersen and Chaiken (1961), Guinet (1965), Coates (1965a), Lieberherr (1967)) or wire meshes (Lieberberr (1969))],

or:

(2) diffusion flames established above the pyrolyzing AP surface via impinging or parallel fuel gas streams (Powling (1967), Jacobs and Powling (1969)).

II. A. 1a "Hot-Plate" and Heated-Wire-Mesh Techniques

The hot-plate (and heated wire-mesh) techniques suffer the major disadvantages of:

(i) possible mechanical and/or fluid mechanical disruption of the pyrolyzing surface,

(ii) possible chemical interaction between the hot-plate and the pyrolyzing material,

(iii) inherent masking of the pyrolyzing surface from photographic or visual access during pyrolysis,

(iv) the necessity of measuring surface temperature with a thermocouple on or within the heated metallic surface, and

(v) inability to characterize the surface state during pyrolysis, i.e. the pressure at which gasification occurs and the composition of the gas phase at and near the pyrolyzing surface.

The first disadvantage has been noted earlier (Nachbar and Williams (1963), McAlevy et al. (1968)) as have the second (Pearson (1967)) and the fourth (Nachbar and Williams (1963)). The significance of the third is apparent when it is noted that surface cracking of AP specimens is not uncommon (Barrere and Williams (1968), p.57) and when it is noted that powerful optical methods for measuring surface temperature are necessarily excluded by hot-plates.

The fifth disadvantage cited has not been emphasized previously. As suggested above (Section I.B.2d), however, it is very significant

in determining the usefulness of pyrolysis data vis-a-vis pyrolysis models. The inability to measure or otherwise determine total pressures (and, therefore, partial pressures) at the pyrolyzing surface is primarily and inherently a consequence of the loading force required to hold a pyrolyzing specimen in intimate contact with a heated metal surface. Loading pressures (force/nominal "contact" area) in hot-plate and heated wire-mesh experiments have, without exception, been appreciable relative to nominal "ambient" pressures. High loading pressures are required in order to achieve r vs. T_S data which are independent of these pressures (Chaiken et al. (1962), Guinet (1965), Lieberherr (1969)). In extreme cases (Chaiken et al. (1962), Lieberherr (1969)), loading pressures (e.g. 18 atm., Lieberherr (1969)) have greatly exceeded ambient pressures*. In any event, the uncertainty in actual contact area and the possibility of appreciable pressure nonuniformity across the surface diminish the utility of hot-plate or wire-mesh techniques appreciably. This is true, even in strictly empirical studies, because of the need for a full characterization of test conditions. It is also true because of the necessity of at least estimating the surface partial pressures of pyrolysis products for identification of pyrolysis regimes and thereby for comparison with models of the pyrolysis process.

The major advantages of the hot-plate and hot-mesh techniques are their apparent conceptual simplicity, their successful use in some non-AP pyrolysis studies (Chaiken et al. (1962)), and the very wide

*Very significant relative to (i). See also Section V. A, below).

range of test data (e.g., measured temperatures) which can be obtained from them.

II. A. 1b Diffusion-Flame Technique

The diffusion-flame technique is capable of overcoming all of the disadvantages cited above for the hot-plate and hot-mesh methods. This technique may well bear development and use beyond the already-substantial efforts of Powling (1967). The diffusion-flame method may, however, be excessively limited in its useful range by flammability limits (McAlevy et al. (1968)). Furthermore, the presence of a necessarily-reactive flow field near the pyrolyzing surface complicates, perhaps prohibitively, the important task of determining gas-phase composition at the pyrolyzing surface.

II. A. 2 Experimental Results from Combustion in Porous AP Beds and in AP-Fuel Mixtures

While certainly complimentary to linear-pyrolysis data, results from porous-bed and mixture combustion are felt to be of only indirect relevence to characterizing the linear pyrolysis of AP. The liklihood of difficulty in interpreting these combustion data from particulate rather than continuous surfaces has already been mentioned (Section I. C.1). For this reason, these results are not considered farther at this point.

II. A. 3 Hot-Plate and Hot-Mesh Data

II. A. 3a Solid Hot-Plate Data

Data for the linear-pyrolysis of pressed AP heated by a solid hot-plate (containing a thermocouple) have been reported by Andersen et al. (1959) and by Andersen and Chaiken (1961). Andersen's most recently reported data are listed in Table J-1 (Appendix J), and the envelope of these data is shown, as implied by Eq. I-7, in Fig. II-1*. The data evidence an apparent activation energy of approximately 23 kcal/mole and are scattered. They were obtained, as summarized in Table II-1, under conditions comparable to those of earlier hot-plate tests on NH_4Cl (Chaiken (1970)).

It was noted during testing that the region of the electrically heated hot-plate nearer the sample was less bright (cooler). This was taken to imply that the pyrolysis process was endothermic overall. However, attempts to determine heat flux to the specimen during pyrolysis were unsuccessful according to Chaiken (1970).

The pressure at the pyrolyzing surface is unknown for these solid hot-plate experiments. Conceivably, effective surface pressures might fall within a large range - from the low ambient pressure (ca. 10^{-3} atm) to the high loading pressures (1.3 to 5 atm). Despite the high loading pressures, it appears that surface pressures were actually very near the lower ambient pressures. Since ambient pressures in these experiments were far below the corresponding AP vapor pressures**, these AP pyrolysis

*The solid hot-plate data of Guinet (1965) are excluded; they depend on loading pressures, indicative of errors in measuring surface temperature.

**AP vapor-pressure data were unavailable at the time of these experiments.

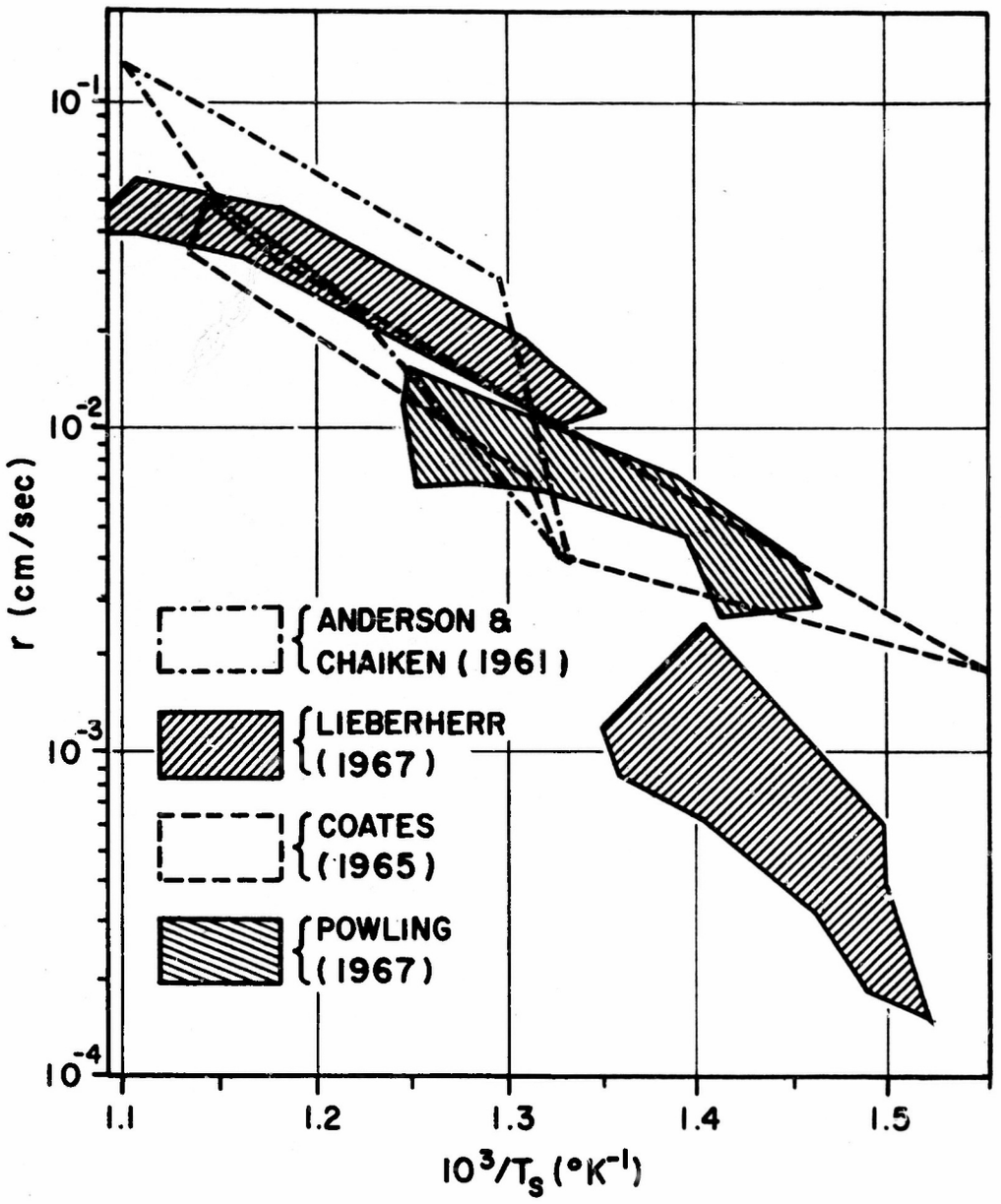

FIGURE II-1: ENVELOPES OF PRIOR LINEAR-PYROLYSIS DATA FOR AP

Source	Temperature Range (°C)	Corresponding AP Vapor Pressures[a] (atm)	Hot-Plate Loading Pressures[b] (atm)	Ambient Pressures[c] (atm)
Andersen and Chaiken (1959)	475° to 640°	0.25 to 20	1.3 to 5	0.001 to 0.003
Coates (1965)	475° to 600° (additional single point at 370°C)	0.25 to 18	1.8	0.05 to 0.1
Lieberherr (1967)	375° to 475°	0.013 to 0.25	1.5	1
	475° to 730°	0.25 to 20	1.5	1

NOTES:

[a] Inami et al. (1963)

[b] Nominal loading pressures plus ambient pressures

[c] Surrounding specimens and hot plates for experiments of Lieberherr and of Andersen and Chaiken

TABLE II-1: AMBIENT, LOADING, AND VAPOR PRESSURES IN HOT-PLATE PYROLYSIS EXPERIMENTS

data probably represent essentially unopposed sublimation. This likli-hood can be deduced from the results of similar linear-pyrolysis tests on NH_4Cl with the same high loading pressures. Pyrolysis results for NH_4Cl definitely indicate that the total pressure at the pyrolyzing surface essentially equalled the very low ambient pressures used (see Appendix H).

The accuracy of the temperature data reported by Andersen and Chaiken is questionable (Cantrell (1963)). The attempt of Nachbar and Williams (1963) to correct for this error is, however, probably very rough due to their unsupported assumption of a gas film of uniform and constant thickness between the hot plate and the pyrolyzing surface. The low pressures which were apparently sustained at the pyrolyzing surface (see above) suggest solid-solid contact or at least some channeling.

II. A. 3b Porous Hot-Plate Data

Data for AP pyrolysis experiments using porous (sintered-metal) hot-plates have been obtained by Guinet (1965), Coates (1965), and by Lieberherr (1967). The data of Coates and Lieberherr are listed in Table J-1 (Appendix J), and the envelopes of these data are shown in Fig. II-1. Guinet's data and similar data mentioned by Barrère and Williams (1968) have not been shown since they are known to be subject to inaccuracies in surface temperature measurement (Lieberherr (1967),

(1969)). The data of Lieberherr (1967) are based on essentially the same apparatus but with an improved temperature-measurement method.*

At high surface temperatures ($T_S \geq 475^oC$), both Coates and Lieberherr report similar r vs. T_S results. For these temperatures, Lieberherr also reports a visible flame near the surface similar to that observed by Guinet (1965). Below 475^oC, Coates reports but a single datum point (at $T_S \tilde{=} 370^oC$, $10^3/T_S \tilde{=} 1.55$) while Lieberherr reports a striking discontinuity in rates (toward lower rates at lower temperatures, see Fig. II-1) coincident with disappearance of a visible flame.

Comparisons of ambient pressures, loading pressures, and AP vapor-pressures for these experiments bring several additional points to light+. First, in the higher temperature range ($\geq 475^oC$), ambient pressures in both experiments were appreciably below the corresponding AP vapor-pressures, though more so in Coates' case (see Table II-1). Indications of gas-phase reactions were reported for high surface temperatures by both Lieberherr and Coates. These facts suggest that pyrolyzate partial pressures were well below corresponding vapor pressures.++ Unopposed sublimation may, then, have existed in each case for tempera-

---

*Guinet deduced surface temperatures from temperatures measured on the downstream face of the porous plate and a correlation of the temperature drop across the plate with the flow rate of gas through the plate; Lieberherr measured the temperature of a thermocouple inserted between the plate and the specimen.

+Neither Coates nor Lieberherr reportedly considered AP vapor pressures vis-a-vis their data though such data were available (Inami et al. (1963)).

++Reactions in the gas phase may depress surface partial pressure by acting as "sinks" for the pyrolyzate.

tures above 475°C. This observation is, however, made uncertain by the high loading pressures used. Over the range of surface temperatures measured, AP vapor pressures range from well above to well below the loading pressures (see Table II-1). Second, below 475°C, Lieberherr's ambient pressure (1.5 atm) is 8 to 100 times higher than corresponding AP vapor pressures*. This suggests diffusion-controlled sublimation at these low temperatures, in contrast with the unopposed sublimation which may exist at higher temperatures. Third, the discontinuity in rate observed by Lieberherr at about 475°C is in the correct direction (and of the correct magnitude, approximately) to be attributed to a transition from low-temperature, diffusion-controlled sublimation to unopposed sublimation coupled with gas-phase reaction (the "visible flame") at higher temperatures.

Finally, it must be observed that the inherent surface irregularity of the porous plates used (pore size, approx. 40 μm) is:

(i) of the same order as the characteristic dimension for heat transfer in the near-surface gas phase (at least for high regression rates, e.g., 0.03 cm/sec), and

(ii) not much greater than the scale of the temperature profile in the solid phase, and

(iii) of the same scale as topological details of subliming-surface structures (see Section IV. B. 2, below).

Therefore there is substantial doubt as to the interpretation of

*Coates' single datum below 475°C has been neglected due to its uniqueness and due to the disparity between Coates' ambient and loading pressures (ca. 35 mm Hg and 1.8 atm, respectively) and the corresponding vapor pressure of AP (ca. 6 mm Hg).

pyrolysis rate and temperature data from such a two-dimensional pyrolyzing surface which is necessarily perturbed by the proximity of the porous plate. Only Guinet touches on the sensitivity of pyrolysis rates and temperatures to porous-plate construction; no one has reported any systematic testing of this potential influence.

II. A. 3c Heated Wire-Mesh Data

Pyrolysis rate vs. temperature data from experiments using electrically heated wire-meshes have been reported by Lieberherr (1969). Only the low-temperature results ($T \leq 500^{o}C$) are considered here since there are substantial current questions regarding the validity (and certainly the interpretation) of Lieberherr's higher-temperature results. (These results indicate, among other features, negative apparent activation energies and strong dependence on ambient pressure). The envelope of the highly-scattered date for 1 atm is shown in Fig. II-2.

As in porous-plate experiments, the fact that the total pressure (and, therefore, AP partial-pressure) at the pyrolyzing surface is not well known interferes considerably with interpretation of the data. The surface pressure is quite possibly greater than any of the ambient pressures tested, however. Lieberherr has estimated a value as high as 18 atm. , based on the loading force and the projected area of the mesh used.

A notable physical feature of these data is that an extremely two-dimensional surface is likely. "Needles" of AP as long as several

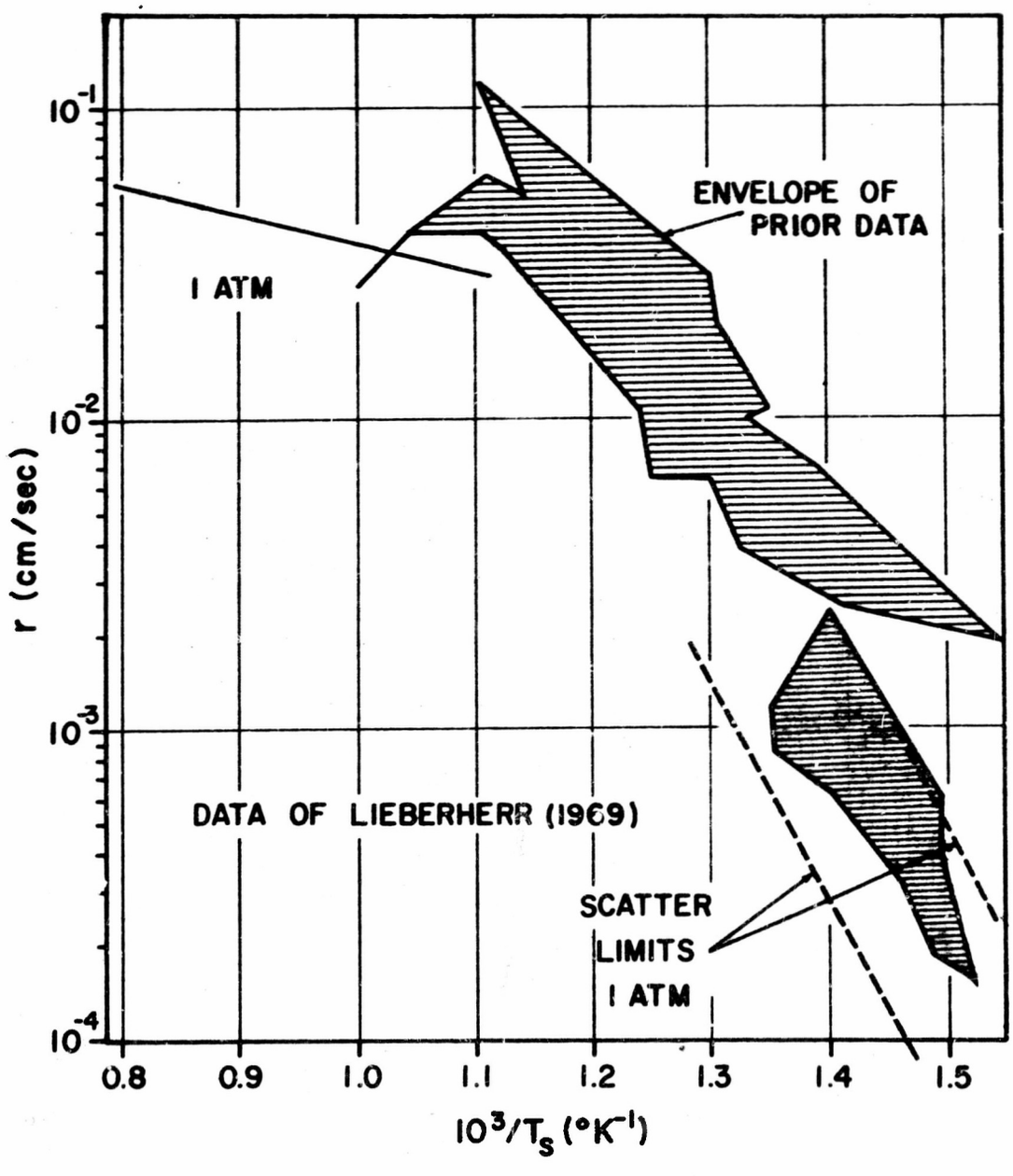

FIGURE II-2: SELECTED RECENT AP PYROLYSIS DATA FROM HEATED-WIRE-MESH EXPERIMENTS (AFTER LIEBERHERR(1969))

millimeters were observed projecting through the mesh during pyrolysis (Lieberherr (1969)). Lieberherr has suggested that these are not necessarily significant since temperatures are measured and regression occurs at the area of contact between the specimen and the hot wire-mesh. In a sense, it is suggested, each wire (or each grain of a porous hot-plate) may be viewed as a single, very small "hot-plate". Lieberherr reported, further, that, over a factor of 2 variation in wire diameter and a factor of 16 variation in pore size, no influence on measured rates and temperatures was observed. Wire type (steel vs. platinum) is apparently also not influential.

III. A. 4 Diffusion-Flame Pyrolysis Data

Powling has reported results of numerous experiments involving the deflagration of pressed AP in a counter-flow diffusion flame fueled by various combustible gases (CH_4; H_2 diluted with N_2). These experiments were at ambient pressures between 30 and 760 mm. Hg (Powling (1967), Jacobs & Powling (1969)). Infrared spectraradiometry was used to determine surface temperatures, apparently on the basis of the same emittance (0.83) used in other spectraradiometric measurements on burning, particulate AP (Powling and Smith (1965)). The data, taken from a plot by Powling and Smith (1965), are listed in Table J-2 (Appendix J), and the envelope of them is shown in Fig. II-1.

These results have also been represented (along with combustion data from particulate systems) on semi-logarithmic plots of ambient pressure vs. inverse surface temperature, a form suggested because of

the possibility of diffusion-controlled sublimation at the surface (Eq. I-9) (Powling (1967)). Powling has noted that the data are more scattered and not as well fitted by a single line on such a plot as on an Arrhenius plot of the pyrolysis rate. He has not, however, called attention to the fact that substantial scatter should be expected on such a plot; ideally, partial pressures of AP pyrolysis product should be considered rather than total, ambient pressures. Depending on the combustion situation, partial pressures might be considerably below ambient, total pressures leading to the appearance of data "scatter" toward higher total pressures at a given surface temperature even if diffusion-control did exist. In fact, consistent with this view, the great majority of such data can be seen to lie at higher pressures than the AP vapor pressures corresponding to the measured surface temperatures (Powling (1967)).

II. A. 5 Summary of Prior Linear Pyrolysis Data

Table II-2 summarizes prior data in terms of Eq's. (I-7) and (I-8) (rate-controlled view) and with reference to temperature range, test method and data scatter.

Figure II-3 summarizes prior data, so far as possible, in terms of Eq. (I-9) (diffusion-controlled view), by comparison with an extrapolation of reported AP vapor pressure data (Inami et al. (1963)). In this ght, it is clear that a major stumbling block to this view is the difficulty in characterizing these data appropriately via partial pressures at the surface rather than via nominal, ambient pressures.

SOURCE	NO. OF DATA POINTS	A (cm/sec)	E_S (kcal/mole)
Solid Hot-plate (1959) Andersen et al.	10	$10^{4.51}$	22.6 ± 3.8
Porous Hot-plate (1965) Coates	12(a)	$10^{3.03}$	17.9 ± 2.1
Porous Hot-plate (1967) Lieberherr	13(b) 10(c)	$10^{3.56}$ $10^{1.56}$	21.6 ± 4.2 11.8 ± 1.2
Diffusion Flame (1967) Powling	36	$10^{1.33}$	12.1 ± 0.7

NOTES:

(a) Point at $10^3/T_S = 1.55$ omitted

(b) Below discontinuity at $10^3/T_S = 1.35$

(c) Above discontinuity at $10^3/T_S = 1.35$

TABLE II-2 - SUMMARY OF KINETIC PARAMETERS FROM LEAST-SQUARES FITS TO PRIOR AP LINEAR-PYROLYSIS DATA [$r = A \exp(-E_S/RT_S)$]

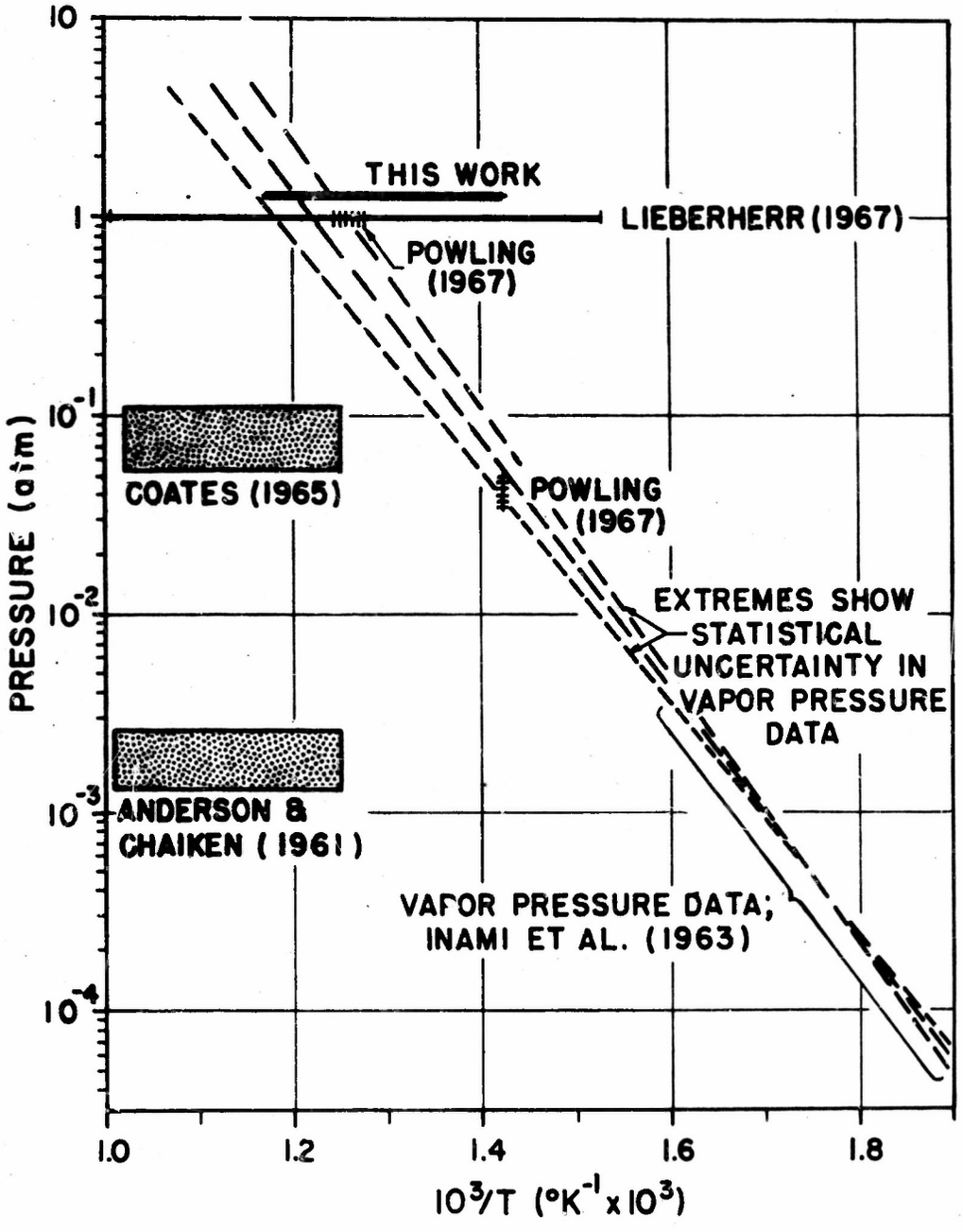

FIGURE II-3: AMBIENT PRESSURES FOR LINEAR PYROLYSIS EXPERIMENTS COMPARED WITH AP VAPOR PRESSURES

II. B RELATED EXPERIMENTAL STUDIES

II. B. 1 Low-Temperature Decomposition Studies

Since data and results concerning the low-temperature decomposition of AP have been amply reviewed recently (Pittman (1966), Hall & Pearson (1967), Jacobs & Whitehead (1969)), this subject need not be discussed in detail here. This low-temperature decomposition may be dominant at low temperatures (e.g., below about 290°C) and is believed to be a surface reaction (e.g., the reaction of adsorbed NH_3 and $HClO_4$ on the crystal surface; Jacobs and Whitehead (1969)). The reaction is generally held to be too slow to contribute substantially to the linear pyrolysis or deflagration of AP at elevated temperatures. For this reason, major emphasis is given in this investigation to the higher-temperature reaction route for AP that apparently involving dissociative sublimation (possibly followed by gas-phase reaction of NH_3 and $HClO_4$). Figure II-4 summarizes a current view (Jacobs and Whitehead (1969)) of the various competing processes (including low-temperature decomposition, Step 7) of AP pyrolysis.

II. B. 2 Isothermal Sublimation Studies

II. B. 2a Vapor-Pressure Measurements

Inami et al. (1963) have measured the vapor pressure of AP at temperatures between 150° and 340°C using a transpiration method. Helium carrier gas was passed through beds (e.g., 2-cm. diameter, 1-cm. height) of AP particles (either 50 μm or larger-than-61 μm

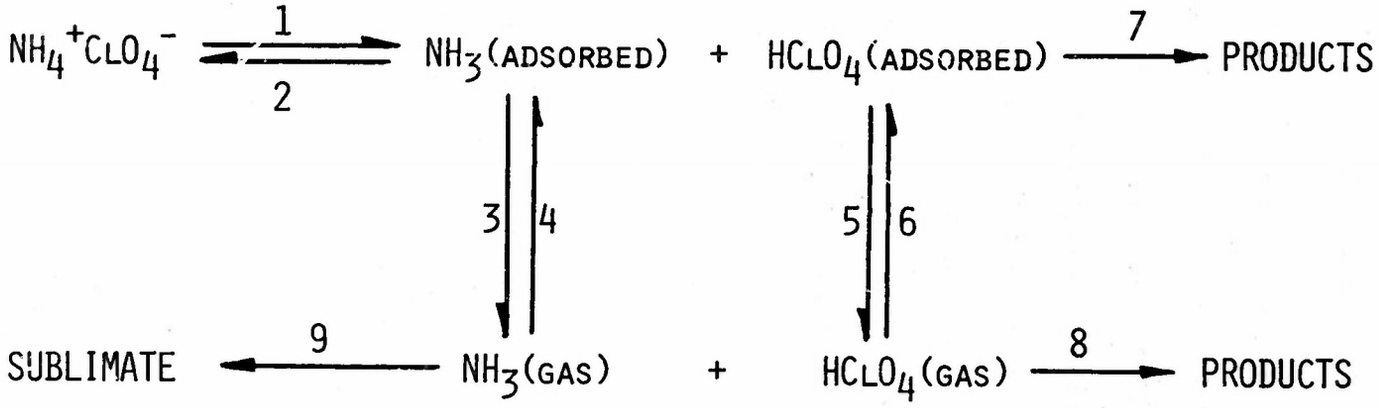

FIGURE II-4: REACTION SCHEME FOR AP DECOMPOSITION (AFTER JACOBS AND RUSSELL-JONES(1968))

particle-size). A sublimate was condensed out on a cold-finger and chemically analyzed. The vapor-pressure results were found to be well-represented by the relation:

$$P_{dissocation} = 10^{10.56} \exp[(-58 \pm 2)/2RT)]$$

where $P_{dissociation}$ is the total pressure of the two sublimation species (NH_3 and $HClO_4$).* The exponent is consistent with dissociative sublimation at the thermodynamic heat-of-sublimation (59.3 kcal/mole) as was the equimolar composition of NH_4^+ and $HClO_4^-$ found in the sublimate.

II. B. 2b Sublimation Kinetics

II. B. 2b (1) Thermogravimetry

Jacobs and Russell-Jones (1968) have made thermogravimetric measurements on pressed AP pellets (ca .3mm diameter, 3 mm height) subliming in the temperature ranges 213° to 270°C (in vacuo) and 304° to 375°C (in 1 atm. air). The pressure dependence of the observed kinetics was studied in an N_2 environment (0.01 to 1.0 atm.) at 270°C. The results were found consistent with a Langmuir-Fuchs sublimation model for a single, "effective" subliming species.

The model balances evaporation rate with recondensation and gas-phase diffusion rates, basing these latter rates on the partial pressure of the sublimed species at one mean-free-path from the surface. Analysis

*The presence of two gas-phase species account for the factor of 2 in the exponential. See footnote, page 11.

of Russell-Jones' data (1964) in these terms allowed parameters appearing in the model to be determined; variations in the values of these parameters with temperature were found to be highly consistent with the vapor-pressure and thermodynamic heat-of-sublimation data of other workers.

In the context of the model, the sublimation rates observed by Jacobs and Russell-Jones were essentially unopposed by recondensation over the range of temperature 213°C (*in vacuo*) and 304° to 375°C (1 atm). Likewise, in the context of their model, Jacobs and Russell-Jones explain the apparent activation energy of their measured reaction-rate constants (ca. 30 kcal/mole) as arising from the heat of sublimation, ΔH_{sub} (*via*, essentially, Eq.I-4). This explanation is consistent with their model which, through use of the Knudsen equation, assumes effectively a unimolecular sublimation. However, there appear to be two objections to the view that the apparent activation energy observed is a direct result of ΔH_{sub}.

First, the sublimation process is, in fact, accepted as bimolecular (NH_3 and $HClO_4$). This bimolecularity appears inconsistent with Jacobs and Russell-Jones' proposal that the apparent activation energy for sublimation is derived directly from ΔH_{sub} since (see Section I.B.2a (2)) the activation energy for rate-controlled or unopposed multi-step sublimation ought not to derive from ΔH_{sub} (see Section I.B.2a(2)); in such a case, the apparent activation energy ought derive from the kinetics of that step which is rate-controlling (and relate to ΔH_{sub} only coincidently, if at all).

A second objection to relating apparent activation energy to H_{sub} arises from Jacobs and Russell-Jones' treatment of an observed pressure-dependence of the evaporation coefficient. This pressure dependence was first attributed to the pressure dependence of the diffusion rate in the gas phase (Russell-Jones (1964)). Later, this pressure dependence was attributed to adsorbed N_2 on the subliming surface; inert gases like nitrogen were proposed as adsorbing on the surface and thereby interfering with surface diffusion of the subliming species prior to their desorption*. This treatment serves to explain a pressure dependence of the evaporation coefficient. However, it appears that it also leads to a temperature dependence of the evaporation coefficient because of temperature-dependent terms which are necessarily introduced whenever N_2 adsorption is treated as a pressure-dependent influence. This temperature dependence, in effect, renders β, the evaporation coefficient, temperature dependent since, from Jacobs and Russell-Jones' Eq's. (25) and (26):

$$\beta = \frac{1}{1 + \chi(T)P} \; k_1(T) + k_2(T)$$

By definition, $\chi(T)$ should be expected to show exponential temperature dependence with appreciable activation energy (potential energy of N_2 adsorption); $k_1(T)$ and $k_2(T)$ are essentially diffusion rate-constants

*Though no independent evidence was cited for N_2 adsorption on AP, this phenomenon was found sufficient to account for the pressure dependence by invoking arguments based on two different, parallel surface-diffusion routes to desorption. One of these routes (the dominant one) allows N_2 adsorption to interfere with surface diffusion. A Langmuir adsorption isotherm was invoked to account for the extent of N_2 adsorption.

which might also be expected to show exponential temperature dependence with appreciable activation energies. It is clear, via Eq. (I-4), that temperature dependence in β must influence the apparent activation energy for sublimation beyond that temperature dependence of the exponential factor in Eq.(I-4) which involves ΔH_{sub}.

Guirao and Williams (1969) have proposed (on more rigorous grounds than Jacobs and Russell-Jones') an alternate view of the data of Jacobs and Russell-Jones; these data can be interpreted as representative of diffusion-controlled, equilibrium sublimation with a small contribution to overall pyrolysis rate from the low-temperature decomposition of AP. This proposal is appealing in that such a mechanism accounts rationally for the relationship between Jacobs and Russell-Jones observed activation energy and ΔH_{sub}.

II.B.2b(2) Surface Regression Measurements

Krauetle (1969) has reported the results of measuring the surface regression rate of large spheroidal crystals of AP (ca. 450 μm diameter) on the hot-stage of a microscope. Hot-stage temperatures of 333° to 463°C and ambient pressures of 0.4 to 0.9 atm were used. Temperatures were limited by the onset of rapid and violent reaction (Boggs (1970)).

Krauetle's results for an abmient pressure of 0.9 atm are shown in Fig. II-5. Data for lower pressures at temperatures below about 380°C were reported but are omitted from Fig. II-5 for clarity. These data show pyrolysis rates approximately inversely proportional to ambient pressure, and Krauetle attributed this to recondensation or reassocia-

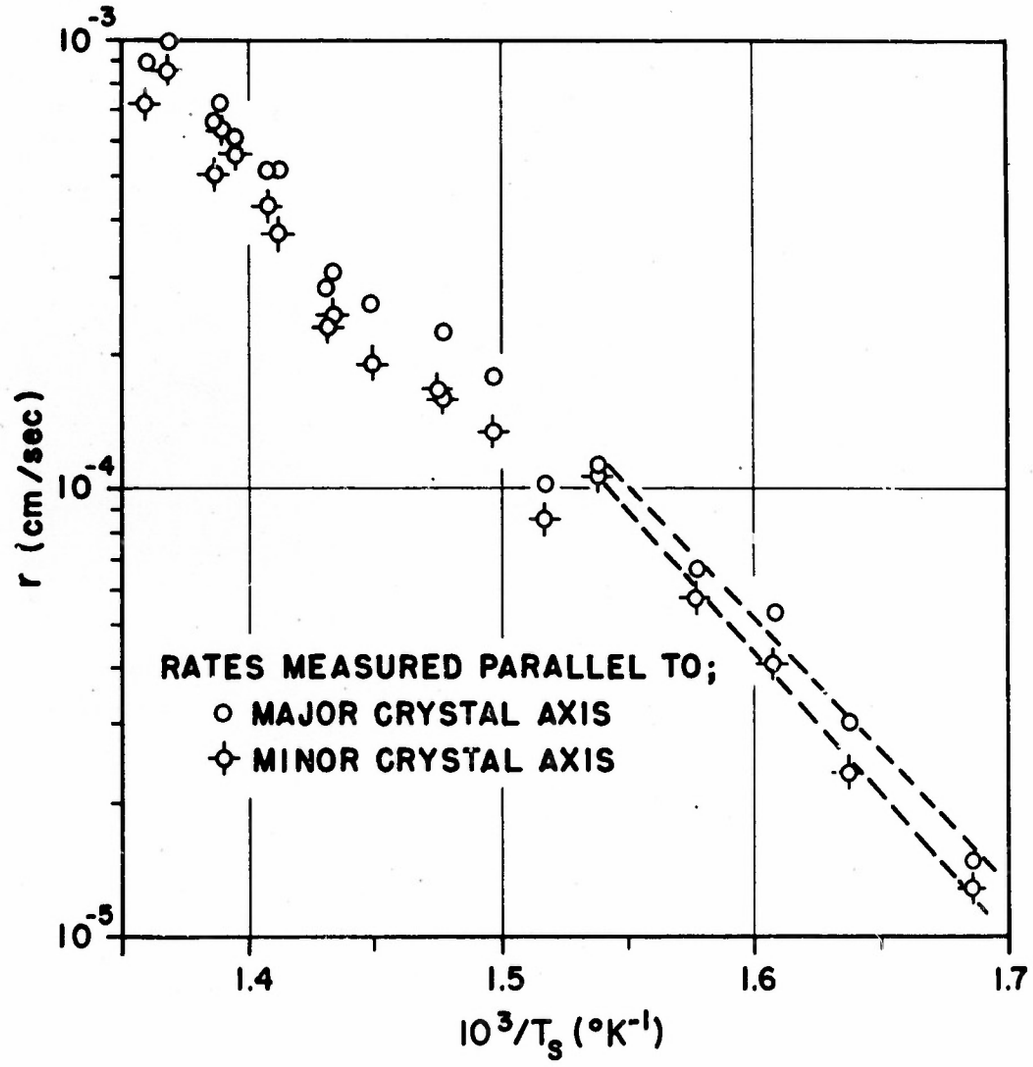

FIGURE II-5: RECENT ISOTHERMAL LINEAR-PYROLYSIS DATA FOR AP (AFTER KRAUETLE (1969))

tion reactions steps of the dissociative sublimation process. In the temperature range for which they overlap the data of Lieberherr (1967), these rates are at the lower extreme of Lieberherr's data scatter (cp., Fig's. II-1 and II-5).

In Fig. II-5, activation energies of 27 to 29 kcal/mole are apparent at the lower temperatures, but above 380°C, this trend is interrupted by what may be either a discontinuity or a decrease in apparent activation energy. It is significent that the temperature cited coincides with that at which Jacobs and Russell-Jones (1969) apparently encountered anomalous effects (acceleratory decomposition rates). Krauetle attributed this effect both to difficulties in obtaining sublimation rates which did not increase with time and to the possibility of non-uniform temperatures; the abruptness of the observed change in trend was not, however, rationalized.

Also reported were scanning-electron micrographs of several sublimed surfaces, and these indicated a highly porous surface with pores of order 3 to 30 μm both across and in depth.

II. C SUMMARY

It appears that up to at least 380°C there is a strong liklih ood that AP pyrolysis experiments (isothermal) have involved diffusion-controlled sublimation. The apparent activation energies (ca. 30 kcal/mole) and the pressure dependencies of the isothermal pyrolysis data of Russell-Jones (1964) and Krauetle (1969) project such a view in light of the diffusion-controlled AP sublimation model of Guirao and

Williams (1969).

The more-scattered linear-pyrolysis data show, on the other hand, lower apparent activation energies (12 to 23 kcal/mole) at higher surface temperatures (above about 475°C). For the test conditions used, rate-controlled sublimation coupled with visible gas-phase reaction of the pyrolyzate is indicated; while not inconsistent with any experimental results, this speculation is not well-supported by them largely because of the impossibility of estimating surface conditions (e.g., pyrolyzate partial-pressures) accurately enough.

At intermediate surface temperatures (in the range 380° to 475°C), linear-pyrolysis experiments have shown either a discontinuous, order-of-magnitude decrease in rates for 1-atm test-pressures (Lieberherr (1967)) or no abrupt decrease for lower test pressures (Powling (1967)). These facts can be speculated as arising from sublimation which is unopposed by recondensation even at high pressures so long as pyrolyzate is consumed by the visible gas-phase reaction (at high temperatures); recondensation can be negligible even at low temperatures without gas-phase reaction if the pressure is low enough. Higher pressures and low temperatures may, however, lead to opposing recondensation (due to the absence of gas-phase reaction at low temperatures). Again, however, it is impossible to estimate actual surface conditions accurately enough to test such a speculation.

The linear-pyrolysis data typically evidence lower apparent energies than do isothermal-pyrolysis data. This may arise from errors in surface temperature measurements for the linear-pyrolysis experiments

or it may reflect a change in mechanism between the two cases, possibly related to the discontinuity in rates observed by Krauetle (1969) at about 380°C.

These matters could be largely resolved by a linear-pyrolysis technique which allows more accurate prediction (and control) of surface conditions during pyrolysis and by a technique which is not subject to the same temperature-measurement errors as hot-plate, linear-pyrolysis experiments. Such a technique is reported in the next chapter.

CHAPTER III - EXPERIMENTAL APPROACH

The purpose of this chapter is to describe both pyrolysis experiments and various supporting experiments and calculations which were carried out in order to characterize the linear pyrolysis of AP.

III. A MEASUREMENT OF LINEAR-PYROLYSIS CHARACTERISTICS OF AP

As a compliment and an extension of the previously described linear pyrolysis techniques and as an independent check on previous experimental and theoretical results, a new linear-pyrolysis technique for AP was developed. The technique is similar to that used earlier with polymeric pyrolysis specimens (McAlevy and Hansel (1965), Hansel and McAlevy (1966)). It involves convective heating of the AP specimen by a hot gas jet and monitoring of the infrared emission from the pyrolyzing surface as a measure of surface temperature. In this way, the relationship between regression rate and surface temperature during pyrolysis is obtained. Figure III-1 depicts the overall experimental arrangement and Figure III-2 details the specimen holder. Experimental details are described below.

The advantages of this pyrolysis method are the same as those attributed above to the diffusion-flame approach (relative to other AP pyrolysis techniques used previously). In addition (relative to the diffusion flame approach), this method has the advantage of eliminating the need for a high-temperature diffusion flame as a driving force for heat transfer to the surface. This advantage has two

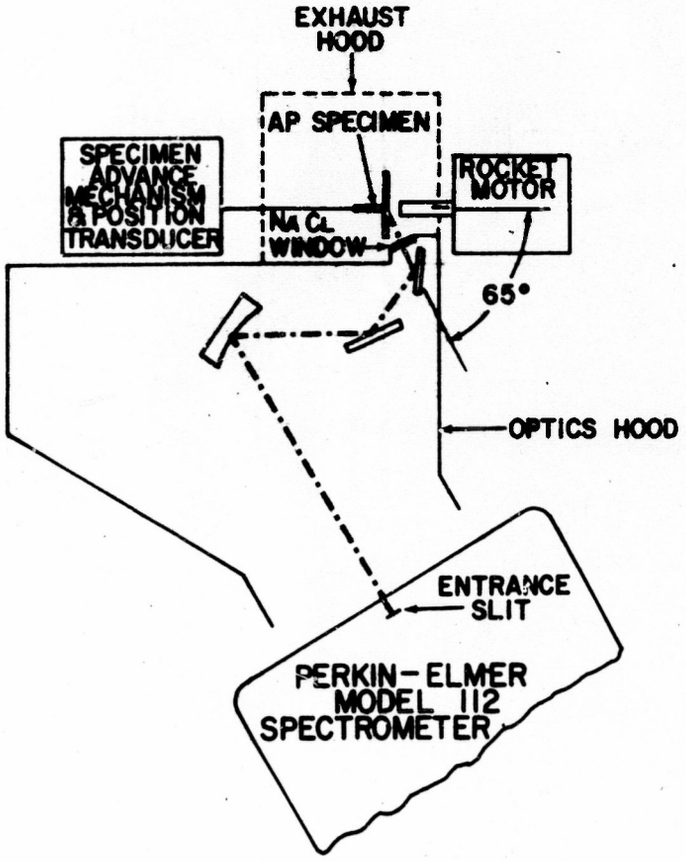

FIGURE III-1: SCHEMATIC OF EXPERIMENTAL APPARATUS FOR LINEAR-PYROLYSIS OF AP VIA CONVECTIVE HEATING WITH INFRARED SPECTRARADIOMETRY

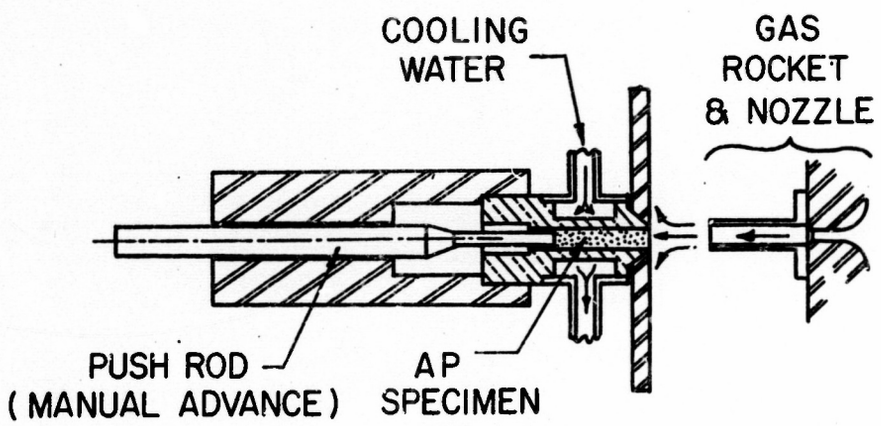

FIGURE III-2: DETAIL OF SPECIMEN HOLDER FOR AP LINEAR-PYROLYSIS APPARATUS

aspects: first, it is not inherently necessary to make radiometric measurements via a line-of-sight through the high-temperature diffusion flame and its products; second, it is much more straightforward to estimate surface conditions (e.g., pyrolyzate partial pressure) if the gas-phase above the pyrolyzing surface is not complicated by the presence of a diffusion flame which serves as a "sink" for reactive pyrolysis products, thereby influencing surface conditions.

The main disadvantage of the infrared method for determining surface temperatures is the need for knowing the spectral emittance of the radiating, pyrolyzing surface at high temperatures.

III.A.1 AP Specimens

The AP specimens used in the work reported here were made by pressing 16-μm AP powder (hammer-milled from commercial, uncoated stock)* at a nominal pressure of 16,000 psi. Appendix A describes details of sample preparation. Most of the specimens were "wet-pressed" after exposing this powder to a water-saturated air atmosphere (1 atm., 25°C) for several days. The resulting pressings were then dried for several days over silica gel. This wet-pressing method was found to minimize break-up of samples during sample preparation and pyrolysis testing. Such fracture and breakup of specimens was a recurrent problem in early stages of the present study and has been reported by others (Friedman (1967), Barrère and Williams (1968)).

*This material was graciously provided by the Solid Propellant Laboratory, Princeton University.

After drying; the specimens were formed into cylinders of $.156"^{+.000"}_{-.003"}$ diameter and of .5" to 1.5" length. Because of the fragility of such specimens, a jig was designed and used for this forming (see Appendix A).

The sample diameter was selected so as to be small enough to allow the end of the sample to be uniformly heated by the 0.20" diameter hot-gas jet available from an existing laboratory gas rocket (Hansel (1964)). To allow rational selection of specimen diameter, assessment of the area of uniform heating by such a jet was made by impinging the jet on large, flat Plexiglas specimen and measuring the area over which the Plexiglas ablated to a nearly uniform depth during short firings of the gas rocket.

Specimen diameter was carefully controlled in order to provide a close fit between the specimen and the bore of a specimen holder. A close fit was found necessary in order to preclude hot-gas jet penetration between the specimen and its holder. Such penetration had been found earlier in this program to be a cause of specimen breakup during pyrolysis testing.

III.A.2 Apparatus

III.A.2a Gas Rocket

The gas rocket was fired with methane and O_2-enriched air (37% O_2-N_2) under conditions close to those used previously (Hansel (1964)). Details of the operating characteristics are contained in Appendix B. The range of operating conditions used in the present

study involved fuel-lean mixtures in the combustion chamber and provided exhaust gas-jet velocities of about 600 ft/sec to 1800 ft/sec and jet temperatures of about 500°C to 2000°C.

III.A.2b AP Specimen Holder

The cylindrical specimens of pressed AP were held during pyrolysis testing within a specimen holder (shown partially in Fig. III-3). This holder restricted exposure to the impinging hot-gas jet to the exposed end of the specimen and prohibited heating on the sample sides. The holder also was equipped with a circular flat plate surrounding the exposed specimen face; this plate was provided in order to force the impinging jet into a configuration which could be aerodynamically modeled in the neighborhood of the specimen face; previous use of impinging jets for heating pyrolyzing (plastic) specimens did not provide so tractible a flow field at the sample face (Hansel (1964)). The specimen holder was water-cooled in order to preclude pre-heating of the specimen by heat conducted from the flat plate through the holder parts to the sample.

III.A.2c Infrared Spectraradiometer

An unmodified Perkin-Elmer Model 112 spectrometer was used to monitor infrared emission from the pyrolyzing surface. The spectrometer included a double-pass Littrow monochromator with thermocouple detector, NaCl prism, amplifier, and chart recorder. Radiant fluxes were measured over a spectral slit width (half-energy) of 0.069 μm

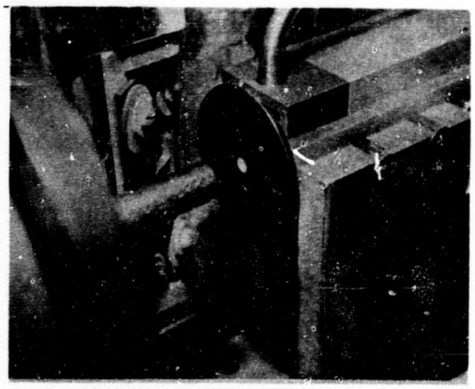

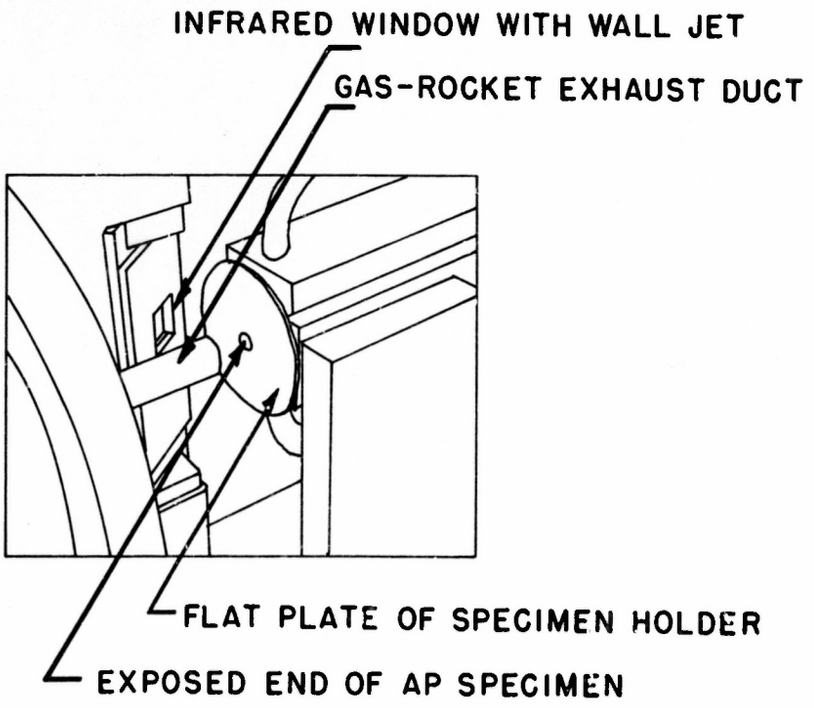

FIGURE III-3: PHOTOGRAPH OF AP SPECIMEN HOLDER

centered at wavelength of 3.05 μm., the center of a (stretching) vibrational band of the ammonium ion.* A resonant absorption wavelength was chosen so as to minimize the optical transparency of the pyrolyzing surface. This particular wavelength was selected in order to maximize radiant emission; at the temperatures of concern in this investigation, the 3.05 μm wavelength yields almost two orders of magnitude more radiant emissive power than other, longer wavelengths of resonant absorption by AP (7.1 μm and 9.3 μm). The 3.05 μm wavelength was also convenient for radiometry because an infrared window was found near this wavelength in the gas-rocket exhaust jet (see Appendix C). The spectral slit width was approximately one-third the spectral width of the ammonium-ion absorption band (as indicated by thin-film transmission data at low temperatures, ca. 100°C; Powling and Smith (1962)).

The slit height used was about 1.5 mm. and the physical slit width was 250 μm. A toroidal mirror was used to image the pyrolyzing surface at a magnification of 1.3 on the slit. The optical axis of the emitted radiation which was monitored was inclined at about 65° to the surface normal in order that the monitored radiation clear the gas rocket (Fig. III-1). This oblique view along with the given slit dimensions and magnification led the spectrometer to collect radiation from an area about 1.1mm x 0.65mm on the specimen surface.

---

*This center wavelength was established from the absorption measurements by the author on a thin AP film graciously provided by J. Powling of E.R.D.E., United Kingdom. The band is due to vibrational stretching of the N-H bond of the ammonium ion (Bellamy (1958)).

III.A.2d Auxiliary Equipment

A lead-screw and push-rod were provided in order to advance the AP specimen manually and maintain the pyrolyzing surface in the plane of the specimen holder plate (Fig. III-2). A potentiometric, linear-motion transducer and chart recorder were used to record specimen displacement as a function of time.

In order to protect the auxiliary, external optics and to minimize escape of pyrolysis products into the laboratory, hoods were provided, one over the optics and one over the sample holder. The optics hood included a 12 x 12 x 2mm NaCl window which allowed radiation to pass though the hood to the spectrometer; the window was protected from corrosive gases by a wall jet of cool, compressed air from a specially-designed window mount (visible in Fig. III-3). The sample-holder hood had a Plexiglas window on one side to allow the pyrolyzing surface to be seen during testing; a 6"-diameter exhaust duct was mounted atop the hood.

III.A.3 Test Procedure

During each test run, the spectrometer was used to record successively the radiation from: (i) an accurate ($\pm 2.5^{\circ}C$) blackbody source (Barnes Eng'g. Model 11-200), (ii) the pyrolyzing specimen, and (iii) from the blackbody (again). The 1/2"-dia. aperture of the blackbody was aligned normal to and centered on the optical axis of the spectrometer at the same axial station as that where the specimen was mounted. This provided reference radiation levels with which the

radiation from the pyrolyzing surface could be compared. After each test firing (with simultaneous recording of radiant emission from the pyrolyzing surface and of specimen displacement *vs.* time), the blackbody was replaced for a check of the originally-recorded reference levels. The last step was necessary as a check that the window near the test specimen had not been fogged during the test and that excessive drift of the instrumentation system had not occurred during firing. Since experience gradually showed this check to be normally unnecessary, it was eventually discontinued and checks were taken only at the beginning and completion of each series of tests. The only data lost because of window-fogging were those obtained when the wall jet over the window was inadvertently left off.

III.A.4 Data Reduction

Example records of reference radiation levels and test radiation levels as obtained from the chart recorder of the spectrometer are shown in Fig. III-4. In Fig. III-5, an example displacement-*vs*-time record for the specimen is shown.

III.A.4a Regression Rate

Each rate reported is a mean rate obtained from the slope of a visually-fitted straight line on the displacement-*vs*-time record. During some tests, fracture of the specimen led to one or several discontinuities in these records; in such cases, the uniform regression between discontinuities were treated separately along with

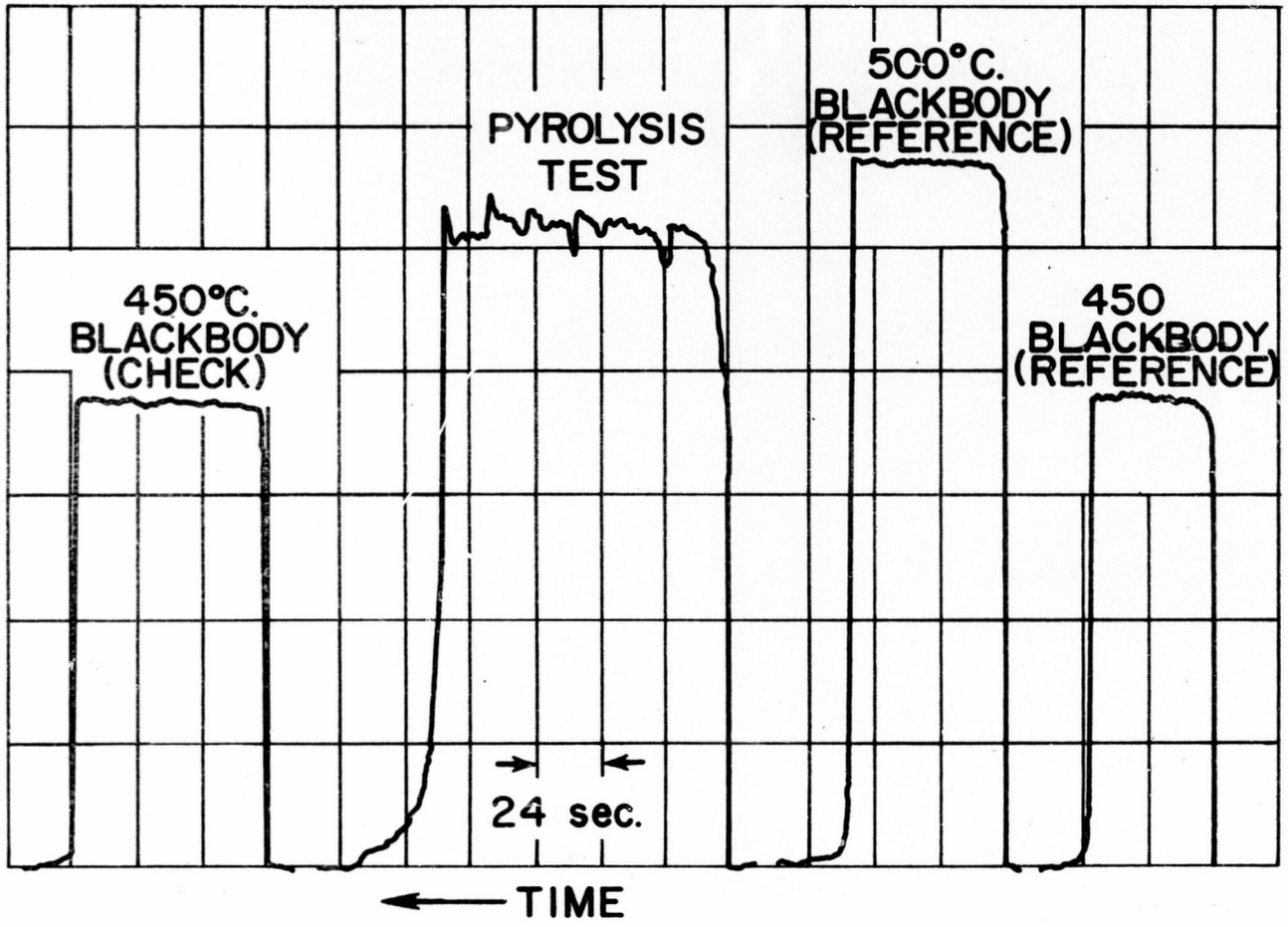

FIGURE III-4: EXAMPLE RECORD OF MEASURED INFRARED RADIATION LEVELS (AT 3.05 um)

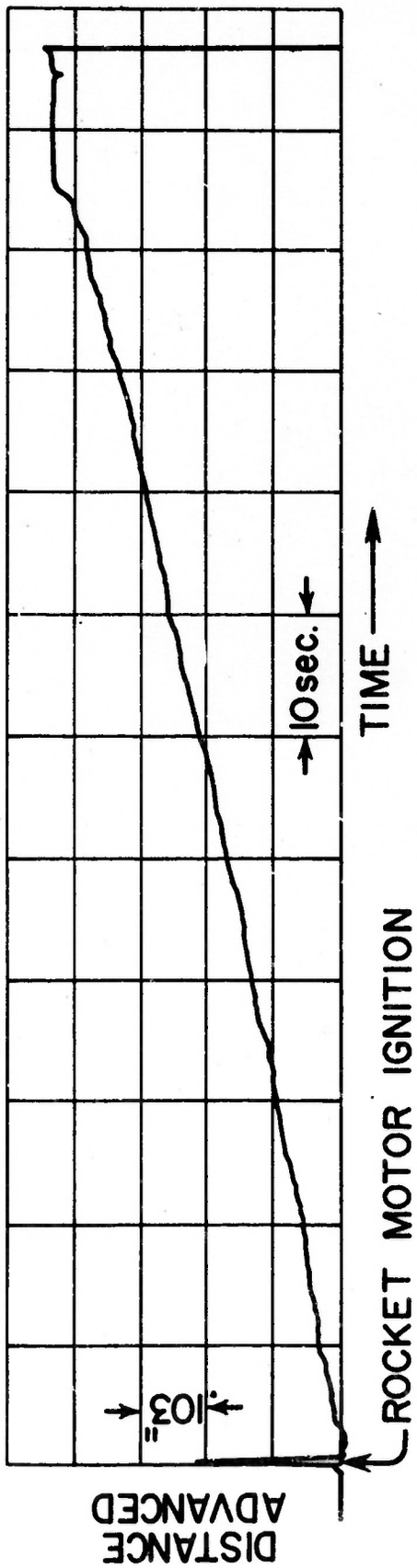

FIGURE III-5: EXAMPLE RECORD OF SPECIMEN DISPLACEMENT HISTORY DURING LINEAR-PYROLYSIS TEST

corresponding time-intervals on the spectrometer record.

It was assumed that any irregularities in the displacement-vs-time records would be evidenced as scatter in the regression rate-vs-surface temperature data, and therefore, no attempt was made to estimate possible errors in measuring regression rates. It was ascertained, however, that there were no visually-apparent systematic variations in the displacement-vs-time records, e.g., no trends toward more non-uniform regression at higher regression rates.

III.A.4b Surface Brightness Temperature

Surface brightness temperatures were determined by comparing recorded reference and test radiation levels. Variations in test levels* were accounted for by determining brightness temperatures at the extremes of such fluctuations. Since test radiation levels were not generally identical with black-body reference levels, surface brightness temperatures (T_B) were calculated using Planck's law and assuming that the recorded levels, $S_{\Delta\lambda}(T_B)$ and $S_{\Delta\lambda}(T_{REF})$ (from the surface and black body, respectively), were proportional to corresponding values of Planck's (spectral) specific-intensity function expressed on a wavelength basis, $B_\lambda(T_B)$ and $B_\lambda(T_{REF})$, respectively.

Thus:
$$B_\lambda(T_B) = B_\lambda(T_{REF}) \frac{S_{\Delta\lambda}(T_B)}{S_{\Delta\lambda}(T_{REF})}$$

From $B_\lambda(T_B)$, the surface brightness temperature follows immediately.

---

*Arising from small variations in specimen location, occasional specimen fracture, and spectrometer noise.

This temperature and its inverse ($10^3/T_B$) were determined, in practice, directly from the ratio of recorded signal levels with the aid of pre-calculated tables relating T_B and $10^3/T_B$ to T_{REF}, λ, and signal ratio, $S_\lambda(T_B)/S_\lambda(T_{REF})$.

III.B SUPPORTING EXPERIMENTS AND CALCULATIONS

Various supporting experiments were carried out in order to characterize: the gas-dynamic behavior of the convective-heating source, the extent of gas-phase infrared emission, and the influence of various experimental parameters (e.g., source of AP) on the measured relation between regression rate and surface temperature. These supporting experiments and calculations are described below.

III.B.1 Influence of Source of AP and Preparation of Samples

Pressed AP was obtained from other laboratories where AP pyrolysis and deflagration studies have been carried out. Specifications of these samples are contained in Appendix A. No significant differences in pyrolysis were detected using the samples from the various sources. The results of those tests on comparison samples in which surface temperatures were determined are reported in Table A-3 along with results from samples made during the present investigation. Some comparisons were made early in this study simply on the basis of the equality of regression rates obtained with a fixed gas-rocket operating condition. These results appear only in Appendix A.

Tests of the sensitivity of pyrolysis data to the manner of

pressing ("wet" vs. "dry"; see Appendix A) also indicated, within normal data scatter, no dependence on AP pressing method. The results of all such tests are reported here, undifferentiated except in Table J-3 (Appendix J).

III.B.2 Influence of Monitoring Wavelength

Comparable regression rate vs. surface-brightness-temperature data were taken at two different wavelengths within the 3 μm. absorption band of AP, 3.05 μm. and 3.14 μm.; 3.05 μm. being the best estimate of the center of the band as mentioned above (see Section III. A.2, above).

These two wavelengths differ by more than the spectral slit-width (.07 μm) used in the measurements. There was no evidence of any dependence of measured pyrolysis characteristics on radiometric wavelength (Appendix C). This indicated that the surface-temperature measurement method was not critically dependent on spectraradiometric parameters such as central (nominal) wavelength or spectral slit width. Checks of this sort have not been reported in previous spectraradiometric pyrolysis studies (Hansel (1964), Powling and Smith (1962, 1963, 1965)). Apparently, under the conditions of this study, the AP surface is radiatively "gray" in the neighborhood of the wavelengths tested. Spectral scans taken during pyrolysis test also suggested that such was the case (Appendix C).

The physical cause of such favorable wavelength independence may be either (or a combination) of several phenomena. First, the surface

may be so rough as to make surface emittance a very weak function of material properties and, therefore, to yield an emittance which is near unity and is essentially constant over at least small wavelength range. This possibility seems unlikely in the present case, judging from the low emittances (e.g., 0.8) which have been measured at the resonant wavelength of AP by Powling and Smith (1965). Second, the absorption band may become broad at elevated temperatures. This could result in little change in emittance over wavelength ranges which, in contrast, might still show substantial spectral variations in emittance or absorption coefficient at low temperatures. Sufficient data are neither available nor readily obtained to allow judging the liklihood of this possibility. Third, sub-surface temperature gradients during pyrolysis may be so small as to render effectively isothermal even the relatively thick surface layers contributing to surface emission at non-resonant wavelengths*. However, by itself, this effect will not be manifested as "gray" behaviour since, within strong absorption bands, even isothermal emitters do not show spectrally invariant emittances (see Ditchburn (1963), p. 553)**.

The results of tests at different radiometric wavelengths are reported, undifferentiated except in Table J-3 of Appendix J.

---

*Based on Powling and Smith's absorption data for AP (1962), the photon mean-free-path at the resonant wavelength of 3.05 μm is less than 1μm. Under the conditions of the present experiments, the largest temperature change over a distance of 1 μm in the solid is about 3°C.

**If the absorption data of Powling and Smith (1962) and Fresnel's reflection law (Sparrow and Cess (1966), pp. 67-69) are used, the emittance of AP can be estimated to decrease by 10 to 15% at the center of the 3.5 μm absorption band.

III.B.3 Influence of Gas-Rocket Operating Conditions

To check the sensitivity of the results to details of the impinging hot-gas jet used for heating, pyrolysis data were taken for two different oxidizer-gas supply-pressures. In terms of r *vs.* T_S, the data appeared superimposed (see Table J-3). This implied that trade-offs between jet velocity and temperature could be made without observable influence on r-*vs.*-T_S trends despite, for example, a factor of two variation in jet velocity. All such data are reported here undifferentiated, except in Table J-3.

III.B.4 Influence of Gas-Phase Emission

The influences of two different types of gas-phase emission were checked: that from the gas-rocket exhaust gas used for heating and that from pyrolysis products immediately above the pyrolyzing surface; either or both of these sources could contribute, as errors, to the radiation attributed to the pyrolyzing (solid) surface only. Details of these checks appear in Appendix C.

Spectral scans and single wavelength measurements of radiant emission from the hot-gas jet were made by sighting the spectrometer transversely across the hot jet at the mouth of the exhaust duct. Spectrometer settings identical to those used during pyrolysis tests were used. The spectral scans indicated a spectral "window" in the jet at the 3 μm wavelength whereas jet emission was appreciable at wavelengths corresponding with the others AP absorption bands at 7 μm

and 9 μm . Measurements of jet emission at 3.05 μm (spectral slit width 0.069 μm) over a range of operating conditions showed such emission to be negligible relative to recorded levels during pyrolysis at the same conditions.

The second potential source of error due to gas-phase emission was also checked. Three independent theoretical and experimental checks indicated no appreciable gas-phase emission effects due to pyrolysis products above the surface.

First, experimental checks of whether or not gas-phase emission is appreciable were carried out using the pyrolysis apparatus itself. The spectrometer was aligned so as to view a portion of the (steel) specimen-holder plate immediately adjacent to the hole through which the specimen is normally passed. Comparisons of the emission levels recorded with a pyrolyzing AP specimen in the holder and with an inert (steel) specimen in place (during firing) showed no differences within the reproducibility of the tests (about $5^{\circ}C$ for a brightness temperature of about $500^{\circ}C$ and a regression rate of about 0.02 cm/sec).

Second, as one of two possible cases, the emission from ammonia above the pyrolyzing surface was estimated assuming that the ammonia reacts with perchloric acid above the surface much as it is thought to during deflagration of AP. Gaseous ammonia with its broad absorption band of about 3 μm. is the most likely contributor to gas-phase emission. Using data from the high-pressure deflagration of AP (Levy and Friedman (1962)), Steinz and Summerfield (1969) have estimated, as did Levy and Friedman, that the gas-phase reaction between NH_3 and

$HClO_4$ (the presumed products of AP gasification) occurs very close to the gasifying AP surface, e.g., 10 μm at 1 atm. If such is the case, emission from the gas-phase in the present experiments can be expected to be quite small since the mass of gas participating is quite small. The emission from the thin gas-layer between a gasifying AP surface and the plane of completion of the ammonia-perchloric acid reaction can be estimated at appreciably less than 1%* of the emission at 3.05 μm. from the solid surface (see Appendix C).

Finally, the boundary-layer calculations of Howe and Mersman (1959) were used to estimate roughly the contribution of NH_3 emission in the event that the NH_3 did not react appreciably above the pyrolyzing surface. While the calculations of Howe and Mersman are for a homogeneous flow field, they are thought to provide a reasonable estimate owing to the modest effect of molecular weight differences on transpired boundary-layers. Heat and mass transfer coefficients, for example, vary approximately as the molecular weight to a small fractional power, e.g., 0.25 to 0.50 (Anfimov (1966)). Through a small extrapolation of Howe and Mersman's calculated trend of thermal boundary-layer thickness versus mass-injection rate from the surface, it was found that 95% of the layer was, in an extreme case, within about 0.25 mm. of the surface. For the purpose of radiation

---

*Calculated assuming a reference spectral absorption coefficient at 1 atm, 300°K (ca. 0.17 cm^{-1} at 3.05 μm) implied by the measurements of France and Williams (1964) and assuming (conservatively) that a linear temperature gradient exists between the surface temperature the AP flame-temperature (conservatively estimated, ca.970°C., based on experimental data 'see Hall and Pearson (1967), Table 21).

estimates, similarity of NH_3 concentration and temperature distributions was assumed, and the distribution of each was approximated linearly. On this basis, emission from the ammonia was found to be less than 1% of that from surface for a reference absorption coefficient of 0.17 cm^{-1}. at 1 atm and 300°K (see Appendix C).

III.B. 5 Scanning-Electron Micrographs

For the purposes of surface microscopy, approximately 15 pyrolysis tests were made by interrupting pyrolysis before the entire AP specimen had been pyrolyzed. This was done simply by shutting the solenoid valves of the gas-rocket gas-supply during the test.

Pyrolysis was interrupted at a time when the specimen was still long enough so that the "thermal wave" had not fully penetrated the solid AP, i.e., such that the surface process might still be expected to be independent of the finite specimen length.

After interruption of heating, the specimen was advanced until it fell from the specimen holder into a padded retrieval box. Because of this process, some chipping at the edges of the specimens was observed, but there was no serious damage of the pyrolyzed surface. The specimens were then mounted within glass vials containing silica gel and dry nitrogen, and these were shipped to the Naval Weapons Center, China Lake, California, for micrography*.

Scanning-electron micrographs of the pyrolyzed surfaces were taken at a variety of magnifications. Before microscopy, the specimens received a vacuum coating of a few hundred Angstroms of gold-palladium.

*Through the good offices of E.Price and T. L. Boggs, Naval Weapons Center

CHAPTER IV - EXPERIMENTAL AND ANALYTICAL RESULTS

IV.A AP PYROLYSIS CHARACTERISTICS

Table J-3 of Appendix J summarizes the regression rate vs. surface brightness-temperature data obtained in this investigation, including data from the various checks of validity described in Section III.B. Figure IV-1 illustrates these data* along with the fitted-lines obtained from least-squares, linear regressions for the data (see Appendix E). Table IV-1 shows the parameters derived from the least-squares fits to the data and allows comparisons with the regression rate vs. surface temperature results of others (see Table II-1).

As detailed in Appendix E, the least-squares fits allow, by way of corresponding standard estimates of error, discernment of a small discontinuity in the observed trend, i.e., an abrupt increase in regression rate for surface brightness temperatures on the order of 475°C. This discontinuity appears to involve only a small change in apparent activation energy. The fitted lines also indicate a regime at high surface brightness temperature for which this temperature is nearly constant. It is noteworthy that the low scatter of the present results has made these observations possible; they would have been impossible to draw from data as highly scattered as the earlier linear pyrolysis data of other workers.

---

*Horizontal lines indicate range of temperatures recorded during each test (see III.A.4b, above).

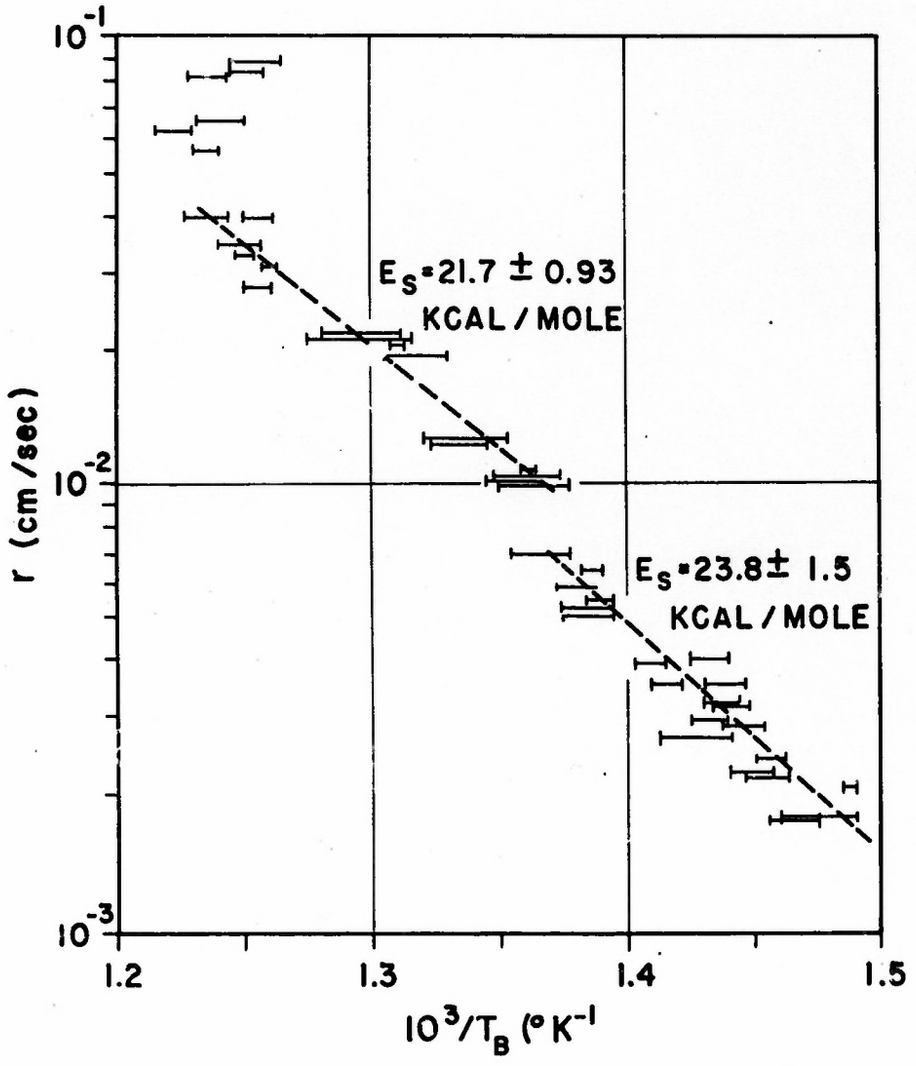

FIGURE IV-1: PYROLYSIS RATES (r) vs. INVERSE SURFACE BRIGHTNESS TEMPERATURE ($10^3/T_B$) FROM CONVECTIVE HEATING OF PRESSED AP (WITH LEAST-SQUARES FITS)

T_B (°C)	$10^3/T_B$ ($-K^{-1} \times 10^3$)	Eq'n Fitted	A (cm/sec)	E_S (kcal/mole)
398 - 457	1.37 - 1.49	1	$10^{4.93}$	23.8 ± 1.5
398 - 457	1.37 - 1.49	2	$10^{3.29}$	23.1
398 - 457	1.37 - 1.49	3	$10^{1.65}$	22.3
463 - 533	1.23 - 1.36	1	$10^{4.45}$	21.7 ± 0.9
463 - 533	1.23 - 1.36	2	$10^{2.79}$	20.9
463 - 533	1.23 - 1.36	3	$10^{1.13}$	20.2
398 - 533	1.23 - 1.49	1	$10^{5.71}$	26.2 ± 0.6
398 - 533	1.23 - 1.49	2	$10^{4.06}$	25.5
398 - 533	1.23 - 1.49	3	$10^{2.41}$	24.7

EQUATIONS: 1: $r = A \exp(-E_S/RT_B)$

2: $r = A_{(½)}(T_B)^{1/2} \exp(-E_S/RT_B)$

3: $r = A_{(1)} T_B \exp(-E_S/RT_B)$

TABLE IV-1 - SUMMARY OF KINETIC PARAMETERS FROM SEVERAL LEAST-SQUARES FITS TO THE PRESENT LINEAR-PYROLYSIS DATA (SEVERAL FUNCTIONAL FORMS)

IV. B SUPPORTING EXPERIMENTAL RESULTS

IV. B.1 Photographs of the Surfaces of Specimens Quenched During Pyrolysis

Scanning electron micrographs of quenched surfaces are shown in Figures IV-2 and IV-3 for both intermediate and extreme test conditions. Photographs like these showed no systematic trend in surface structure and corroborated that regression during pyrolysis was macroscopically planar (Fig. IV-2) but microscopically stepped and/or porous on a scale of approximately 10 to 30 μm (Fig. IV-3). There is some evidence, though inconclusive, that the "steps" on the surface grow less distinct at higher rates and surface temperatures. Many of the structures observed compare closely with those reported by Krauetle (1969) from isothermal sublimation studies at lower temperatures and with those reported by Boggs and Krauetle (1969) for CH_4-AP diffusion flames at near-atmospheric pressures.

Figure IV-2 shows some cracking and a locally near-planar surface but with some "dishing"*. Dishing was often apparent macroscopically, but often visual inspection of the specimens showed much less surface irregularity than is apparent in Fig. IV-2. Much or all of the surface cracking may result from the polymorphic phase-change (and density change) of AP during cooling of the surface layer from test conditions; cracking has been observed by Boggs (1970) on single-crystals of AP which have been cooled from deflagration conditions.

---

*The chipping apparent at the edges is probably due to the retrieval method used to obtain the specimens; see page 64, above.

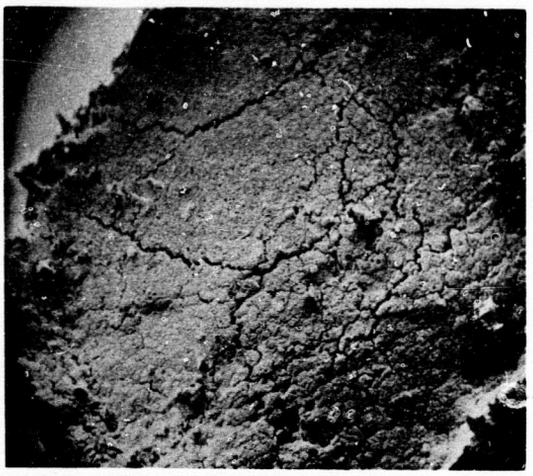

r = 0.08 CM/SEC
(17 X MAGNIFICATION)

r = 0.06 CM/SEC
(170 X MAGNIFICATION)

FIGURE IV-2: LOW-MAGNIFICATION SCANNING-ELECTRON MICROGRAPHS OF QUENCHED PYROLYSIS SURFACES

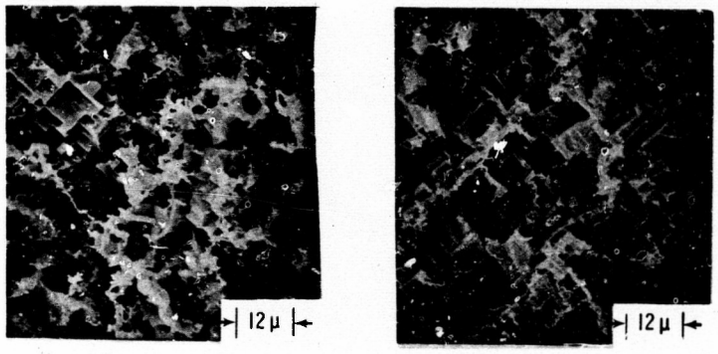

r = 0.004 CM/SEC

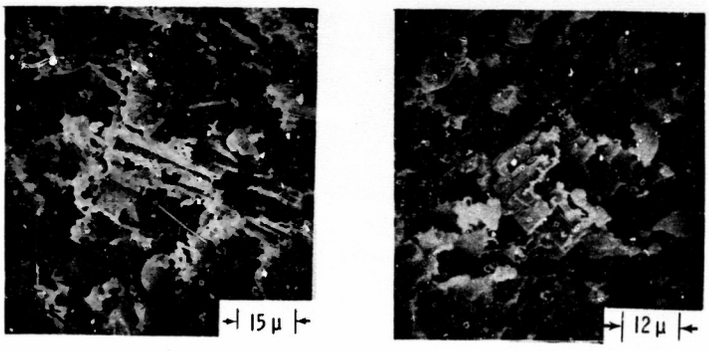

r = 0.02 CM/SEC

FIGURE IV-3: HIGH-MAGNIFICATION SCANNING-ELECTRON MICROGRAPHS OF QUENCHED PYROLYSIS SURFACES

IV.C SUPPORTING ANALYTICAL RESULTS

IV.C.1 Estimates of Convective Surface Heat Fluxes

Stagnation-point convective heat-transfer analysis was used as a basis for estimating surface heat-flux during pyrolysis. Details of the simplified analysis used are presented in Appendix F; the results of the analysis (based on numerical solution for laminar, convective heating by a compressible fluid near a stagnation point (Reshotko and Cohen (1955)) are shown in Figure IV-4 as plots of surface heat flux vs. pyrolysis rates for several different cases. The results shown are based on surface temperatures derived from brightness temperatures with the assumption of an emittance value of 0.72*. As pointed out below (Section V.A), this is a likely minimum value for the emittance. Larger values (up to unity) have little effect on the good correlation shown in Fig. IV-4. Appendix F also notes other alternative approaches to estimating heat flux, these having been judged impractical for the present purposes.

IV.C.2 Estimates of Pyrolyzate Partial Pressures at the Surface and Corresponding Vacuum Sublimation Rates

Partial-pressures of the gaseous products of pyrolysis above the pyrolyzing surface were estimated. These estimates were obtained using

*For simplicity, most references to specific surface temperatures in the following sections deal with temperatures derived by assuming $\varepsilon = 0.72$. It should be recognized (see Section V.A, below) that this value is neither certain nor crucial to the interpretations given herein.

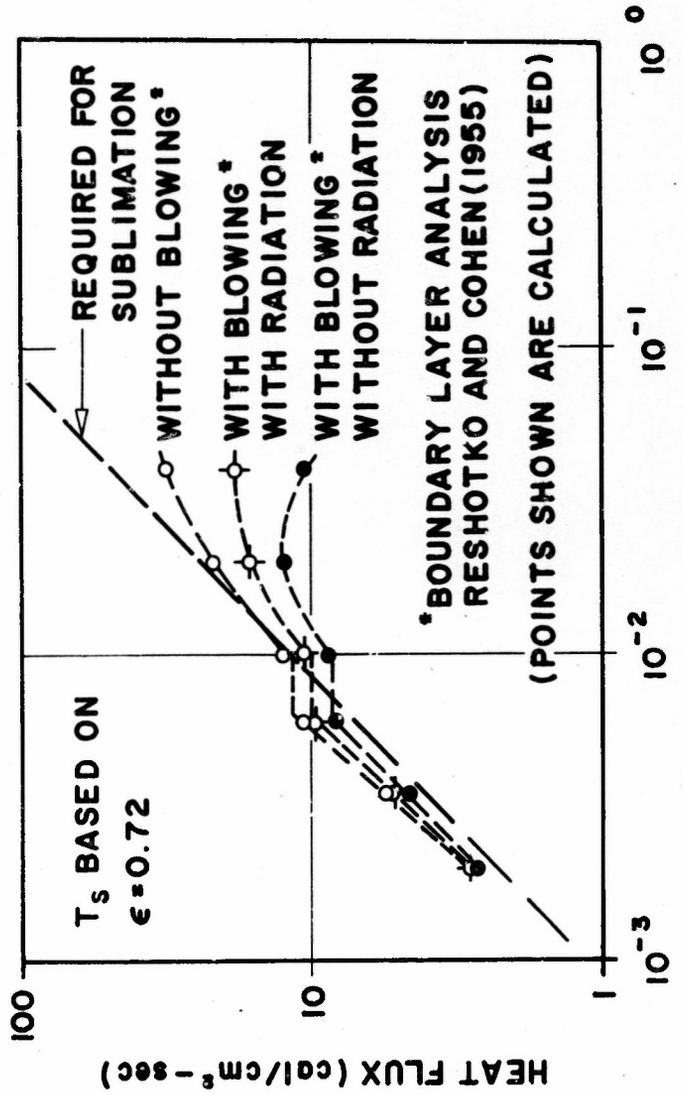

FIGURE IV-4: ESTIMATED HEAT-FLUX vs. REGRESSION RATE FOR AP PYROLYSIS VIA CONVECTIVE HEATING

the approach of Spalding to relate heat and mass transfer in convective flow fields (Spalding (1963)). This approach, based on Reynolds Hypothesis and the assumption of unity Lewis Number, was used along with the following assumptions to deduce the mass fractions and, hence, the partial pressures of the pyrolyzate gas at the surface:

(1) the pyrolyzate can be considered as a single species which is an equimolar mixture of NH_3 and $HClO_4$, the products of dissociative sublimation of AP,

(2) specific heat and thermal conductivity do not vary in the gas phase,

(3) the specific heat of solid AP is constant at 0.30 cal/gm-°K,

(4) reaction occurs at the surface only and is endothermic at 58.2 kcal/mole of AP (heat of sublimation of AP, Inami et al. (1963)),

(5) the pyrolyzate and the impinging-jet gas are ideal gases,

(6) the impinging gas-jet has the (measured) temperatures and stagnation pressures described in Appendix B.

The results of these estimates are given in Table IV-2. The details of the estimation procedure are given in Appendix D, and the results are indicated in Figure IV-5. In this figure, measured rates (r) have been scaled up to represent pyrolysis rates *in vacuo* (r_{vac}) according to Eq. (I-5). Only those rates corresponding to surface temperatures below 500°C have been scaled in this way because of evidence that higher-temperature rates are already essentially vacuum rates owing to gas-phase reactions at high temperatures (see Section V.B.1b, below.)

$10^3/T_S$ [a] ($^oK^{-1} \times 10^3$)	T_S [a] (^oK)	r [a] (cm/sec)	P [b] (atm)	$P_{i,eq}(T_S)$ [c] (atm)	T_E [d] (^oK)	$P_{i,S}/P$	$P_{i,S}/P_{i,eq}$	r_{vac} (cm/sec)
1.397	716	0.0022	1.15	0.083	853	0.0278	.387	0.0036
1.351	740	0.0035	1.17	0.15?	973	0.0455	.345	0.0053
1.304	766	0.0060	1.19	0.301	1183	0.0775	.306	0.0087

NOTES:

(a) Based on measured regression-rate vs. brightness-temperature data and surface emittance = 0.72
(b) Based on measured stagnation pressures (Appendix B)
(c) Based on vapor-pressure data of Inami et al (1963)
(d) Based on measured impinging jet temperatures (Appendix B)

TABLE IV-2 - RESULTS OF SURFACE PARTIAL-PRESSURE AND (VACUUM) SUBLIMATION-RATE ESTIMATES

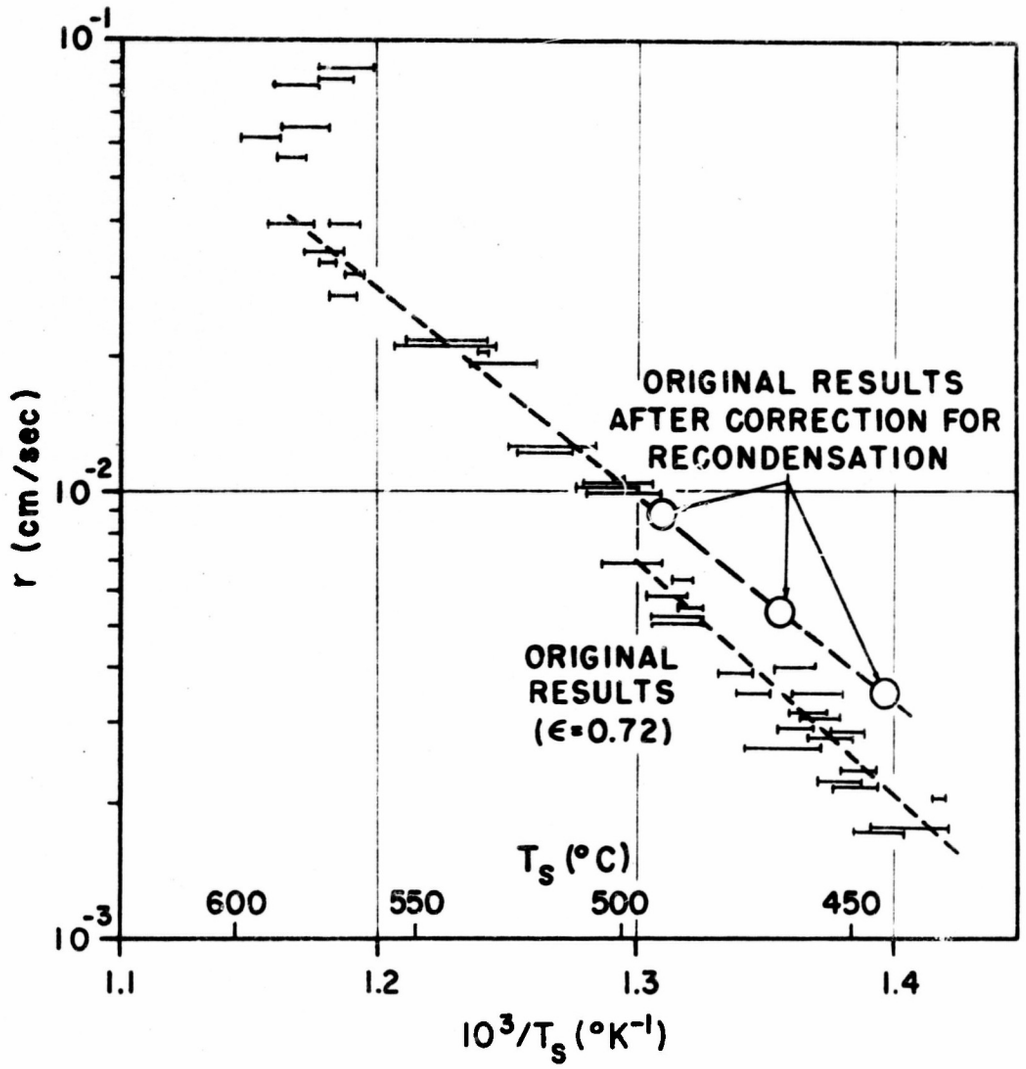

FIGURE IV-5: AP PYROLYSIS (SUBLIMATION) RATES VS. SURFACE TEMPERATURE FOR ϵ = 0.72 WITH CORRECTION FOR RECONDENSATION

CHAPTER V - INTERPRETATION OF RESULTS

V.A SURFACE TEMPERATURES

Surface brightness temperatures (T_B) were measured in the present investigation, and these may serve as a basis for deducing surface temperatures (T_S). Such deductions depend on the value(s) of surface emittance during pyrolysis. Earlier studies involving radiometric measurements of the surface temperature of AP have employed extrapolations of emittance measurements at low temperatures to deduce surface temperatures (Powling and Smith (1962, 1963)).

Extrapolation of low-temperature AP emittances is apparently tenable for deducing surface temperatures over most of the range of the present results but has little foundation if the high brightness-temperature regime ($T_B \cong 530^{\circ}C$) of the present data is being considered (see Fig. IV-1). This high-temperature regime may involve a different sublimation mechanism and, hence, a different surface structure. Of the regimes studied, this regime is probably the most closely related to the pyrolysis occuring during propellant combustion. In the context of describing combustion situations, prime interest in the future will probably lie in this regime rather than those at lower temperatures for which emittance measurements and extrapolations are tenable. for these reasons, re-measurement of AP emittance values at low temperature was judged of marginal value, and earlier measurements were used as a basis for deducing surface temperatures from the brightness temperatures of this investigation.

Reasonable limits for the surface temperatures implied by the present brightness temperature measurements can be set on the basis of the normal emittance measurements of Powling and Smith (1962). As a reasonable upper limit on surface emittance, the most recently reported emittance value of Powling and Smith (1965) was chosen (0.83). This value was measured normal to heated AP surfaces (200° to 360°C), and the emittance is reportedly nearly independent of temperature. As a reasonable lower limit for the emittance in the present circumstances, Fresnel's reflection law (Sparrow and Cess (1966)) for optically flat surfaces of optically absorbing materials was used*. With an estimate of the absorption coefficient of AP at 3.1 μm ($\kappa_{3.1\ \mu m} = 15{,}000 cm^{-1}$; Powling and Smith (1965)) and a conservative estimate for the index of refraction of AP at the same wavelength ($n_{\lambda} = 1.00$), the ratio of normal and oblique spectral emittances was established for the emission direction used in the present experiments (65° to the normal). This value (0.87) multiplied by the normal emittance (0.83) gave a lower bound for the emittance characteristic of the present measurements (0.72). On this basis, the pyrolysis characteristics of AP may be expressed as shown in Fig. V-1 which is based on the results in Fig's. IV-1 and IV-5.

If the emittance is assumed constant over the temperature range of interest, the effect of considering different (constant) emittances

---

*This approach is based on the premise that scattering of infrared radiation within pressed AP samples is unimportant. The data of Powling and Smith (1962) for the transmittance of an 80-μm-thick, pressed AP sample support this premise.

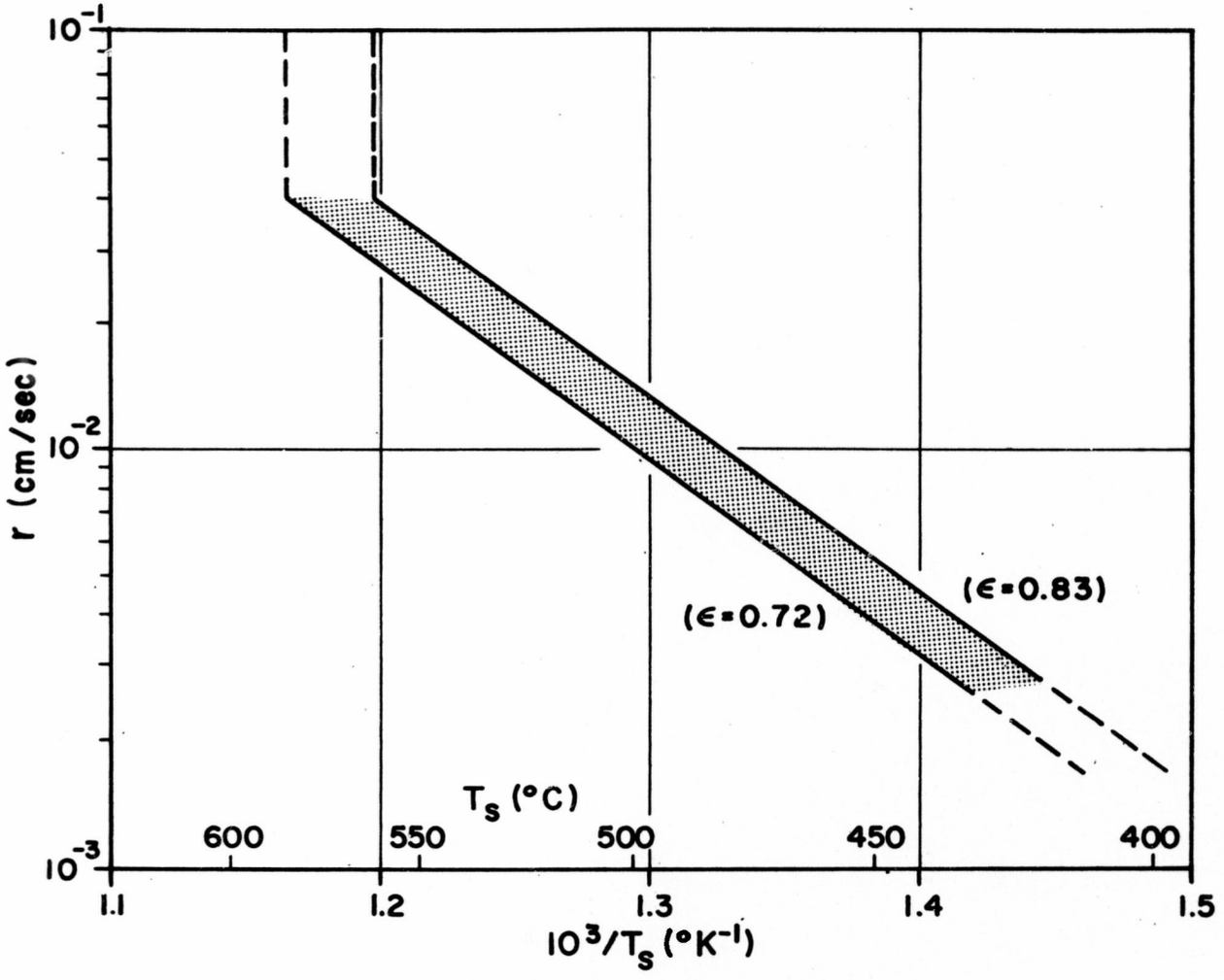

FIGURE V-1: AP PYROLYSIS RATE (r) vs. SURFACE TEMPERATURE (T_S)

is very nearly a simple, uniform displacement of data points (horizontally) on coordinates like those of Fig. V-1. That is, for the wavelength and brightness temperatures of this study, Wien's law approximates Planck's function very closely (within 0.3% or less), and a consequence of Wien's law is that inverse real and inverse brightness temperatures differ by a value which depends only on wavelength and emittance values and is independent of the actual temperatures involved. For this reason, apparent activation energies were not recalculated in the process of considering surface temperatures rather than brightness temperatures; any correction of the least-squares fits of the data (shown in Fig. IV-1) in order to account for non-unity emittance would fall well within the uncertainties listed in Table IV-1.

V.B IMPLICATIONS OF THE PRESENT RESULTS

The present results suggest the existence of two different pyrolysis regimes within the range of surface temperature and pyrolysis rates observed. The regimes are indicated in Fig. V-2 and are termed Regime B and Regime C. The low-temperature, isothermal sublimation regime is termed Regime A. These Regimes are summarized in Table V-1.

V.B.1 Regime B

The various results provide a self-consistent view of the mechanism of the linear pyrolysis of AP within Regime B.

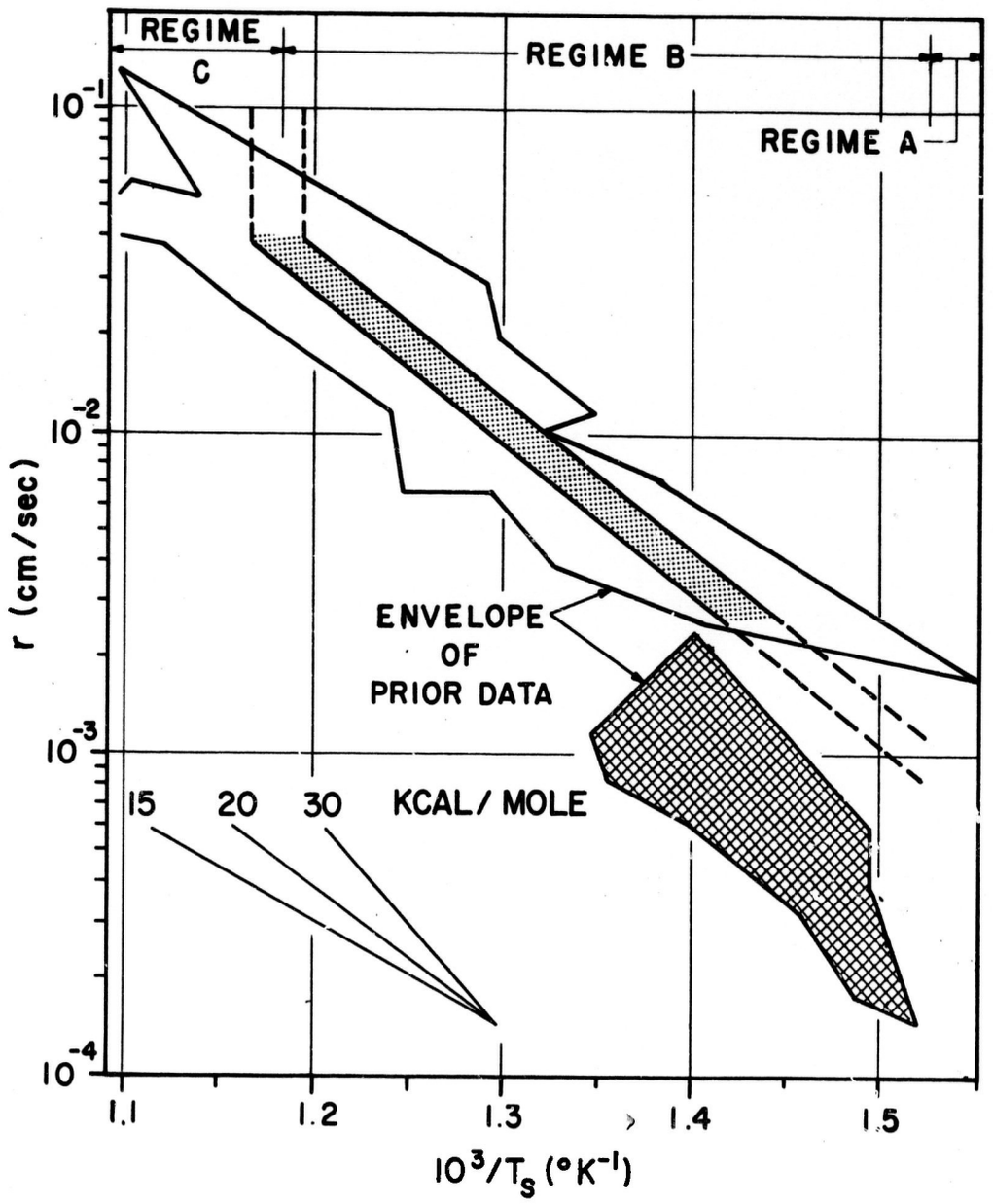

FIGURE V-2: AP (VACUUM) PYROLYSIS RATES (r) vs. SURFACE TEMPERATURES (T_S) FOR ϵ = 0.72 TO 0.83 WITH THE REGIMES DEDUCED IN THIS STUDY

T_S (°C)	REGIME	TYPE OF PYROLYSIS	RATE-CONTROLLING PROCESS(ES)	APPARENT ACTIVATION ENERGY, E_S (KCAL/MOLE)	PYROLYSIS STEP ACCOUNTING FOR E_S
< 380	A	Isothermal Sublimation	Diffusion or sublimation-kinetics-controlled	ca.30	Proton-Transfer
< 490 > 380	B1	Sublimation without postreaction	Diffusion or kinetics-controlled depending on ambient pressure, mode of heating, etc. Postreaction typically yields kinetics control	ca.22	Desorption(?)
< 580 > 490	B2	Sublimation with postreaction, probably in gas phase			
> 580[a]	C	Sublimation and/or new reaction with probable change in surface structure (liquid phase?)	?	?	?

NOTE: At 1 atm pressure; influence of ambient pressure uninvestigated to date

TABLE V-1 - SUMMARY OF AP PYROLYSIS REGIMES

V.B.1a Heat Flux and Partial Pressure Estimates

Estimated values of surface heat flux and partial pressures of pyrolyzate are highly consistent with a reasonable mechanistic hypothesis, i.e., that pyrolysis data (regression rate vs. surface temperature) which were obtained in Regime B are representative of sublimation, endothermic to the extent of about 58 kcal/mole and rate-limited by a currently unidentified kinetic step in the overall sublimation process. Apparently, the present investigation is the first in which any such checks for consistency have been made. Earlier studies have suffered from profound difficulties in modeling the situation in which pyrolysis occurs.

V.B.1b Discontinuity in Trend of Regression Rate v. Surface Temperature (Onset of Gas-Phase Reaction)

Though a discontinuity in the relation between pyrolysis rate and surface temperature was observed within Regime B (Fig. IV-1), this does not apparently evidence a change in pyrolysis mechanism from the sublimation mechanism described above. The discontinuity in pyrolysis rate at a surface brightness temperature of about 460°C can be attributed to the onset of gas-phase reaction of the pyrolyzate and to a resulting decrease in pyrolyzate partial pressure at the pyrolyzing surface. This decreased partial pressure, occurring abruptly with the onset of gas-phase reaction, should be expected to increase pyrolysis rates abruptly by nearly eliminating the recondensation which partially opposes sublimation at higher partial pressures.

The results of Fig. IV-6 are highly consistent with this view. The discontinuity in regression rates may be discounted by "correcting" regression rates at low surface temperatures via estimates of partial pressures at the surface (Appendix D). This "eliminates" the discontinuity, and the slope of the resulting Arrhenius plot does not change at the discontinuity (Fig. IV-6). These facts suggest maintenance of a single sublimation mechanism across the discontinuity.

Heat-flux estimates (Fig. IV-5) are consistent with the idea of non-reactive, convective heating at low temperatures but indicate a new heat source, such as exothermic gas-phase reaction, at higher surface temperatures. The idea of a gas-phase reaction is supported by a variety of observations: (i) the onset of visible flames observed by Guinet (1965) and Lieberherr (1967), (ii) indications of reaction within porous hot-plates (Coates (1965)), and (iii) the excellent correlation obtained from partial-pressure estimates (see above).

Further evidence for reaction in addition to sublimation can be found in the close similarity of the regression rate observed at the discontinuity in this study and in Lieberherr's work, i.e., about 0.01 cm/sec. This rate is also strikingly similar to rates observed during AP deflagration. For example, rates extrapolated (for 1 atm ambient pressure) from higher-pressure self-deflagration data for AP (0.015 cm/sec, Levy and Friedman (1962)) and rates for threshold radiation-augmentation of AP self-deflagration at 1 atm (e.g.; 0.02 cm/sec, Levy and Friedman (1962); 0.009 to 0.02 cm/sec, Hertzberg (1970)) are

all close to the lowest rate at which reaction is postulated to occur in the present investigation. The later evidence does not, however, necessarily indicate reaction in the gas-phase, as contrasted with the solid-phase.

V.B.1c Pyrolysis Mechanism

The mechanism of pyrolysis in Regime B appears to differ from that of either of the extant models of the low-temperature sublimation process or their extrapolations to linear-pyrolysis conditions (see Section I.C.2). Both of these models involve an apparent activation energy of about 30 kcal/mole. The apparent activation energy found in the present investigation (ca. 22 kcal/mole) compares unfavorably with this value, but, on the other hand, favorably with earlier values from other linear-pyrolysis experiments (Table II-1). None of these earlier pyrolysis experiments support a simple extrapolation of isothermal pyrolysis data to non-isothermal, higher-heating-rate conditions; the results of the present investigation considerably reinforce earlier work in this regard, since the present results derive from a completely independent method.

The greatly-reduced scatter of the present results (compared with earlier linear-pyrolysis data) contributes to further mechanistic interpretation than has been possible earlier. The observed constancy of apparent activation energy through Regime B, a range of about 170°C, strongly implies rate-control by a single reaction mechanism; in the past, data scatter would have allowed interpretation in terms

of temperature-dependent activation energies reflecting a changing mechanism, e.g., transition between rate-control by different reaction steps.

Though the present results do not provide a basis for identifying the particular reaction step involved in Regime-B pyrolysis, they do bring considerably more insight to bear on this identification problem. Contrary to the situation before the present results, it is possible to state several apparently requisite features of any mechanism proposed to explain pyrolysis in Regime B:

(i) such a mechanism should evidence an apparent activation energy in the neighborhood of 22 kcal/mole,

(ii) there should be no obvious competitive processes to subvert this value into a value varying more than one or two kcal/mole within Regime B,

(iii) the mechanism must provide such an apparent activation at pyrolyzate partial pressures an order of magnitude or more below corresponding equilibrium vapor pressures for AP (at the surface temperatures of Regime B),

(iv) the mechanism should not be strongly influenced by the presence of normal combustion products, e.g., CO_2, H_2O, or of O_2 or N_2 in the gas phase near the pyrolyzing surface (since concentrations of these species doubtless varied appreciably but not systematically over the present pyrolysis tests*).

* See Section III.B.3 relative to variations in hot-gas-jet temperature and therefore, in composition.

Apparently, one of the more complex sublimations models of Guirao and Williams (1969) or the earlier model of Schultz and Dekker (1957) may apply in describing linear pyrolysis in Regime B. There does not appear to be any obstacle to considering, for example, the latter model. However, it must be recognized that even the information available from the present, improved type of linear pyrolysis test is an insufficient basis for establishing any such detailed mechanistic view to the exclusion of all others.

V.B.1d Summary

Within Regime B, with surface temperatures in the range of 380° to 570°C, it appears that pyrolysis rates are determined by a step controlling the rate of dissociative sublimation and that this step is a different one than that controlling lower-temperature sublimation. This step appears to be dominant whether gas-phase reaction is present or not. While it is possible that the step controlling higher-temperature sublimation is one of desorption from the pyrolyzing surface, current evidence is insufficient to corroborate this view. It does appear, however, that pyrolysis rates in this regime are not consistent with either of the two present models of the low-temperature sublimation process. The data are, therefore, not consistent with extrapolations of these models to higher temperatures, e. g., that of Jacobs and Powling (1969).

V.B.2 Regime C

V.B.2a Validity of Data in Regime C

Though subject to further experimental study, Regime C appears not to be simply a result of experimental idiosyncracies. It is noteworthy in this regard that specimens used in Regime C pyrolysis tests were generally more carefully prepared of any used in the present study*. Possibly for this reason it appeared that, despite higher regression rates, these specimens regressed even more steadily and with more nearly planar surfaces than others did. Because of these facts, the results for high heating rates were expected, before data reduction, to lie on a simple extrapolation of the trend of earlier data.

The trend of pyrolysis data in Regime C (Fig. V-2) is such an abrupt and striking variation from the trend of lower-temperature data, that there is cause to expect that the recorded trend of the data in Regime C is not necessarily real. A change in structure of the pyrolyzing surface might, for example, sufficiently alter the surface emittance from its lower-temperature value as to invalidate the constant-emittance assumption used in reducing lower-temperature data. It is quite possible that the actual relation between regression rate and surface temperature has not changed within Regime C, but rather that infrared radiometry simply indicates changes in surface

*In anticipation of difficulty in maintaining specimen-integrity during testing at high heating rates, most of the specimens used were processed more carefully than those used in other tests. The specimens were pressed with longer dwell-times in the press (e.g., 30 min.) and were formed carefully into cylinders with diametral tolerances which were appreciably smaller (e.g., ±0.001" , see Appendix A) than those normally encountered with other test specimens (e.g., ±0.002").

structure in this Regime. Thus, the temperatures and rates at which Regime C begins are probably more physically significant than the apparent trend within Regime C .

V.B.2b Speculations Regarding Regime C

It is striking that the onset of Regime C occurs, apparently, at about 580 to 590°C (subject to previously cited uncertainty owing to uncertainty in surface emittance). This temperature is remarkably close to the constant surface temperature (590°C) inferred by Beckstead and Hightower (1967) and by Boggs (1970) from measurements of the depth of planes of polymorphic phase transformation below the surfaces of AP crystals which were quenched during self-deflagration. The 580° to 590°C range is remarkably close to the only known estimates of the triple-point temperature of AP (Cordes (1969)). Since Beckstead and Hightower's crystals showed evidence of a liquid layer on the pyrolyzing surface, it is tempting to suggest that Regime C (unlike Regime B) involves a liquid phase, possibly AP, on the pyrolyzing surface. Simple sublimation seems well established as the central process in AP pyrolysis at low temperatures, and the more complex processes likely in AP pyrolysis with a liquid phase are likely during AP pyrolysis at deflagration conditions (Boggs (1970)). Regime C might, in this context, be postulated as a regime in which surface condition and r vs. T_S relations are developing into those occurring during the deflagration of AP. Such a postulate would place the present data in the role of bridging, for the first time, the gap between low-temperature pyrolysis

of AP and the higher-temperature self-deflagration of AP.

V.B.2c Obstacles to Speculations

There are two obstacles to postulating that Regime III involves a liquid phase and that, for example, its gradual increase accounts for the observed relation between regression rate and surface brightness temperature in Regime C . While neither of these objections seems, however, well enough established to invalidate such a postulate conclusively, the obstacles raised are appreciable.

V.B.2c (1) Vapor Pressure Discrepancies

Estimates of the triple-point of AP (Cordes (1969)) as being at 590°C include estimates of the vapor pressure at the triple-point as being approximately 2000 mm Hg. Such a pressure is considerably higher than even the maximum total (stagnation) pressures in the present experiments (935 mm Hg). The partial pressures of AP pyrolyzate vapor are expected to be lower yet, perhaps by a factor of 0.2 or less, considering the scheme for partial pressure estimates which was used in this investigation*. This implies partial pressures lower than the triple-point vapor pressures by a factor at least an order of magnitude which is not consistent with postulate that Regime C

*The partial pressure of pyrolyzate at the surface for a regression rate of 0.04 cm/sec may be estimated at about 0.15 times the total pressure if it is assumed that the convective flow field near the pyrolyzing surface is nonreactive (see Appendix D). This factor is higher than what would be estimated by taking into appropriate consideration reactions in the flow field.

involves liquid AP.

It is significant that the vapor pressure of AP in the neighborhood of the triple-point enters the estimate of the triple-point temperature only as a ratio since the estimation method is based on a "corresponding-states" model. (see Cordes (1969)). In effect, then, so long as the latent heat of sublimation is known reasonably precisely, the corresponding-states basis for predicting triple-point temperature may be accurate. Since the vapor pressure at the triple-point is determined by extrapolation of the usual exponential vapor-pressure data over 3 to 4 orders of magnitude, it is quite possible that this vapor pressure may be appreciably in error though its temperature dependence may be only slightly so. Thus, Cordes' well-correlated estimates of triple-point temperatures do not necessarily imply such a well-known vapor pressure at the triple point. For example, an error of 2 kcal/mole (ca. 3%) in latent heat of sublimation implies about the same proportional error (ca. 30°C) in determining melting point in the method cited (Cordes). In contrast, such an error implies about 30% error (about 600 mm Hg) in extrapolating vapor-pressure data to the melting point. It is, however, difficult to rationalize the previously-cited order-of-magnitude error in vapor pressure as arising from such an error.

V.B.2c(2) Lack of Physical Evidence for a Liquid Phase

A second objection exists against identifying Regime C as one involving a liquid phase on the pyrolyzing surface. The scanning-

electron micrographs of the present investigation show little or no evidence of a liquid phase on surfaces quenched during pyrolysis. It does appear possible, however, that a thin layer of liquid on the surface could be vaporized during the quenching process; at the steady regression rates observed before quenching, a surface layer of 1 μm thickness is pyrolyzed in approximately 1 msec., probably faster than the duration of the quenching process. While quenching may be fast enough to preserve large surface features, then, a thin layer of pyrolyzing liquid might easily vanish during the process*.

V.B.2d Summary

In summary, Regime C is not readily characterized; it was not investigated as fully in the present study as Regime B. The surface temperature at which Regime C appears correlates well with both surface temperatures estimates for the self-deflagration of AP and with melting-point estimates for AP. However, inconsistencies arise in attempting to postulate the occurrence of molten AP on the surface and to relate this postulate with other data involving a liquid phase for AP. It appears that there may be transition at surface temperatures of about 580°C from Regime B to a pyrolysis regime more nearly resembling pyrolysis during self-deflagration of AP and of composite propellants, but appearances are not conclusive.

---

*Such appears not to be the case during quenching of self-deflagrating AP crystals. However, these are quenched by a different means (see Beckstead and Hightower (1967)) which may preserve liquid layers more effectively.

V.C RELATION OF PRESENT RESULTS TO PRIOR PYROLYSIS RESULTS OF OTHERS

Consideration of particulate systems is omitted from this section for the reasons cited above (Section II.A.2). It is notable that recent thoughts regarding pyrolysis of particulate systems (Jacobs and Powling (1969)), have suggested a tendency of such systems to overestimate sublimation rates and apparent activation energies relative to linear pyrolysis. This observation is consistent with the relationship between the present results and those from particulate systems. It remains to compare the present pyrolysis results with those from the several other sources of linear pyrolysis data cited earlier.

V.C.1 Pyrolysis in AP-Gaseous Fuel Diffusion Flames

The diffusion-flame results of Powling suffer, in interpretation, from uncertainty as to the environment in which pyrolysis occurs. As the preceding section of the present work shows, estimates of surface-environment are imperative for the sake of interpreting pyrolysis results. Reports of diffusion-flame data have not, however, been complete enough to allow such estimates; combustible fuel-gas compositions have not, for example, been reported. Even with such data, however, estimates of surface conditions accompanying diffusion flames would be difficult to achieve because of the probably need for considering reaction kinetics in attempting to estimate heat fluxes and partial pressures at the surface; appropriate quantitative kinetic data are insufficient for the task. One must be content, then, with judging simply whether or not pyrolysis data from diffusion flames are

reasonably consistent with a particular pyrolysis scheme of interest.

In this regard, Powling's diffusion-flame data are, at least, consistent with the view of sublimative pyrolysis as described in the preceding section. The pyrolysis rates at various surface temperatures are of the same order as the present results. Viewed overall, Powling's data suggest a lower apparent activation energy than that of the present data. However, the possibility is strong that changes in mass diffusion rates may be significant; diffusion is impeded by the higher total pressures involved in the diffusion-flame experiments with higher rates. This might be expected to result in recondensation being more significant at the higher measured surface temperatures which accompany higher pressures in Powling's data. This would imply that higher pyrolysis rates may actually be lower in proportion to corresponding unopposed reaction rates than are the lower pyrolysis rates. This possibility is in accord with the observation that, at a given measured surface temperature, diffusion-flame pyrolysis rates (e.g., Fig. 4, Jacobs and Powling (1969)) exceed by little if any the pyrolysis rates reported in the present study. Unfortunately, however, there are some inconsistencies in reports of apparently comparable diffusion-flame pyrolysis rates*.

Diffusion-flame pyrolysis data do not include rates or surface temperatures quite high enough to necessitate their consideration relative to the data of Regime C of the present study.

*Compare, for example, the data of Fig. 4, Jacobs and Powling (1969) and Fig. 3, Powling (1967).

V.C.2 Porous Hot-Plate Pyrolysis Data

V.C.2a Data of Lieberherr

As mentioned above (Section II.A.3b), two sub-regimes are identifiable in the porous hot-plate data of Lieberherr which cover what was termed above as "Regime B". These sub-regimes are separated by an order-of-magnatude discontinuity in regression rate and are termed here "Regime B1" (lower temperature) and "Regime B2" (higher temperature).

Below about 475°C (termed Regime B1), the porous hot-plate data of Lieberherr are consistent with the present results and the interpretation given in Section V.A.1 above. As would be expected from that interpretation, Lieberherr's data show (with considerably scatter; see Table I-1) nearly the same activation energy as do the present results but appreciably lower pyrolysis rates. These lower rates may be considered a consequence of higher pyrolyzate partial pressures at the regressing surface. This possibility is particularly evident as a likely cause for the abrupt, order-of-magnitude increase in pyrolysis rates between Regimes B1 and B2; unopposed surface reaction is a distinct possibility at the higher surface temperatures of Regime B2 if gas-phase reactions serve as pyrolyzate "sinks" in Regime B2 but not in Regime B1.

To check this interpretation, partial pressures were estimated for Lieberherr's data in Regime IIA. The aim was to check roughly for consistency of Lieberherr's rates relative to the corresponding rates

of the present results, i.e., with the vacuum pyrolysis rates deduced in Appendix D, above. An additional aim was to check the consistency of Lieberherr's order-of-magnitude discontinuity in pyrolysis rate (at $10^3/T_S = 1.35$; $T_S = 475^oC$) with the idea of a suddenly-reduced partial pressure at higher temperatures due to the onset of gas-phase reactions.

The basis for estimates of partial pressures for Lieberherr's case is necessarily different from that used with the data of the present investigation. For the present convective-heating results (see Appendix D), the assumption of similarity of mass and heat transport was used to estimate partial pressures of pyrolyzate at the pyrolyzing surface; this was possible because the same gas phase flow field is involved in the two processes when heating is by convection. In the case of Lieberherr's porous hot-plate pyrolysis, such is not the case; the boundary conditions for heat and mass transport in the gas phase are sufficiently different as to preclude the assumption of similarity of heat and mass transport. In this context, pyrolyzate partial-pressures must be estimated directly from the appropriate gas-phase mass-transport relations.

In Appendix G, a model for estimating surface partial pressures is developed for a one-dimensional, binary flow-field composed of pyrolyzate "vapor" and an inert ambient gas. The model allows estimation of surface partial pressures of pyrolyzate, $P_{1,S}$, based on input values for:

the vacuum sublimation rate, r_{vac}

the characteristic diffusion length, L

the temperature-dependent vapor-pressure of pyrolyzate, $P_{1,eq}$

the surface temperature, T_S

the molecular weights, M_1 and M_2, of the species involved (pyrolyzate and inert, respectively)

the (binary) diffusion coefficient of pyrolyzate into inert, D.

This model was used to estimate the pyrolyzate partial pressures corresponding with Lieberherr's low-temperature data (Regime B1). Values for L and D appropriate to Lieberherr's situation are, unfortunately, uncertain as is the validity of the assumption of one-dimensionality for his porous-plate situation.

Partial pressure ratios $P_{1,s}/P_{1,eq}$, were calculated from the model using somewhat arbitrary though reasonable estimates:

$L = 0.1$ cm (approximately the porous-plate thickness)

$D = D_{std} (T/T_{std})^{3/2}(P_{std}/P)$; $D_{std} = 0.05$ cm^2/sec

$M_1 = 58$ (mean molecular weight of equimolar NH_3 - $HClO_4$ mixture)

r_{vac} = value indicated (at T_S of interest) in Fig. IV-5

The estimated partial-pressure ratios were used to calculate the ratio:

$$r/r_{vac} = 1 - P_{1,s}/P_{1,eq}$$

At $10^3/T_S = 1.4$ (Regime B1), the results of this calculation were:

$r/r_{vac} = 0.05$

The same ratio evaluated directly from a least-squares fit to Lieberherr's data and r_{vac} as deduced in the present investigation (see Fig. V-1) is:

$r/r_{vac} = 0.25$ at $10^3/T_S = 1.4$

These two values are, then, within order-of-magnitude agreement, their difference is not surprising in light of the substantial uncertainties in calculating the first value. The rough calculation is consistent with the idea of substantial recondensation being a possible cause of Lieberherr's rates being lower in Regime Bi than those of the present study (at the same temperature, $r/r_{vac} = 0.6$ for the present study).

Lieberherr's order-of-magnitude discontinuity in rate at $10^3/T_S = 1.35$ also appears to be consistent with the idea of a sudden decrease in pyrolyzate partial pressure with the onset of gas-phase reaction. It may be assumed, as for the present results, that gas-phase reaction reduces partial-pressures ratios to very low values in Lieberherr's situation. Since:

$r/r_{vac} = 0.05$ for Lieberherr's low-temperature data,

an order-of-magnitude increase in r might be expected at higher temperature if gas-phase reactions become very significant in depressing surface partial pressures of pyrolyzate.

In summary, rough estimates of surface partial-pressures of AP pyrolyzate for Lieberherr's data of Regime IIA appear to be as consistent as might be expected with the present results. This is apparently true both in terms of values for r_{vac} and in terms of the large discontinuity in rate observed by Lieberherr at $10^3/T_S = 1.35$ ($475^{\circ}C$). These estimates must, however, be viewed cautiously in light of the uncertainty which accompanies partial-pressure estimates for the porous hot-plate configuration. At least, the estimates do not appear to be inconsistent with the present results.

V.C.2b Data of Coates

Coates' data from porous-plate experiments at temperatures below 480°C are limited to a single, isolated datum point at $10^3/T_S = 1.55$ ($T_S = 370°C$) (see Table J-1, Appendix J). This point shows a pyrolysis rate an order-of-magnitude higher than that implied (with slight extrapolation) by Lieberherr's data at the same measured surface temperature. This difference may be rationalized as resulting from Coates' test-pressure being about an order-of-magnitude lower than Lieberherr's. This lower pressure should result in a higher diffusion coefficient in Coates' case and, therefore, in a much lower partial-pressure of pyrolyzate at the surface in Coates' case. An estimate of this partial pressure (made on the basis described above) led to prediction of an order-of-magnitude increase in r/r_{vac} from Eq. (IV-1). This is consistent with the relationship between Coates' and Lieberherr's experimental data.

Above about 475°C* but below about 570°C (termed Regime B2), both Coates' and Lieberherr's results show activation energies which are lower than that of the present study (see Tables II-1 and IV-1) and lower than that of Lieberherr in Regime B1. The fact that the present data show the same activation energy in both regimes suggests validity for these data and questionability for the porous hot-plate data.

*If the differences in experimental techniques are considered, it is not surprising that the discontinuity in Lieberherr's data occurs at a somewhat different temperature than that of the present data. Flammability limits are known to be notably apparatus-dependent (Lewis and von Elbe (1961)).

The flimsy, porous surface structure of sublimed AP observed using the scanning electron microscope (Fig. IV-4; also Boggs and Krauetle (1969)) suggests a strong possibility of physical influence on surface structure by the porous-metal hot-plate against which pyrolysis specimens are forced (see also Andersen (1964)). The liklihood of gas-phase reactions also suggests the possibility of complex thermal coupling between this reaction zone and the porous plate, thereby perturbing "normal" pyrolysis. Either this coupling or systematic errors in the surface temperature indicated by thermocouples may be responsible for the discrepancy between the present results and those of Lieberherr and Coates. An indication of anomalous pyrolysis with porous hot-plates can be drawn from the apparent occurrence of a maximum regression rate in Lieberherr's results near a reported surface temperature of 630°C. This is not in accord with the observed trend in the present results, or the expected trend, i.e., increasing regression rates with increasing heating rates. In general, the strong internal consistency of the present results seems to favor them over the earlier porous-plate data. The latter remain as untested in terms of consistency with other results such as heat-flux and partial-pressure estimates.

V.C.3 Solid Hot-Plate Pyrolysis Data

Again as in the case of data from porous hot-plates, the earlier data from solid hot-plates are forced to stand by themselves without the aid of heat-flux estimates, etc. Neither the validity nor

invalidity of these data and the present ones is much clarified by the agreement of apparent activation energies for the two cases (Tables II-1 and IV-1); this agreement may be coincidental. Alternatively, it is possible that, despite conjectured errors in surface temperature measurement (see Section II.A.3a), the solid hot-plate data do represent unopposed sublimation rates. Certainly the very low ambient pressures used in these early tests should have been conducive to unopposed sublimation.

V.C.4 High-Temperature Isothermal Sublimation Data

In comparison with the present results, those of Krauetle are of particular interest. The activation energy indicated by the present results (compared with isothermal sublimation studies) suggests that, at some surface temperature lower than those of the present study, a change in apparent activation energy ought to be observable. This transition may be manifested in the apparent discontinuity of Krauetle's data in the neighborhood of 380°C (Fig. II-5). At surface temperatures below this point, Krauetle's data strongly evidence an apparent activation energy in agreement with other lower-temperature isothermal sublimation data (Jacobs and Russell-Jones (1968)). At higher surface temperatures, however, systematic evidence of a lower activation energy is apparent. Finally, at Krauetle's highest temperatures (430° to 470°C), interpretation of his data is subject to uncertainty due to the nonuniformity of regression and the possibility of non-isothermal test conditions which he cites.

CHAPTER VI - CONCLUSIONS

VI.A. THE PRESENT PYROLYSIS TECHNIQUE

The present results promote the view that the combination of convective heating and infrared radiometry now constitute a proven technique for characterizing linear pyrolysis. This technique is more potent in both concept and practice than previous ones. The convective-heating-infrared-radiometry combination has been used previously in polymer pyrolysis studies, but its full potential for allowing checks of the self-consistency of pyrolysis results and for aiding mechanistic interpretation of them has been much more nearly achieved in the present investigation.

VI.A.1 Convective Heating

A particular innovation in the present experimental method is the use of a convective heating configuration which provides not only for regression rate and optical surface-temperature measurements but also for estimates of surface partial pressures and heat fluxes. Estimates like these have either not been made previously or have been so uncertain as to compromise their use. They are, however, a clear necessity in checking the consistency of experimental data with mechanistic models of pyrolysis and in successfully delineating, even empirically, th. various regimes which may arise during the pyrolysis of various materials. These estimates of surface partial pressurs and heat fluxes, along with the increased reproducibility of the data obtained by the

present technique, provide a much more valuable approach to investigating pyrolysis then has previously been possible.

The convective-heating configuration of the present investigation owes its utility to the fact that it was shown experimentally to involve a constant radial velocity gradient in the flow external to a transpired boundary layer. This fact justified fluid-dynamic analysis in terms of the well-developed theory of compressible, laminar, stagnation-point flow. Apparently for the first time, the present investigation demonstrates the applicability of this theory to the case of a finite gas jet impinging on a flat plate with a high ratio of jet temperature to ambient temperature and substantial temperature variations in the flow field.

The major drawback of the convective-heating mode of driving pyrolysis seems to be the surface shear stresses which necessarily accompany it though these were not a problem in the present investigation of AP. Convective-heating of polymers and fusible crystalline solids suffers from the possibility of substantial flow of liquid surface layers due to shear stresses. This effect is a serious detriment to the pyrolysis testing of some materials by convective heating because it interjects the complication of mechanistic modeling of uncertain viscous flow situations into the modeling of the overall pyrolysis process.

VI.A.2 Surface-Temperature Measurement by Infrared Spectraradiometry

Infrared spectraradiometry has been shown to be a technique for surface-temperature measurement which is viable for at least some linear-pyrolysis experiments. The present investigation exemplifies how the utility of this technique depends on a variety of preconditions for its use, most notably:

(i) checks on the extent of undesirable emission from the convective-heating jet and from pyrolyzate near the pyrolyzing surface, and

(ii) prior determination of surface-emittance values and a basis for the extrapolation of low-temperature data to high surface temperatures.

While not apparently a factor in the present investigation, influences of sub-surface temperature variations must also be of concern in applying the technique of the present investigation to other situations. The possibility of such influences is a detriment to use of the technique with materials which do not have spectral regions of high infrared absorptivity.

VI.A.3 Summary

In summary, the pyrolysis technique used in the present investigation has been shown to offer substantial advantage relative to other methods used previously. It cannot be proposed, however, as a universally-applicable method which supercedes others; it must rather be viewed as a viable and potent compliment to other experimental methods

for characterizing linear pyrolysis.

VI.B. PYROLYSIS CHARACTERISTICS OF AP

The experimental results of this investigations and the interpretation given to them lead to the delineation of three pyrolysis regimes. These are summarized in Table V-1. It appears that, subject to further study of Regime C, the present investigation goes far in bridging the gap which has existed to date between the data and models of isothermal AP pyrolysis on the one hand and those for AP self-deflagration on the other.

VI.B.1 Regimes A and B

The present investigation indicates that the sublimation mechanism operative in lower-temperature, isothermal pyrolysis (Regime A) is not dominant at the higher temperatures of Regime B (or beyond). Apparently, then, because of the higher heat fluxes, temperatures, and regression rates involved, linear-pyrolysis experiments like the present one relate more directly to the pyrolysis occuring during combustion. The mechanism of Regime A is manifested in apparent activation energies near 29 kcal/mole while the present results (and some earlier ones) for Regime B indicate a lower value, ca. 22 kcal/mole. This lower value is not directly related to the heat of sublimation of AP as the higher value from isothermal experiments is (according to two current views of low-temperature pyrolysis).

There is, nonetheless, substantial evidence (prior and present)

that sublimation is still the dominant process in Regime B. The present results are notable in this regard since they evidence high consistency between heat flux estimates and sublimation energetics and also between pyrolyzate partial-pressure estimates and several recondensation effects which might be expected from a reversible, sublimation process. For example, present and prior studies have shown discontinuities in the trend of regression rate vs. surface temperature which can be explained in terms of partial-pressure estimates and a recondensation process.

In contrast with either current mechanistic view of Regime-A pyrolysis, it is possible to postulate that pyrolysis in Regime B is rate-controlled by the desorption of NH_3 and $HClO_4$ from the subliming surface. Such a possibility was proposed much earlier but in a different context and without conclusive support. The present heat-flux and partial-pressure estimates appear to be consistent with such a sublimation mechanism, but they will not discriminate it from other possibilities.

Finally, it can be concluded that macroscopic differences in surface structure do, as has been suggested by prior workers, influence apparent activation energy. The present results support the earlier evidences of low activation energy for the linear pyrolysis of continuous AP surfaces. Therefore, the present results also reinforce earlier suggestions that the higher values of apparent activation energy observed with particulate surfaces (e.g., porous beds) are a result of particulate surface structure.

VI.B.2 Regime C

Some evidence of a third pyrolysis regime has been found in Regime C though without as exhaustive investigation as will ultimately be desireable. This regime apparently occurs at pyrolysis rates bordering on the lowest observed in the self-deflagration of AP. The lowest surface temperatures of this regime coincide with those predicted for the melting point of AP and with the temperatures attributed to a liquid-solid interface in experimental determinations of the surface temperature of self-deflagrating AP. Appearance of this regime in the present experiments may be a result of the radiometric method used for surface temperature measurements; this method is expected to be more sensitive than thermocouple measurements to surface structure changes, for example, to the appearance of a liquid-phase on the surface. This sensitivity arises from the sensitivity of the radiometric method to changes in surface emittance; hence, the appearance of Regime C as a changed relationship between regression rate and surface temperature may be fictitious and may conceivably reflect only a changed surface structure (without major influence on regression rate-surface temperature relationships).

VI.C. RECOMMENDATIONS FOR FUTURE RESEARCH

The most pressing need arising from the present research is for further research into the pyrolysis process which manifests itself as Regime C of the present study. An attempt to extend the present kind of pyrolysis characterization to higher heating rates and pyrolysis

rates is an obvious and desirable next step in making pyrolysis data useful for describing combustion situations.

The success of the present research in making deductions based on heat-flux and partial-pressure estimates at the pyrolyzing surface should be extended in application to other materials for which convective heating is suited, i.e., non-melting solids such as Teflon.

The present pyrolysis technique might be extended to use at variable ambient pressures both above and below atmospheric. Such data should be paramount in characterizing pyrolyzing materials and in testing various mechanistic views of pyrolysis.

The capability for varying gas-phase composition at a pyrolyzing surface (which is unique to the convective-heating linear-pyrolysis technique) should be exploited.

REFERENCES

Andersen, W. H., 1964, Comments on "Gas-Film Effects in the Linear Pyrolysis of Solids", AIAA J., Vol. 2, No. 2, pp. 404-407.

Andersen, W. H., Bills, K. W., Mishuck, E. and Schultz, R. D., 1959, A Model Describing Combustion of Solid Composite Propellants Containing Ammonium Nitrate, Comb. and Fl., Vol. 3, No. 3, pp. 301-317.

Andersen, W. H. and Chaiken, R. F., 1961, Detonability of Solid Composite Propellants, ARS J., Vol. 31, No. 10, pp. 1379-1387.

Anfimov, N. A., 1966, Heat and Mass Transfer Near the Stagnation Point with Injection and Suction of Various Gases through the Body Surface, Mekh. Zhid. i Gaza, Vol. 1, No. 1, pp. 22-31.

Barrère, M. and Williams, F. A., (1968), Analytical and Experimental Studies of the Steady-State Combustion Mechanism of Solid Propellants in Advances in Tactical Rocket Propulsion (AGARD Conference Proc. No. One), Editor: S. S. Penner, Technivision Services, Maidenhead, England, pp. 49-137.

Beckstead, M. W., Derr, R. L., and Price, C. F., 1970, A Model of Composite Solid-Propellant Combustion Based on Multiple Flames, AIAA J., Vol. 8, No. 12, pp. 2200-2207.

Beckstead, M. W. and Hightower, J. D., 1967, Surface Temperature

of Deflagrating Ammonium Perchlorate Crystals, AIAA J.,Vol. 5, No. 10, pp. 1785- 1790.

Bellamy, L., 1958, The Infra Red Spectra of Complex Molecules (2nd Ed.), J. Wiley, New York.

Boggs, T. L., 1970, Deflagration Rate, Surface Structure, and Subsurface Profile of Self-Deflagrating Single Crystals of Ammonium Perchlorate, AIAA J. Vol. 8, No. 5, pp. 867-873.

Boggs, T. L., 1970, Personal Communication, Aug. 1970.

Boggs, T. L. and Krauetle, K. J., 1969, Role of the Scanning Electron Microscope in the Study of Solid Rocket Propellant Combustion, I. Ammonium Perchlorate Decomposition and Deflagration, Comb. Sci. and Tech., Vol. 1, pp. 75-93.

Cantrell, R. H., 1963, Gas-Film Effects in the Linear Pyrolysis of Solids, AIAA J., Vol. 1, No. 7, pp. 1544-1550.

Carslaw, H. S. and Jaeger, J. C., 1959, Conduction of Heat in Solids (2nd Ed.), Oxford University Press, London.

Chaiken, R. F., 1970, Personal Communication, June 1970.

Chaiken, R. F., Andersen, W. H., Barsh, M. K., Mishuck, E., Moe, G., and Schultz, R. D., 1960, Kinetics of the Surface Degradation of Polymethylmethacrylate, J. Chem. Phys., Vol 32, No. 1, pp. 141-146.

Chaiken, R. F., Sibbett, D. J., Sutherland, J. E., Van de Mark, D. K., and Wheeler, A., 1962, Rate of Sublimation of Ammonium Halides, J. Chem. Phys., Vol. 37, No. 10, pp. 2311-2318.

Coates, R. L., 1965, Linear Pyrolysis Rate Measurements of Propellant Constituents, AIAA J., Vol. 3, No. 7, pp. 1257-1261.

Coates, R. L., 1965, Final Report: Research on Combustion of Solid Propellants, Lockheed Propulsion Co., Redlands, Cal., Report No. LPC-641-F.

Comfort, E. H., O'Connor, T. J., and Cass, L. A., 1966, Heat Transfer Resulting from the Normal Impingement of a Turbulent High Temperature Jet on an Infinitely Large Flat Plate, Proceedings of the 1966 Heat Transfer and Fluid Mechanics Institute (Ed's: Saad, M. A. and Miller, J. A.), Stanford Univ. Press, Stanford, Cal.

Cordes, H. F., 1969, An Estimate of the Melting Point of Ammonium Perchlorate, AIAA J., Vol. 7, No. 6, pp. 1193-1195.

Ditchburn, R. W., 1963, Light (2nd ed.), Interscience, New York.

Fay, J. A. and Riddell, F. R., 1958, Theory of Stagnation Point Heat Transfer in Dissociated Air, J. Aero. Sci., Vol. 25, No. 2, pp. 73-121.

France, W. L. and Williams, D., 1964, Total Absorptance of Ammonia in the Infrared, Air Force Cambridge Research Lab., Bedford, Mass., AFCRL-64-652.

Friedman, R., 1967, Personal Communication, Jan. 1967.

Gardon, R. and Akfirat, J. C., 1965, The Role of Turbulence in Determining the Heat-Transfer Characteristics of Impinging Jets, Int. J. Ht. Mass Transf., Vol, 8, No. , pp. 1261-1272.

Gardon, R. and Cabonpue, J., 1962, Heat Transfer Between a Flat Plate and Jets of Air Impinging on It, International Developments in Heat Transfer, A.S.M.E., New York, pp. 454-460.

Goulden, C. H., 1952, Methods of Statistical Analysis (2nd ed.), J. Wiley, New York.

Guinet, M., 1965, Vitesse linéaire de pyrolyse du perchlorate d'ammonium en écoulement unidimensionnel, Recherche Aerospatiale, No. 109, pp. 41-49.

Guirao, C. and Williams, F. A., 1969, Models for the Sublimation of Ammonium Perchlorate, Paper No. 69-22, Western States Section/The Combustion Inst. 1969-Spring Meeting, China Lake, Cal.

Hall, A. R. and Pearson, G. S., 1967, Ammonium Perchlorate: A Review of Its Role in Composite Propellant Combustion, Rocket Propulsion Establishment, Westcott, England, Tech. Report No. 67/1.

Hansel, J. G., 1964, Studies of the Linear Pyrolysis of Thermoplastics in Chemically Reactive Environments, Sc.D. thesis, Dept. of Mech. Eng. Stevens Inst. of Tech.

Hansel, J. G. and McAlevy, R. F., III, 1966, Energetics and Chemical Kinetics of Poylstyrene Surface Degradation in Inert and Chemically

Reactive Environments, AIAA J., Vol. 4, No. 5, pp. 841-848.

Hertzberg, M., 1970, The Free-Laminar and Laser-Induced Combustion of Ammonium Perchlorate, Comb. Sci. and Tech., Vol. 1, pp. 449-460.

Howe, J. T. and Mersman, W. A., 1959, Solutions of the Laminar Compressible Boundary-Layer Equations with Transpiration Which are Applicable to the Stagnation Regions of Axisymmetric Blunt Bodies, National Aeronautics and Space Administration, Washington, NASA TN D-12.

Inami, S. H., Rosser, W. A., and Wise, H., 1963, Dissociation Pressure of Ammonium Perchlorate, J. Phys. Chem., Vol. 67, No. 5, pp. 1077-1079.

Jacobs, P. W. M. and Powling, 1969, The Role of Sublimation in the Combustion of Ammonium Perchlorate Propellants, Comb. and Flame, Vol. 13, No. 1, pp. 71-81.

Jacobs, P. W. M. and Russell-Jones, A., 1968, Sublimation of Ammonium Perchlorate, J. Phys. Chem., Vol. 72, No.1, pp. 202-207.

Jacobs, P. W. M. and Whitehead, H. M., 1969, Decomposition and Combustion of Ammonium Perchlorate, Chem. Rev., Vol. 69, No. 4, pp.551-590.

Johnson, W. E. and Nachbar, W., 1962, Deflagration Limits in the Steady Linear Burning of a Monopropellant with Application to Ammonium Perchlorate, Eighth Symp. (Int.) on Combustion, Williams and Wilkins, Baltimore, pp. 678-689.

Keenan, J. H. and Kaye, J., 1948, Gas Tables, J. Wiley, New York.

Kennard, E. H., 1938, Kinetic Theory of Gases, McGraw-Hill, New York p. 69.

Krauetle, K. J., 1969, The Study of the Thermal Decomposition of Ammonium Perchlorate at High Temperatures, Expanded Abstracts from 6th ICRPG Combustion Conference, Vol. I, Chemical Propulsion Information Agency, Silver Spring, Md., pp. 477-485.

Laidler, K. J., 1950, Chemical Kinetics, McGraw-Hill, New York, Chapt. 6.

Leclerc, A., 1950, Deviation d'un jet liquide par une plaque normal à son axe, Houille Blanche, pp. 816-821.

Levy, J. B. and Friedman, R., 1962, Further Studies of Pure Ammonium Perchlorate Deflagration, Eighth Symp. (Int.) on Combustion, Williams and Wilkins, Baltimore, pp. 663-677.

Lewis B. and von Elbe, G., 1961, Combustion, Flames, and Explosions of Gases (2nd ed.), Academic Press, New York, pp.310-323.

Libby, P. A. and Sepri, P., 1968, Stagnation Point Flow with Complex Composition, Phys. Fluids, Vol. 11, No. 8, pp. 1621-1627.

Lieberherr, J-F., 1967, Personal Communication (Sept. 1967).

Lieberherr, J-F., 1969, High Temperature Pyrolysis of Ammonium Perch-

lorate, Twelfth Symp. (Int.) on Combustion, Combustion Inst., Pittsburgh, Pa., pp. 533-541.

McAdams, W. H., 1954, Heat Transmission (3rd ed.), McGraw-Hill, New York.

McAlevy, R. F., III and Hansel, J. G., 1965, Linear Pyrolysis of Thermoplastics in Chemically Reactive Environments, AIAA J., Vol. 3, No. 2, pp. 244-249.

McAlevy, R. F., III, Lee, S. Y., and Smith, W. H., 1968, Linear Pyrolysis of Polymethylmethacrylate during Combustion, AIAA J., Vol. 6, pp. 1137-1142.

Madorsky, S. L., 1964, Thermal Degradation of Organic Polymers, Interscience, New York.

Nachbar, W. and Williams, F. A., 1963, On the Analysis of Linear Pyrolysis Experiments, Ninth Symp. (Int.) on Combustion, Academic Press, New York, pp. 345-357.

Pearson, G. S., 1966, Perchloric Acid, Advances in Inorganic Chemistry and Radiochemistry, Vol. 8 (Ed's.: Emeléus, H. J. and Sharpe, A. G.), Academic Press, New York, pp. 178-224.

Pearson, G. S., 1967, Comment, Eleventh Symp. (Int.) on Combustion, Combustion Inst., Pittsburgh, Pa., p. 456.

Penner, S. S., 1948, Melting and Evaporation as Rate Processes, J.

Phys. Chem., Vol. 52, No's. 6 & 7, pp. 949-954, 1262-1263.

Pittman, C. U., Jr., 1966, The Mechanism of Decomposition of Ammonium Perchlorate: A Review, U. S. Army Missile Command, Redstone Arsenal, Alabama, Report No. RK-TR-66-13.

Powling, J., 1967, Experiments Relating to the Combustion of Ammonium Perchlorate-Based Propellants, Eleventh Symp. (Int.) on Combustion, Combustion Inst., Pittsburgh, Pa., pp. 447-456.

Powling, J. and Smith, W. A. W., 1962, Measurement of the Burning Surface Temperatures of Propellant Compositions by Infra-Red Emission, Comb. and Flame, Vol. 6, No. 3, pp. 173-181.

Powling, J. and Smith, W. A. W., 1963, The Surface Temperature of Burning Ammonium Perchlorate, Comb. and Flame, Vol. 7, No. 3, pp. 269-275.

Powling, J. and Smith, W. A. W., 1965, The Surface Temperature of Ammonium Perchlorate Burning at Elevated Pressures, Tenth Symp. (Int.) on Combustion, Combustion Inst., Pittsburgh, Pa., pp. 1373-1380.

Rabinovitch, B., 1965, Regression Rates and the Kinetics of Polymer Degradation, Tenth Symp. (Int.) on Combustion, Combustion Inst., Pittsburgh, Pa., pp. 1395-1404.

Reshotko, E. and Cohen, C. B., 1955, Heat Transfer at the Forward Stagnation Point of Blunt Bodies, National Advisory Committee for Aeronautics, Washington, NACA Tech. Note 3513.

Russell-Jones, A., 1964, The Thermal Decomposition of Some Inorganic Perchlorates, Ph.D. Thesis, Chemistry Dept., Imperial College of Sci. and Tech., London.

Scala, S. M. and Gilbert, L. M., 1965, Sublimation of Graphite at Hypersonic Speeds, AIAA J., Vol. 3, No. 9, pp. 1635-1644.

Schlichting, H., 1960, Boundary Layer Theory (4th ed.) McGraw-Hill, New York.

Shrader, H., 1961, Trocknung Feuchter Oberflächen Mittels Warmluft-strahlen; Strömungsvorgänge und Stoffübertragung, VDI, Forschungsheft No. 484.

Schultz, R. D. and Dekker, A. O., 1955, Absolute Thermal Decomposition Rates of Solids. Part II. The Vacuum Sublimation Rates of Molecular Crystals, J. Chem. Phys., Vol. 23, No. 11, pp. 2133-2138.

Schultz, R. D. and Dekker, A. O., 1956, The Effect of Physical Adsorption on the Absolute Decomposition Rates of Crystalline Ammonium Chloride and Cupric Sulfate Trihydrate, J. Phys. Chem., Vol. 60, No. 8, pp. 1095-1100.

Schultz, R. D. and Dekker, A. O., 1957, Transition-State Theory of the Linear Rate of Decomposition of Ammonium Perchlorate, Sixth Symp. (Int.) on Combustion, Reinhold, New York, pp. 618-626.

Schumaker, J. C., 1960, Perchlorates, Their Properties, Manufacture and Uses (Am. Chem. Soc. Monograph No.146), Reinhold, New York, p.93.

Somorjai, G. A., 1968, Mechanism of Sublimation, Science, Vol. 162, No. 3855, pp. 755-760.

Spalding, D. B., 1961, The Prediction of Mass Transfer Rates When Equilibrium Does Not Prevail at the Phase Interface, Int. J. Ht. Mass Transf., Vol. 2, No. 4, pp. 283-313.

Spalding, D. B., 1963, Convective Mass Transfer, McGraw-Hill, New York.

Sparrow, E. M. and Cess, R. D., 1966, Radiation Heat Transfer, Brooks/Cole, Belmont, Cal.

Steinz, J. A. and Summerfield, M., 1969, Low Pressure Burning of Composite Solid Propellants, Propellants Manufacture, Hazards, and Testing, American Chemical Soc., Washington, pp. 244-295.

Waesche, R. H. W., 1967, Research Investigation of the Decomposition of Composite Solid Propellants, Final Report July 5, 1966-July 4, 1967, United Aircraft Research Laboratories, E. Hartford, Conn., Report No. F910476-12.

Walz, D. R., 1964, Spot Cooling and Heating of Surfaces with High Velocity Impinging Air Jets, Dept. of Mech. Eng., Stanford Univ., Stanford, Cal., Tech. Report No. 61 (AD 607727).

Wilfong, R. E., Penner, S. S., and Daniels, F., 1950, An Hypothesis for Propellant Burning, J. Phys. Chem., Vol. 54, No. 6, pp. 863-872.

Williams, F. A., 1965, Combustion Theory, Addison-Wesley, Reading, Mass.

APPENDIX A - AP SPECIMENS

A. 1 Pressing of AP Powders

All in-house pressings of AP specimens used in this preogram were carried out using an existing three-piece hardened-steel die shown in Figure A-1. Two techniques were used for pressing AP powder into monolithic samples: "dry-pressing" and "wet-pressing".

For dry-pressing, the "bottom insert" of the die was inserted in the die block cavity and approximately 11 gm of AP powder which had been dried over silica gel for several days was spread evenly over the insert within the cavity. This charge was selected in order to yield a specimen approximately 1/4" thick. The "top insert" was then inserted, and the top insert was pressed into the die block, compressing the AP, by using a hydraulically-pumped 10-ton laboratory press (Fred. S. Carver, Model C). After the ram force (pressure) of the press once reached its maximum, this force of 10 tons (20,000 psig) was held for several minutes using the hydraulic pump to sustain maximum pressure. The specimen was removed by relieving the pump pressure, inserting several spacers under each side of the die block, and pressing the bottom insert, specimen, and top insert out of the cavity. During this removal process, the pressure applied to the top insert (because of friction in the die) did not exceed 3000 to 4000 psig. Thus, the effective ram pressure (excluding friction) was on the order of 16,000 psig. Accounting for the crossectional areas of the presspiston (2.41" in^2) and of the die cavity (1.25 in^2), the pressure

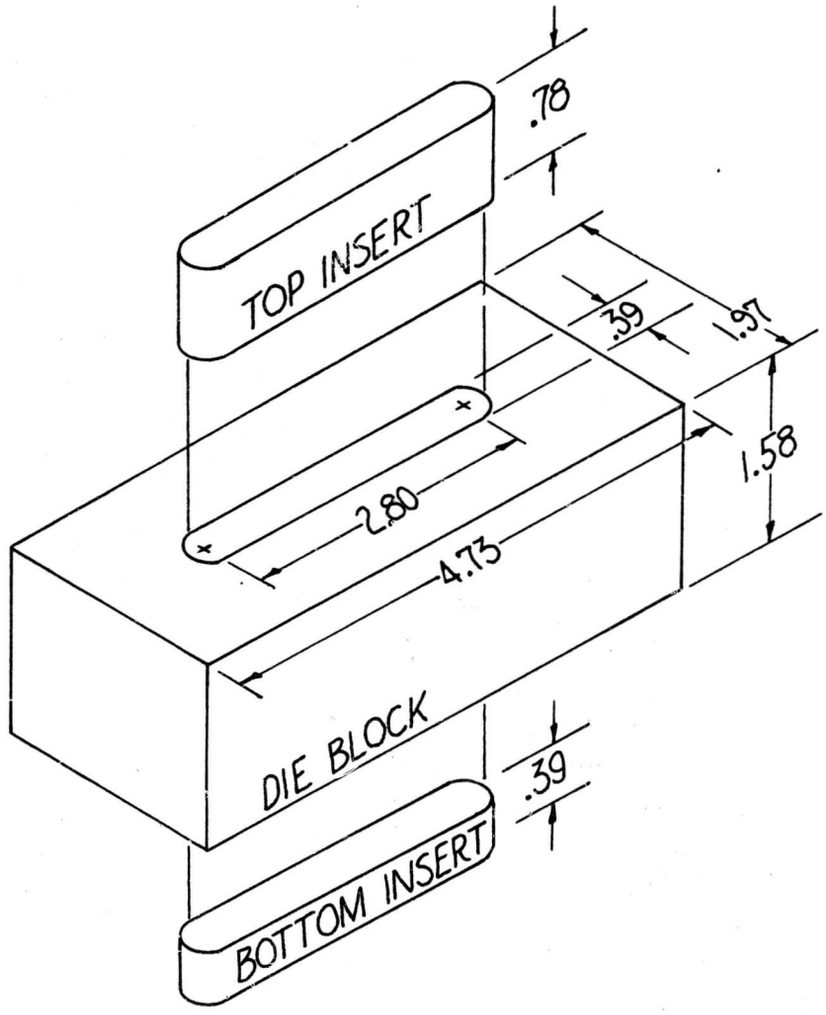

FIGURE A-~~1~~2: DIE FOR PRESSING AP

applied to the sample may be calculated at about 30,000 psig. After pressing, the specimen was "bonded" by exposing it (in a closed dessicator) to a water-saturated air environment at 72°F for several days. The specimen was then dried and stored for at least several days over silica gel before pyrolysis testing.

For wet-pressing, the same procedure was followed except that the AP charged into the die had previously been exposed, as a powder, to a water-saturated air environment for several days. During pressing, water was forced out of the die, and after pressing, the specimen was immediately dried over silica gel.

A.2 Forming of Cylindrical Specimens

Since cylindrical specimens of nominal 0.156" -diameter were desired for testing, the pressed specimens (ca. 0.40" x 2.8" x 0.25") required further forming.

To obtain specimens more nearly the final dimensions desired, the pressings were band-sawed at low cutting speed (e.g., 100 ft/min) typically into four pieces measuring approximately 0.18" x 1.4" x 0.25". Some care had to be exercised during sawing owing to sample fragility, but recovery of sawed samples was high (e.g., 90%). After sawing, the ends of the smaller pieces were squared approximately using a coarse emery cloth mounted on a flat metal back-up plate.

Cylindrical specimens were formed by mounting the rectangular-crossection samples of AP between two lengths of 5/32" drill rod which served as templates. The specimen was then "sanded" with an axial

motion using emery cloth which had been rubber-cemented onto a flat metal back-up plate (see Figure A-2). The ends of the drill rod were fitted with 1/16"-thick soft rubber to provide compliance with the ends of the AP specimen. The abrasive pad used was wide enough so as always to be guided by the pieces of drill rod; this allowed, with axial motion of the pad, abrasion of the AP until it was finally of a crossection approximately matching that of the drill rod. At the beginning of forming, an "extra-coarse" emery cloth was used, and in the final stages, "fine" emery cloth was applied. By checking approach to final dimensions with a micrometer and by removing the last 0.010" in diameter slowly and carefully, the diameter of the final specimen could be held close enough to its nominal value to assure a smooth but not a loose fit within the 5/32"-diameter, reamed hole in the pyrolysis-test sample-holder. Table A-1 shows the results of diametral measurements (twelve per specimen) taken 45^{o} apart at each end and at the center of two specimens after forming; lengths and weights are also indicated. These data are typical of the best that was achieved using the apparatus and method described.

A.3 Density of Test Specimens

The density of the two specimens with measurements appearing in Table A-1 was determined. The purpose of this check was to ascertain whether the densities of the pressed specimens were close to the single-crystal density (1.95 gm/cc, Jacobs and Whitehead (1969)) of AP. This should be the case in order to assure specimens comparable with

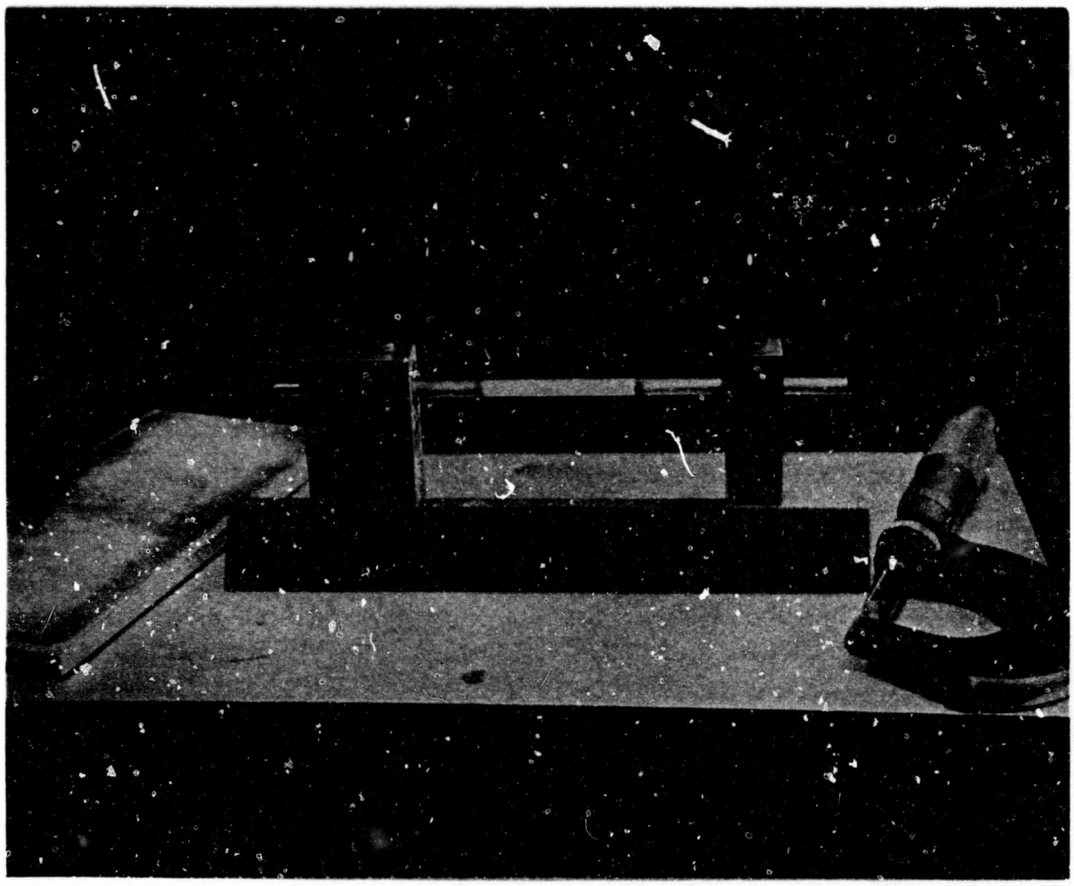

FIGURE A-2: PHOTOGRAPH OF JIG FOR FORMING AP SPECIMENS

SPECIMEN NO. 1			SPECIMEN NO. 2	
MEASURED DIAMETER* (inches)	MEASURED LENGTH (inches)		MEASURED DIAMETER* (inches)	MEASURED LENGTH (inches)
0.1553	1.420		0.1559	1.409
0.1541	1.419		0.1546	1.410
0.1534	1.420		0.1540	1.411
0.1551	1.418		0.1559	1.410
0.1547			0.1558	
0.1540			0.1556	
0.1536			0.1562	
0.1531			0.1560	
0.1530			0.1543	
0.1530			0.1559	
0.1525			0.1556	
0.1521			0.1556	

* Diameters measured at 3 axial stations for 4 transverse directions

TABLE A-1 - DIMENSIONS OF TEST SPECIMENS USED TO DETERMINE DENSITY OF AP PRESSINGS

those of others (Levy and Friedman (1962), Guinet (1965)), to determine if the specimens were reasonable free of voids which could lead to anomalous behavior, and to allow linear regression rates and mass consumption rates to be related conveniently. The specimen lengths were measured and the arithmetic mean of several measurements was used, along with the arithmetic mean of the diameter data of Table A-1 and the weight of each specimen, to determine densities. The results were:

Specimen 1: $\rho = 1.88$ gm/cc

Specimen 2: $\rho = 1.88$ gm/cc

The excellent agreement and the proximity to single-crystal density were deemed sufficient to justify straightforward comparison with results from others' high-density specimens and to allow negligible error in assuming specimen density equal to that of single-crystals.

A.4 Comparison Specimens

In the preliminary stages of the present investigation, comparisons were made between the pyrolysis of specimens dry-pressed (in-house) and specimens provided by other laboratories which have tested the pyrolysis and deflagration of pressed AP*. The comparison specimens had the specifications shown in Table A-2.

---

*Samples provided graciously by M. Barrère, O.N.E.R.A. (Office National des Etudes et de Recherches Aerospatiale, Chatillon, France) and by R. Friedman, A.R.C. (Atlantic Research Corp., Alexandria, Va.)

SOURCE	Original AP Powder Size (μm)	Pressing Pressure (psig)	Pressing Size (mm)	Reported Density (gm/cc)
A.R.C.	51, 15	100,000[2]	4 x 4 x 38	1.89 - 1.91
O.N.E.R.A.	N.A.[1]	44,000	5 x 5 x 15	1.935

[1] Probably approx. 50 μm

[2] or higher (e.g., 136,000 psig)

TABLE A-2 - SPECIFICATIONS OF AP COMPARISON SPECIMENS

At the beginning of the present study, the specimens from O.N.E.R.A. and A.R.C. were, after being formed into cylinders, compared for similar regression rates at each of two different gas-rocket operating conditions. The results were as follows:

Run No.	Specimen Source	Gas-Rocket Supply Pressures		Pyrolysis Rate
		CH_4 (psig)	37%O_2-N_2 (psig)	(cm/sec)
I-1	A.R.C.	90	112	0.00955
I-1	"	"	"	0.0104
II-1	O.N.E.R.A.	"	"	0.0113
II-2	"	"	"	0.0123

II-3	O.N.E.R.A.	90	112	0.0993
II-4	"	"	"	0.0103
I-3	A.R.C.	110	112	0.0203
I-4	"	"	"	0.0237
II-5	O.N.E.R.A.	"	"	0.0210
II-6	"	"	"	0.0215

TABLE A-3 - REGRESSION RATES OF COMPARISON SPECIMENS

On this basis, the specimens from two different sources were judged to be indistinguishable, within the reproducibility of the experiments.

Later in the present program, specimens from O.N.E.R.A. were pyrolyzed with coincident rate and surface temperature measurements. These results were found, within the scatter of collected pyrolysis data, to be indistinguishable from the results obtained from in-house pressings by either the "wet" or "dry-pressing" techniques. At least to the extent of these various tests, then, specimen source and pressing method were not found to influence the pyrolysis characteristics measured.

APPENDIX B - GAS-ROCKET OPERATING CHARACTERISTICS

B.1 General Description of Gas Rocket

The gas-rocket motor used was essentially that described earlier by Hansel (1964). Ignition and (reactant) gas supply systems were modified slightly for convenience, and the "Vycor" (fused silica) exhaust duct used by Hansel was replaced by one of stainless steel. The system is shown schematically in Figure B-1.

Nozzle and exhaust-duct details are as follows:

Minimum diameter (in nozzle end-plate):	0.080"*
Nozzle end-plate thickness:	.38"
Exhaust-duct inside diameter:	.20"
" " outside " :	.38"
" " length :	1.75"

The rocket motor was operated with CH_4 (C.P. grade) as fuel gas and with 37% O_2 - N_2 (extra dry grade) as oxidizer gas. For the most part, the fuel supply pressure was varied between 60 and 170 psig with the oxidizer supply pressure held constant at 112 psig. These values for the control variables (pressures and compositions) are close to those used extensively in Hansel's earlier operation of the same motor.

Owing to the rather large supplier's tolerance allowed for the oxidizer gas mixtures (±5% in O_2 fraction), rocket operating conditions were noticeably variable for given reactant supply pressures.

*with 0.13" x 45° countersink at downstream end

Gas Rocket Assembly

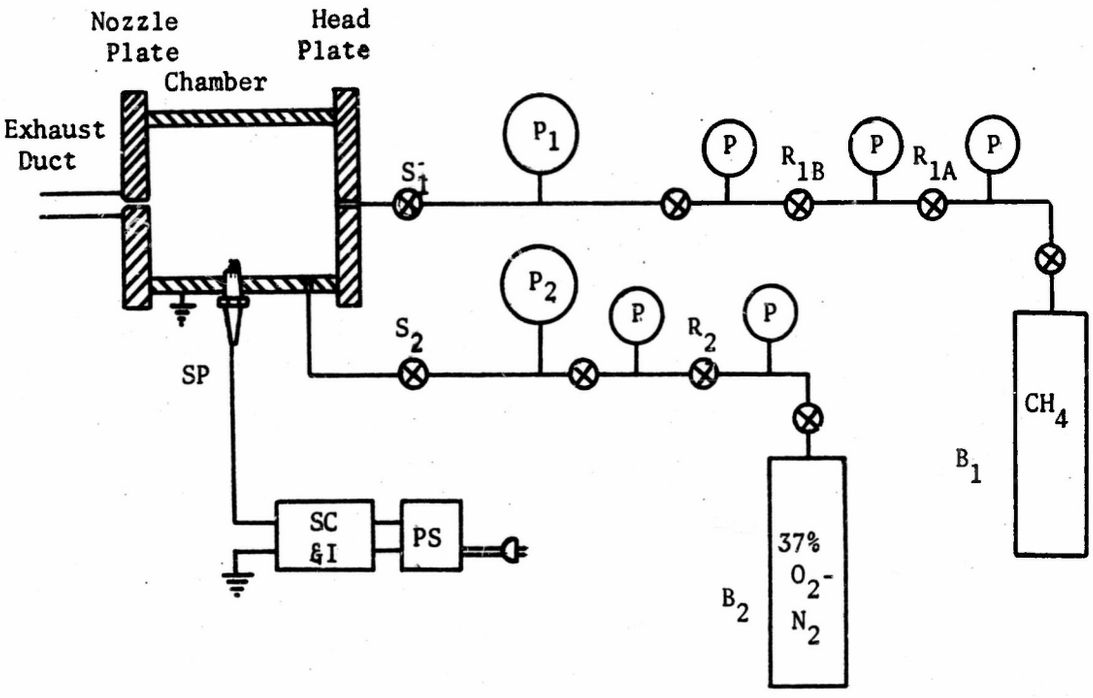

Ignition System

SP = Spark Plug

SC&I = Spark Coil & Interrupter

PS = 0-16 vdc, 0-10 a. power supply

Gas Supply System*

B_i = Gas Bottle

⊗ = Valve: R_i = regulating valve

S_i = solenoid valve

(P) = Pressure Gauges (uncalibrated)

(P_i) = Precision Pressure Gauges (calibrated)

* Subscripts: "1" CH_4 supply

"2" 37% O_2-N_2 supply

FIGURE B-1: SCHEMATIC OF GAS-ROCKET SYSTEM

Reproducibility of pyrolysis-test data was generally excellent, however, and the relationships observed between pyrolysis rate and surface temperature were highly consistent. A given pyrolysis rate and surface temperature were, however, observed for different gas supply pressures from different oxidizer bottles. This suggested appreciable composition variation as a cause of the observed irreproducibility in gas-rocket operating conditons.

A rough check of the influence of oxidizer-gas composition showed the following:

(i) Judging from the influence of mixture ratio on natural gas* -air flames (Lewis and von Elbe (1961), p. 632) a change in adiabatic flame temperature of about 170°C may be accomplished by a 1% change in volume fraction of fuel gas (for slightly lean flames, 6 1/2 to 8 1/2% natural gas),

(ii) A 1% change in fuel-gas fraction is approximately equivalent to a 2% change in O_2 fraction; thus, a ±2% change in O_2 composition might, reasonably, lead to a change of about ±170°C in exhaust jet temperature,

(iii) A change of ±170°C in exhaust jet temperature corresponds to approximately ±10 psig change in fuel supply pressure, and

(iv) Therefore, the fuel supply pressure resulting in a given pyrolysis rate and surface temperature might

*85% methane.

vary by ±10 psig or more depending on oxidizer gas composition.

While such variations are inconvenient, they were judged not to be prohibitive, particularly in consideration of the great increase in operating expense (ca. 10 times) which would have been required by substantially tighter tolerances on oxidizer-gas composition.

It is noteworthy that errors in resetting gas supply pressures (notably that of CH_4) can also contribute to lack of reproducibility via mixture ratio changes, even with oxidizer drawn from a single gas bottle of fixed composition. To minimize such an inconvenience, two precision pressure gauges (P_1, P_2, Fig. B-1) were calibrated to within ±0.25 psi and used for setting supply pressures during most data runs (Run series 16 through 21).

B.2 Exhaust-Jet Temperature Measurements

Exhaust-jet temperatures were measured with various gas-rocket supply pressures, and these data are shown in Figure B-2. The measurements were taken using a 0.005"-diameter, butt-welded thermocouple (Pt-6%R/Pt-30%R) with the junction on centerline and with the axis of the leads traversing the exhaust jet approximately 2mm douwnstream of the exhaust duct exit-plane. The thermocouple was supported by an insulated ring of 2.25"-inside-diameter which was coaxial with the jet axis. A high input-impedance (2 MΩ) potentiometric recorder* (Esterline-Angus Model T171B) was attached directly to the two

*Calibrated before use with a potentiometer.

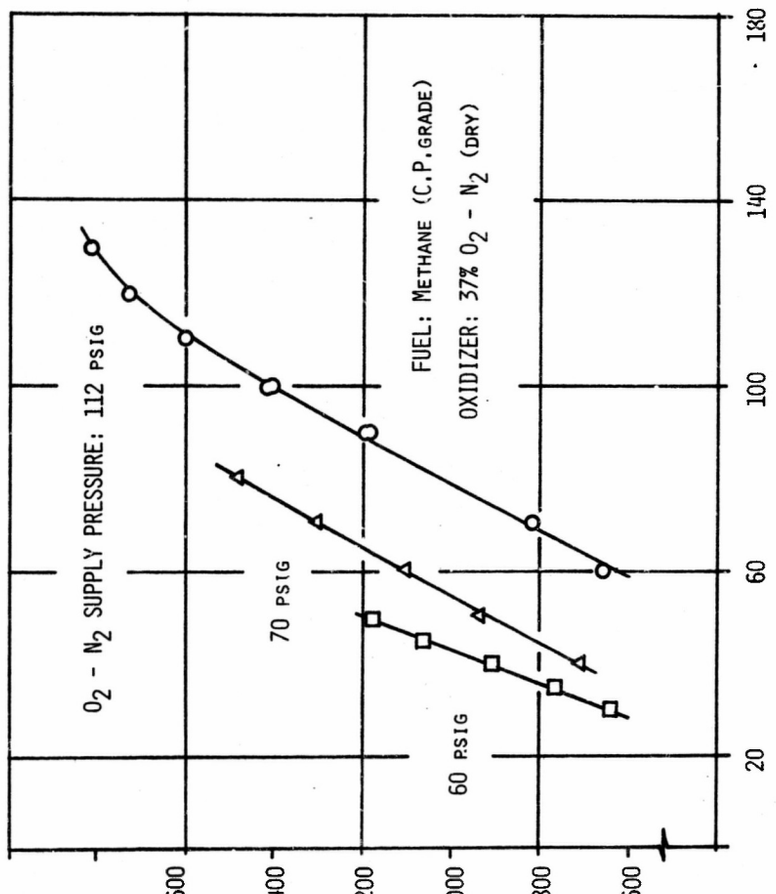

FIGURE B-2: MEASURED GAS-ROCKET EXHAUST-JET TEMPERATURES vs. FUEL SUPPLY PRESSURES

thermocouple leads which were of about 6" length; room temperature served as a suitable reference-junction temperature because of the low sensitivity of the thermocouple at low temperatures.

Radiation corrections for this thermocouple were estimated for a typical operating condition by considering convective heating and radiative loss for a cylinder oriented normal to the flow under the following conditions:

jet velocity:	1700 ft/sec	(measured)
" temperature:	$3372^{\circ}R.$	"
cylinder diameter:	0.005"	"
gas:	air	"
thermocouple emmittance:	0.18	(extreme, Pt-wire)

with the following results (McAdams, (1954); Fig.10.7, p. 259)

Reynolds No. = 300

Nusselt No. = 9 $\Rightarrow$ film coeffic. = 750 $BTU/hr\text{-}ft^2\text{-}^{\circ}F$

Assuming, overall for the transverse cylinder:

$$\gamma \Delta T = \epsilon \sigma T_{jet}^4,$$

then, for the above values, $\Delta T = T_{jet} - T_{thermocouple} = 50^{\circ}F = 28^{\circ}C$ which is sufficiently small (for example, for estimating surface heating rates of AP specimens because of jet impingement).

Conduction lead-losses were also estimated (for the above-cited conditions) by considering each lead to the thermocouple as a cylindrical fin undergoing convective heating with the same film coefficient as calculated above and with its base (at the jet radius) at ambient

temperature. The "standard" solution of this fin problem (Carslaw & Jaeger (1959), p. 140) indicated that, even for the conservative model used, the tip of the "fin" was negligibly different (ca. 0.1°C) from the jet temperature.

On these bases, the measured temperatures were expected to be accurate within approximately 30°C.

Time variations of jet temperatures were obvious during thermocouple tests. First, temperatures indicated by the thermocouple-recorder system were observed to fluctuate substantially, more at higher fuel-supply pressures (e.g., ±20°C at 1400°C) than at lower ones (e.g. ±5°C at 850°C). These fluctuations are possibly a result of large-scale turbulence generated in the gas rocket chamber due to the flame or due to impingement of the oxidizer and fuel injector jets. Second, a moderately long heat-up time of the rocket was evidenced by jet temperatures which required 1 to 2 minutes to stabilize (within 1% of final asymptotic values). This lag in achieving a steady-state is probably a consequence of the heat capacity of the rocket-motor chamber, nozzle end-plate, and exhaust duct. The reported values of jet temperature are the asymptotic values either as observed or as estimated via short extrapolations.

B.3 Exhaust-Jet Velocity Measurements

Jet velocities were measured with various gas-rocket supply pressures; data and corresponding results (including Reynolds Numbers and Mach Numbers) are shown in Table B-1. For calculation of these

GAS-ROCKET FUEL SUPPLY PRESSURE (psig)	T_{jet}[a] (^{o}K)	P_L (psig)	V_{jet} (ft/sec)	M_{jet}[b] (-)	Re_{jet}[c] (-)	a (sec^{-1})
FLAT-PLATE PROBE						
160	1973	3.84	1785	0.635	7500	1.2×10^5
130	1883	3.66	1700	0.64	7800	1.2×10^5
110	1673	3.40	1550	0.60	8500	1.1×10^5
90	1273	3.00	1270	0.56	10,700	$8.6 \times .0^4$
70	903	2.40[d]	950	0.49	14,700	6.4×10^4
50	523	1.64[d]	600	0.40	21,300	4.1×10^4
PITOT-TUBE PROBE						
110	1673	3.76	NOTES:			
90	1273	3.16	(a) From measured values (Fig. B-2) (with short extrapolations)			
70	903	2.48				
50	523	1.68	(b) Based on acoustic veloc. of air at T_{jet}; Keenan and Kaye (1948), Table 2			
			(c) Viscosity data for T_j from Keenan and Kaye (1948), Table 2			
			(d) 0.050"-dia. pressure tap			

TABLE B-1 - GAS-ROCKET EXHAUST-JET VELOCITIES (V_{jet}), MACH NO'S. (M_{jet}), REYNOLDS NO'S (Re_{jet}), AND STAGNATION-POINT VELOCITY-GRADIENTS (a) FOR TYPICAL OPERATING CONDITIONS (OXIDIZER SUPPLY PRESSURE = 112 psig)

quantities, ambiant pressure was assumed to be 14.7 psia., and the jet density was assumed to be that of air as a perfect gas at the measured jet temperatures (see Fig. B-1).

Some measurements of jet velocity were made using a Pitot tube which had been aligned (visually) with the axis of the jet. The open end of the probe was located in the exit plane of the gas-rocket exhaust duct. The probe tip was a 1" length of 18-gauge stainless steel hypodermic tubing, and this had been silver-soldered into the tapered, plugged end of an ell of stainless steel tubing of 1/4"-outside-diameter. Pressures were measured by connecting the Pitot tube to a 0-10 psid variable-reluctance, diaphragm pressure-transducer (Pace, Model P7D) equipped with a demodulator-indicator (Pace, Model CD25). The output jack (0-10 vdc.) of the latter was connected to a potentiometric strip-chart recorder. The zero and sensitivity adjustments of the transducer system were set before use by applying a 10-psig pressure simultaneously to the system and to a 0-30 psig Bourdon-tube pressure gauge which had been checked earlier (±0.1 psi) against a dead-weight tester (at 10 psig increments). Transducer read-out for this step was via a 5-digit digital voltmeter (Hewlett-Packard Model 3440A with Model 3444A Plug-In). Pitot-tube measurements were limited to fuel-supply pressures below 130 psig since the high temperatures at higher fuel-supply pressures led to melting of the stainless-steel tip.

In order to extend velocity measurements beyond the high-temperature limit of the Pitot-tube technique, "flat-plate" measurements were

taken. This was done by impinging the gas-rocket exhaust-jet onto a flat plate of 2"-diameter, centered on and aligned with the jet axis. The plane of the plate was 3/8" downstream of the exhaust-duct exit-plane, the same axial station as that of the AP sample-holder during pyrolysis testing. As a pressure tap, a hole of 0.016"-diameter was located at the center of the circular plate. This was done by drilling a hole (No. 78 drill) of this nominal diameter in the plugged end of a length of stainless-steel tubing of 1/4" diameter; the plugged end of the tubing was then inserted in a close-fitting hole at the center of the plate. The plate was faced with 1/8"-thick asbestos mill-board facing mounted on a similar plate of 1/8" stainless steel which had been silver-soldered to the 1/4" tubing. The probe end was finished flush with the surface of the asbestos plate. The transducer-indicator system described above was used for pressure measurements with this apparatus.

As is indicated in Table B-1, the Pitot-tube measurements were consistently higher (at high fuel supply pressures) then those from the centerline of the flat-plate. The differences dynamic pressures did not exceed 10% (implying 5% disagreement in jet velocity) and were deemed acceptable.

B.4 Pressure Distributions on Flat Plate

Pressure distributions across the impinging jet were also measured by moving the flat plate (described immediately above) transversely across the jet while measuring the pressure at the center tap of the

plate. Results are shown in Figure B-3 in which the measured gauge pressures are shown non-dimensionalized with respect to the centerline gauge pressure.

Of particular note is the fitted curve, a parabola, as suggested by the potential-flow solution for normal impingement of an infinite incompressible stream onto a flat plate, i.e.;

$$u = a x$$

Apparently, the moderate subsonic Mach numbers involved allow this incompressible potential flow-field to describe the jet flow well at least for the modest range of jet velocities measured. This observation is apparently the first such for impinging axisymmetric jets with high ratios of jet temperature to ambient temperature ($1.7 \leq T_{jet}/T_{ambient} \leq 6.6$).*

Using Bernoulli's equation to describe the flow external to the boundary layer, the data of Fig. B-3 may be used to determine a value for the parameter "a" which is the external-flow velocity-gradient; "a" is the sole parameter describing a corresponding potential flow (Schlichting (1960), p. 82):

$$u = a x$$

$$v = -2ay$$

where x is measured outward from the jet centerline in the radial direction and y is measured positive outward from the plate surface.

The values of "a" determined from the measured pressure distri-

---

*Comfort et al. (1966) have measured pressure distributions for an arc jet impinging on a flat plate, but the reported pressure distributions are not notably parabolic.

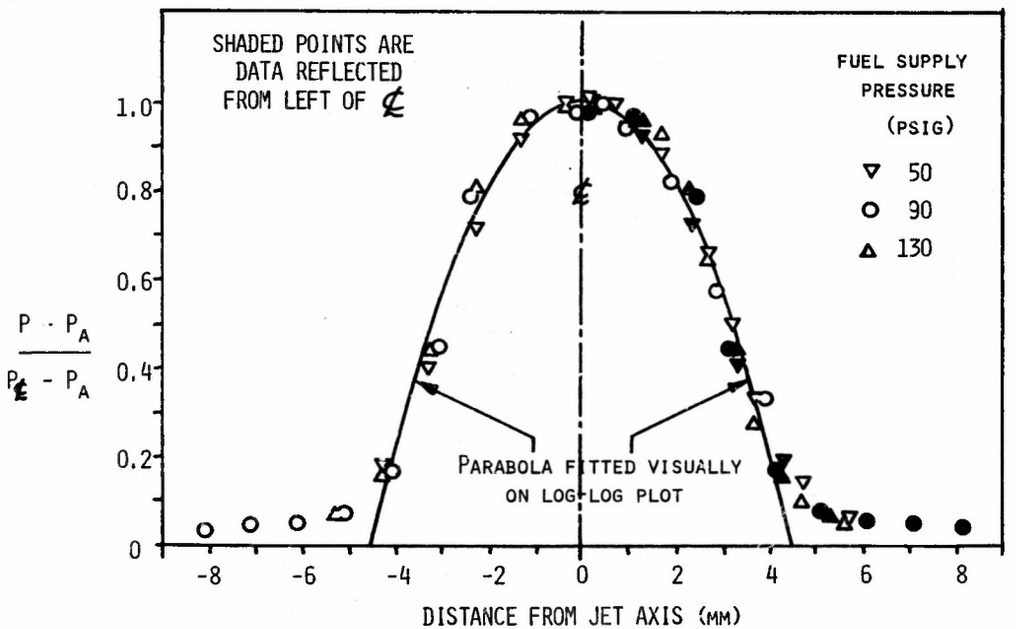

FIGURE B-3: RADIAL STATIC-PRESSURE DISTRIBUTIONS ON FLAT PLATE NORMAL TO IMPINGING-JET AXIS

butions at the plate (see Table B-1) are higher by a constant factor (4.25) than those (a') which might be predicted by attempting to match a semi-infinite, stagnation-point flow to the jet configuration. This could be done by assuming that the jet is simply a portion of a semi-infinite potential flow-field characterized by the normal velocity, V_{jet}, at the axial station "y_N", the distance from the plate to the jet-nozzle exit plane, i.e.:

$$a' = \frac{V_{jet}}{2y_N}$$

The observed difference between a and a' is especially pertinent because calculations of stagnation-point heat-transfer show a direct dependence on the external-flow velocity gradient, a (e.g., heat flux proportional to $(a)^{1/2}$; Reshotko and Cohen (1955)).

It should further be noted that the characteristic dimension of the region on the flat plate within which the potential-flow description appears useful is essentially invariant (ca. 8 mm diameter) and is approximately twice the size of the AP specimens (ca. 3.9 mm) tested with the gas-rocket; this characteristic dimension is apparently fixed by the diameter of the exhaust duct directing the impinging flow at the flat plate (4.8 mm diameter) but is substantially larger than the duct diameter.

APPENDIX C - EXPERIMENTAL AND ANALYTICAL CHECKS ON VALIDITY OF THE EXPERIMENTAL TECHNIQUE

C.1 Spectral Scans During Pyrolysis

Figures C-1 and C-2 show spectral scans of emission from pyrolyzing AP surfaces and from the blackbody comparison source at several temperatures. The scans were made under conditions for which gas-phase emission from the gas-rocket exhaust is negligible (see below). Both scans show some irregularities as a consequence of sample break-up during pyrolysis and /or loss of synchronization between surface regression and sample advance.

Figure C-1 shows the result of a fast scan which covered a bandwidth of approximately 2 μm (in the neighborhood of 3.05 μm) in approximately 150 sec. CO_2 and H_2O absorption bands are labelled in Fig. C-1 and are apparent both in the pyrolysis-test results and, to a lesser extent (due to CO_2 and H_2O in the atmosphere), in the blackbody spectral scan. The 3.05 μm wavelength used radiometrically is labelled. From the results of the lower-speed scan (scan time ca. 100 sec.), it appears (Fig. C-2) that emission from the surface is nearly gray in the neighborhood of 3.05 μm and that this particular test indicated a brightness temperature of about 513°C.

C.2 Wavelength Dependence of r vs. T_c Data

Table J-3 of Appendix J shows r vs. T_B data labelled as to which of two different wavelengths were used radiometrically to

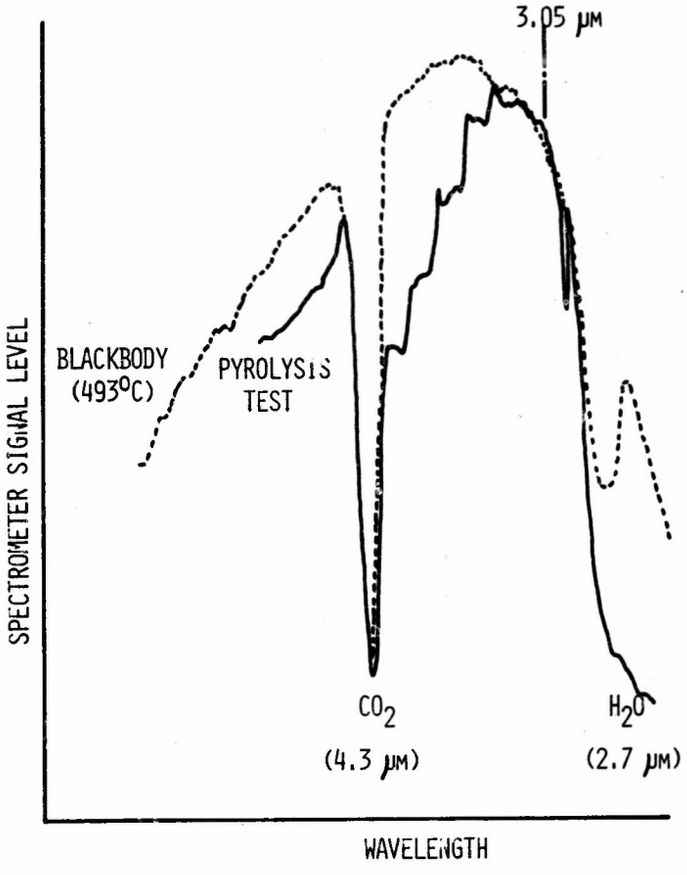

FIGURE C-1: SPECTRAL SCAN (FAST) OF SURFACE EMISSION DURING PYROLYSIS

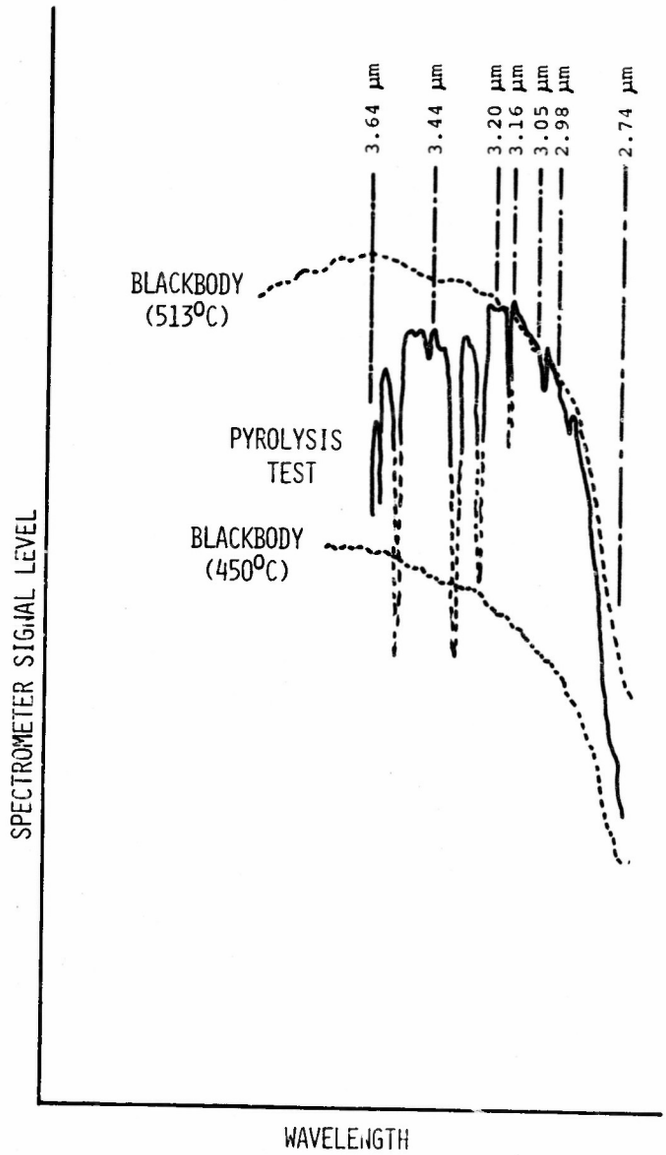

FIGURE C-2: SPECTRAL SCAN (SLOW) OF SURFACE EMISSION DURING PYROLYSIS

measure T_S. Within the scatter of the data, no difference is apparent. This suggests, as did the spectral scans during pyrolysis, that the AP surface is essentially gray in the region of the 3.05 μm absorption band for the NH_4^+ ion. This would not have appeared to be the case if subsurface temperature gradients and volumetric emission in the surface layer were significant. Therefore, these data support the assumption that subsurface gradients are negligible on the scale of the small photon mean-free-path in the solid near the pyrolyzing surface.*

C.3 Gas-Phase Emission Effects

C.3a Emission from the Convective-Heating Jet

Spectral scans were taken by aligning the optic axis of the spectrometer transverse to the gas-rocket exhaust jet immediately downstream (2 to 4 mm) of its exit from the exhaust duct**. Figure C-3 shows the results of scans at two different operating conditions, one corresponding to the highest regression rates and temperatures measured, the other corresponding to an intermediate rate and temperature. The strong, 4.3-μm absorption-emission band of CO_2 and the

*Based on AP transmissivity data of Powling (1967), the photon mean-free-path at 3.05 μm is on the order of 0.1 μm, easily small enough to justify the data observed.

**These preliminary measurements from early in the test program were taken under slightly different gas-rocket operating conditions and with a different exhaust duct (made of fused silica) than were used in later pyrolysis testing.

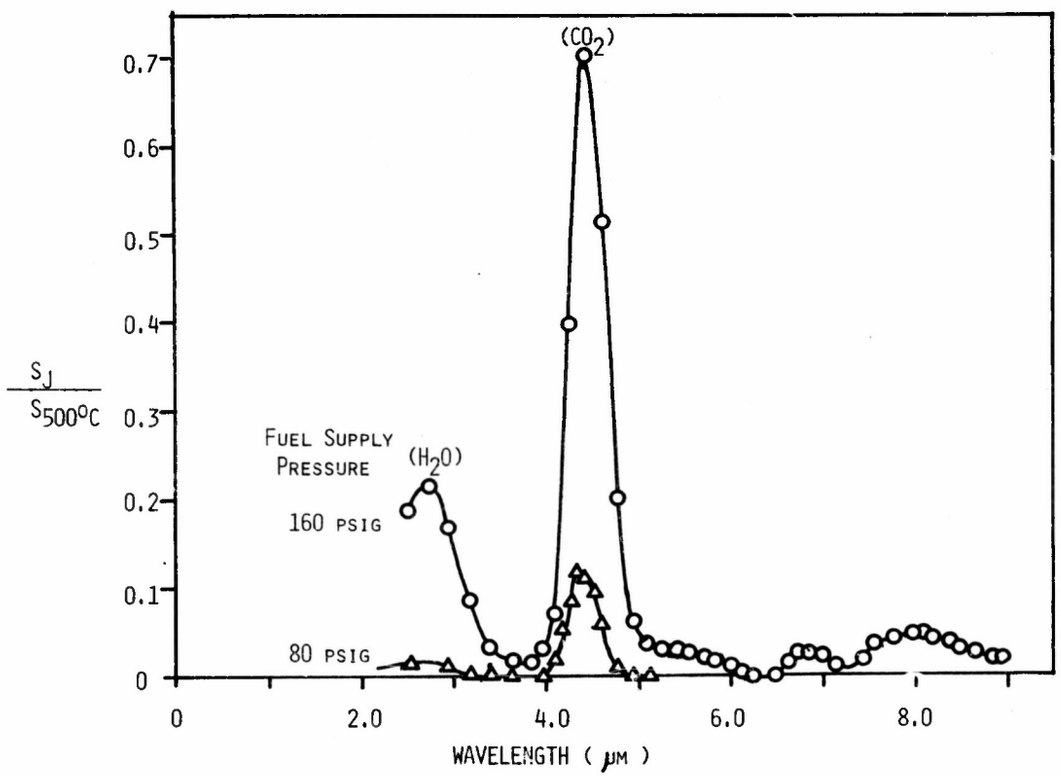

FIGURE C-3: SPECTRAL SCANS OF GAS-ROCKET EXHAUST-JET EMISSION (S_J) RELATIVE TO EMISSION FROM 500°C BLACKBODY (S_{500^oC})

2.7-μm band of H_2O are very obvious, and it is clear that the latter poses some threat to radiometric surface temperature measurements at 3.05 μm.

Table C-1 shows quantitatively the results of measuring gas-rocket exhaust emission at 3.05 μm with the same spectral slit-width as was used in surface radiometry. The "corrections" indicated in Table C-1 are based on measured emission from an optical path length arising from sighting transversely through the gas-rocket exhaust jet close to the exhaust-duct exit-plane. Corrections to measured brightness temperatures should be made, on the other hand, based on the optical path length through the impinging jet as the spectrometer views the pyrolyzing surface obliquely. The relative sizes of these two path lengths depend on the flow fields resulting from the impinging jet; the path lengths contributing to emission measured during pyrolysis testing might reasonably be either larger or smaller than those for a transverse view through the jet.

To estimate actual path lengths through the impinging jet, the shape of a (axisymmetric) potential-flow streamline passing through the outside diameter of the exhaust duct was calculated, based on values of the stagnation-point velocity gradient ("a") as described in Appendix B. With this streamline considered as a jet boundary, the physical path length through the jet to the pyrolyzing surface (with an oblique, 65° line-of-sight) was about 5 mm. This length is essentially the same as the diameter of the jet viewed in collecting the data of Table C-1. Therefore, it can be expected that "correct-

GAS-ROCKET SUPPLY PRESSURE		ΔT_B
OXIDIZER (psig)	FUEL (psig)	(^oC)
112	160	6
112	140	4
112	120	2
112	90	1

TABLE C-1 - ESTIMATED CORRECTIONS (ΔT_B) TO MEASURED SURFACE BRIGHTNESS-TEMPERATURE DUE TO GAS-ROCKET EXHAUST-JET EMISSION

ions" to measured brightness temperatures might be approximately as shown in Table C-1 (or less because of peripheral mixing and cooling of the jet). These corrections are so small as to be neglected for the present purposes; their influences on apparent activation energy, for example, are within the uncertainty in this value due to data scatter.

A brief attempt was made, unsuccessfully, to fuel the gas rocket with CO rather than CH_4. The aim was to minimize possible influence on radiometric measurements by radiation from the 2.7 μm H_2O band. Ignition could not be accomplished with dry CO and the normal 37% $O_2 - N_2$ oxidizer gas. After provision for bubbling CO through H_2O before injection into the gas rocket, ignition was achieved but the maximum jet temperatures which resulted were too low (ca. 600°C) to drive pyrolysis at usefully high rates. It appeared that suitably high jet temperatures would only be likely with pure O_2 as an oxidizer. Use of pure O_2 was judged impractical since it would have required complete replacement of the oxidizer supply system (which was known to be contaminated slightly by oil* and therefore, to be hazardous with pure O_2). The marginal value of highly-refined measurements (see Section V.A) also contributed to this decision.

---

* arising from use of a hydraulic dead-weight tester for pressure-gauge calibration.

C.3b Emission From Pyrolysis Products

C.3b (1) Experimental Checks

As a rough check on the extent of emission from pyrolysis products, a comparative measurement was made. With an intermediate regression rate (ca. 0.02 cm/sec), a portion of the sample-holder plate immediately adjacent to the pyrolyzing AP sample was imaged on the spectrometer slit and the transient emission from the plate (and, possibly, from pyrolysis products) was recorded following gas-rocket ignition; similarly, after ignition with the same gas-rocket conditions, emission from the plate only was measured (with a steel rod in place of the AP specimen). Both records included signal levels corresponding to the brightness temperature of the AP surface under the same gas-rocket conditions. Within the reproducibility of the indicated brightness temperatures (ca. 5°C), the two records were indistinguishable, showing virtually identical brightness temperatures at that time after ignition when the test without AP showed a brightness temperature equal to that at the pyrolyzing AP surface. Several repetitions gave the same result. This result was taken to indicate that substantial emission from pyrolysis products over the pyrolyzing surface was unlikely. However, it could not be conclusively established that the indistinguishibility of the records was not due to simultaneous and counter-balancing quenching by a somewhat cooler plate and emission from the gas-phase.

C.3b (2) Analytical Checks

C.3b (2a) Model Allowing for AP Decomposition Flame

For the sake of an analytical estimate of gas-phase emission from pyrolysis products, a model was considered which accounted for the possible decomposition flame of the AP pyrolysis products, NH_3 and $HClO_4$. As a conservative estimate covering this situation, a flame sheet was considered to lie above the pyrolyzing surface. This flame sheet was presumed to have the temperature of the (adiabatic) AP decomposition flame and to follow a linear temperature profile above the surface. The flame stand-off distance was conservatively estimated on an energetics basis from the surface heat-flux required to sustain sublimation at a rate equal to the deflagration rate of pure AP at 1 atm. This rate (0.015 cm/sec) can be estimated by extrapolating high-pressure deflagration-rate data for AP (Friedman et al.) or by stabilizing self-deflagration of AP at 1 atm. by the addition of an external heat-flux (Levy and Friedman (1962), Hertzberg (1970)). This rate is included in the midrange of the pyrolysis rates measured during this study.

Estimating the flame standoff distance, L_F, from the heat flux at the surface for the AP flame (presumably stabilized by a relatively small external heat flux)*:

$$L_F = \frac{\bar{k}(T_F - T_s)}{\dot{q}_s} = \frac{\bar{k}(T_F - T_s)}{r\rho\left[\bar{c}(T_s - T_0) + \Delta h^\circ_{sub}\right]}$$

* Pure AP has not been observed to burn without fuel at less than about 20 atm ambient pressure unless modest external heat fluxes are provided (Levy and Friedman (1962), Hertzberg (1970)).

For $\bar{k}$ = 2×10^{-4} cal/cm-sec-^{o}K (air at 750^{o}K; Keenan & Kaye (1948))

T_F = 1250^{o}K. (Hall and Pearson (1967), Table 21)

r = 0.015 cm/sec

T_S = 750^{o}K. (measured, this study, at r = 0.015 cm/sec)

ρ = 1.95 gm/cm^3 (Jacobs and Whitehead (1969))

$\bar{c}$ = 0.3 cal/gm-^{o}K.

T_0 = 300^{o}K.

Δh^{o}_{sub} = 495 cal/gm = 58.2 kcal/mole (Hall and Pearson (1967), p. 10)

Then: L_F = 70 μm

Considering one-dimensional, monochromatic radiant transport of specific intensity, J_λ , in an optically-thin, non-scattering medium of homogeneous gas with monochromatic absorption coefficient, κ_λ, (see Fig. C-4):

$$\cos\theta \frac{dJ_\lambda}{dy} = \kappa_\lambda B_\lambda[T(y)]$$

$$J_{\lambda,L_F} = \frac{1}{\cos\theta}\int_0^{L_F} \kappa_\lambda B_\lambda[T(y)]\, dy \qquad \text{(C-1)}$$

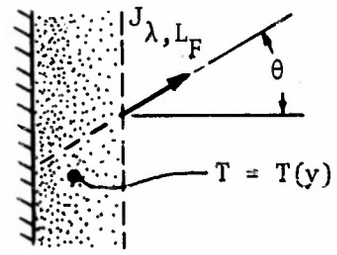

Fig. C-4 - EMITTING GAS-LAYER NEAR PYROLYZING SURFACE

Assuming that, for fixed optics, a spectrometer viewing at the angle θ responds proportionally to J_{λ,L_F}, the fractional error in spectrometer reading arising from gas-phase emission above a surface of emittance ϵ and surface temperature T_S is:

$$\delta_\lambda = \frac{J_{\lambda,L_F}}{\epsilon B_\lambda(T_S)} = \frac{1}{\cos\theta} \frac{\int_0^{L_F} \kappa_\lambda B_\lambda[T(y)]\, dy}{B_\lambda(T_S)} \qquad (C\text{-}2)$$

Since temperature is considered to vary in the field of interest, κ_λ also varies spatially. This variation is a consequence of variations both in absorption band structure with temperature and in concentration of emitting species with temperature (density). Data regarding details in band structure variation are not available for NH_3, the species of interest here, and band structure at ambient temperature will be assumed to apply; density variations are accounted for <u>via</u> the perfect gas law and the partial pressure of NH_3 above the surface:

$$\kappa_\lambda = \kappa_{\lambda,ref} \frac{T_{ref}}{T} \frac{P_{NH_3}}{P_{ref}} \qquad (C\text{-}3)$$

The reference state is that for which spectral absorption data are available (France & Williams (1964)).

Substituting (C-3) into (C-2) and substituting B_λ along with the assumption of a linear temperature profile:

$$T = T_S + \frac{T_F - T_S}{L_F} y$$

Then, in terms of T as an independent variable, (C-2) becomes:

$$\mathcal{J}_\lambda = \frac{1}{\epsilon \cos\theta} \kappa_{\lambda,ref} L_F \frac{T_{ref}}{T_F - T_S} \frac{P}{P_{ref}} \int_{T_S}^{T_F} \frac{1}{T} \frac{\exp\left(\frac{C_2}{\lambda T_S}\right) - 1}{\exp\left(\frac{C_2}{\lambda T}\right) - 1} \, dT \qquad (C\text{-}4)$$

where c_2 is Planck's second radiation constant. For the range of interest (λ = 3.05 μm, $T_S = 750^\circ K \leq T \leq T_F = 1250^\circ K.$), $c_2/\lambda T >> 1$ and (C-4) may be written, in terms of :

$$t \equiv c_2/\lambda T,$$

as

$$\mathcal{J}_\lambda = \frac{1}{\epsilon \cos\theta} \kappa_{\lambda,ref} L_F \frac{T_{ref}}{T_F - T_S} \frac{P}{P_{ref}} \exp\left(\frac{C_2}{\lambda T_S}\right) \int_{\frac{C_2}{\lambda T_S}}^{\frac{C_2}{\lambda T_F}} \frac{\exp(-t)}{t} \, dt$$

or, as:

$$\mathcal{J}_\lambda = \frac{\tau}{\epsilon} \exp\left(\frac{C_2}{\lambda T_S}\right) \left\{ \left[-Ei\left(\frac{C_2}{\lambda T_S}\right) \right] - \left[-Ei\left(-\frac{C_2}{\lambda T_F}\right) \right] \right\} \qquad (C\text{-}5)$$

where $\tau \equiv \frac{\kappa_{\lambda,ref}}{\cos\theta} L_F \frac{T_{ref}}{T_F - T_S} \frac{P}{P_{ref}}$ (quasi-optical-thickness)*

and $$-Ei(-t) \equiv \int_t^\infty \frac{e^{-v}}{v} \, dv$$

is the exponential integral.

For NH_3 (France & Williams (1964) Fig. 37), $\kappa_{\lambda,ref} = .17\ cm^{-1}$ at $T_{ref} = 300^\circ K.$ and $P_{ref} = 1$ atm.** Using this value, assuming

*Of the same order as optical thickness since $T_F - T_S \cong T_S \cong T_F$ within a factor of 2.

**This value was checked within a factor of 2 for the spectrometer conditions of the present study.

$P/P_{ref} = 0.5$ *, $\theta = 65^{o}$, and substituting the previously-cited values into (C-5):

$$\tau = 0.08$$

which justifies the optically-thin assumption. Then from (C-5):

$$\eta_{\lambda} = 0.004 << 1.$$

This result justifies neglect of NH_3 emission from the gas phase. It should be noted that in all regards, excepting possibly the assumption of temperature-invariant absorption-band structure, this estimate is apparently conservative, i.e., an over-estimate of η_{λ}. Finite reaction kinetics, back-diffusion of flame products (which should be appreciable, see Appendix D and Table VI-2) and heat transfer to the flame from the external flow will all tend to decrease the optical thickness below the estimated value and, therefore, decrease η_{λ}.

C.3.b(2b) Model Neglecting Gas-Phase Reaction

In order to estimate emission from pyrolysis products which might react at a negligible rate above the pyrolyzing surface, it is necessary to estimate both temperature and concentration distributions in the flow-field above the surface and to proceed in a direction similar to that above (Section C.3.b(2a)). The practical route to such estimates is necessarily an analytical one since the high-temperature, high-velocity flow-field involved is difficult to probe experimentally on a sufficiently small scale (boundary-layer thicknesses of order 10 to 100 μm might be expected). Such an analytic attempt to estimate

* Surface composition: equimolar NH_3 and $HClO_4$.

temperature and concentration distributions is , however, tenuous since the detailed flow fields arising from impinging jets (even without surface transpiration) have apparently not been investigated.

Studies of the fluid mechanics of impinging jets have typically focussed on essentially incompressible flow-fields and on local heat-transfer coefficients (Walz (1964), Gardon and Cabonpue (1962)). Two works which were not studied (Leclerc (1950), Schrader (1961)) deal with velocity distributions (Gardon and Akfirat (1965)) and another with compressible flow with large temperature variations (Comfort et al. (1966)). The various results have pointed almost exclusively to a square-root dependence of local heat-transfer coefficients on Reynolds Number (Walz (1964)), which is a characteristic of laminar rather than turbulent flow. In addition, local maxima in heat-transfer coefficients at radial locations approximately equal to the nozzle radius of the impinging jet have suggested that transition to turbulence occurs at such a location and that laminar flow exists between that location and the stagnation point (Gardon and Akfirat (1965)). This conclusion is further supported by the disappearance of such local maxima at low jet Reynolds Number (Gardon and Akfirat (1965)). It seems likely, then, that laminar flow existed in the present study. The work reported here was in the same Reynolds Number regime as previous impinging-jet studies which evidenced laminar flow and the present work involved a sample diameter which was appreciably less than the impinging-jet diameter.

Owing to the lack of experimental or theoretical data on details

of flow fields in impinging jets, analytic predictions of temperature distributions were obtained, from classic, stagnation-point boundary-layer analysis. While semi-infinite external flow-fields rather than finite jets are involved in such an approach, this was the only viable approach to the present problem; such approaches have proved useful in correlating impinging jet data (Walz (1964)) and may be expected to be reasonably valid in the present case for which jet diameter exceeds that of the impingement region of interest.

A laminar approach to the present case is consistent with the finding that, for surface temperatures and regression rates lower than those at which "inflammation" sets in, laminar heat transfer theory is capable of predicting quite well the heat flux required from an impinging jet supporting sublimative pyrolysis (see Appendix F). Therefore, for a variety of reasons, it is reasonable and without contradiction to consider a laminar boundary-layer in attempting to estimate temperature and concentration distributions in the present case.

While a substantial body of literature is available dealing with laminar, stagnation-point boundary layers in hypersonic flow situations, the only detailed boundary-layer analysis applicable to the present subsonic case is apparently that of Howe and Mersman (1959). This work deals with temperature and velocity distributions, surface heat fluxes, etc. in homogeneous, "blown", and compressible laminar boundary-layers. A numerical solution of appropriate boundary-layer equations allows for temperature-dependent properties (viscosity, thermal conductivity, and

specific heat).

In the present investigation, low mass fractions of the pyrolysis products (NH_3, $HClO_4$) in the gas-phase were expected (see Table IV-2). Hence, Howe and Mersman's assumption of a homogeneous flow-field was considered applicable. Without detailed analysis of a multi component flow-field comparable with that of the present case, however, the limitations of Howe and Mersman's homogeneous flow-field assumption cannot readily be evaluated. The limited existing studies of such multicomponent boundary layers do, however, offer some encouragement that transpiration of heavy gases (e.g., Xe) into lighter (e.g., N_2) boundary layers do not <u>for the present purpose</u> substantially alter velocity, density, or temperature profiles (Libby and Sepri (1968)).

<u>Radiation Analysis:</u>

From (C-2), considering the entire boundary layer:

$$\mathcal{J}_\lambda \equiv \frac{J_{\lambda,L_F}}{B_\lambda(T_s)} = \frac{1}{\epsilon \cos\theta} \frac{\int_0^\infty \kappa_\lambda B_\lambda[T(y)]\, dy}{B_\lambda(T_s)} \qquad (C\text{-}7)$$

Assuming, as previously, that κ_λ depends only on the local molar concentration of emitters:

$$\kappa_\lambda = \kappa_{\lambda,ref} \frac{n}{n_{ref}} = \kappa_{\lambda,ref} \frac{x}{x_{ref}} \frac{\rho}{\rho_{ref}}$$

Then, in terms of κ_{λ,NH_3} determined from pure NH_3 at standard ("STD") temperature and pressure:

$$\kappa_\lambda = \kappa_{\lambda,NH_3}\, x_{NH_3} \frac{\rho}{\rho_{STD}}$$

$$K_\lambda = K_{\lambda,NH_3} \chi_{NH_3} \frac{P}{P_{STD}} \frac{T_{STD}}{T} \qquad (C\text{-}8)$$

Assuming similarity between temperature and mass fraction profiles and that:

$$\chi_{NH_3,E} = 0$$

then:

$$\chi_{NH_3} = \left(1 - \frac{T - T_S}{T_E - T_S}\right) \chi_{NH_3,S} \qquad (C\text{-}9)$$

Substituting (C-8), (C-7), and the definition of B_λ into (C-7):

$$\vartheta_\lambda = \frac{1}{\epsilon \cos\theta} K_{\lambda,NH_3} \frac{P}{P_{STD}} \chi_{NH_3,S} \int_0^\infty \frac{T_{STD}}{T} \left(\frac{T-T_S}{T_E-T_S}\right) \exp\left[\frac{C_2}{\lambda}\left(\frac{1}{T} - \frac{1}{T_S}\right)\right] dy$$

Then, if $\Theta \equiv (T - T_S)/(T_E - T_S)$, $K_{\lambda,NH_3,S} \equiv K_{\lambda,NH_3} \frac{P}{P_{STD}} \frac{T_{STD}}{T} \chi_{NH_3,S}$ and $\eta \equiv y/y^*$, $y^* \equiv (\mu_S/\rho_S a)^{1/2}$:

$$\vartheta_\lambda = \frac{K_{\lambda,NH_3}}{\epsilon \cos\theta} y^* \int \frac{1-\Theta}{1+\left(\frac{T_E}{T_S}-1\right)\Theta} \exp\left\{\frac{C_2}{\lambda T_S}\left(\frac{T_E}{T_S}-1\right)\Theta \Big/ \left[1+\left(\frac{T_E}{T_S}-1\right)\Theta\right]\right\} d\eta \qquad (C\text{-}10)$$

Coupling of Radiation With Flow Field:

Howe and Mersman (1959) present tabulated numerical results for the non-dimensional boundary-layer temperature profiles in wedge flows:

$$\Theta = \Theta(\eta, T_E/T_S, f_w)$$

where η is the non-dimensional distance from the wall $(y/\sqrt{\rho_w u_E / \mu_w x})$, f_w is the wall "blowing parameter" for the wedge-flow case: $f_w = - v_w/u_E (Re)^{1/2}$. The Mangler transformation provides scaling for these profiles to the axi-symmetric case, such that:

$$\Theta = \Theta\left(\sqrt{3}\,\eta,\ T_E/T_S,\ \frac{\sqrt{3}}{2}\,f_S\right)^*$$

i.e.,

$$(\eta)_{\text{axisymmetric}} = (\eta)_{\text{wedge}}/\sqrt{3}$$

$$(f_S)_{\text{axi-symmetric}} = \frac{2}{\sqrt{3}}\,(f_w)_{\text{wedge}}.$$

Howe and Mersman's results are for five temperature ratios, T_E/T_S = 0.25, 0.5, 1.0, 2.0, and 4.0 and three blowing rates, f_w = 0,-0.5,-1.0 (f_S = 0,-0.577,-1.15). For given f_S and T_E/T_S then, these results can be used to determine Θ and, therefore, to allow numerical integration of (C-10) to estimate the influence of pyrolysis product emission.

In light of the approximate nature of any estimate derivable for the present case from Howe and Mersman's approach, only a representative pyrolysis situation was selected for emission estimation; a comprehensive coverage of the complete pyrolysis regime was felt to be unwarranted.

The external-to-surface-temperature ratio, T_E/T_S, was found to be approximately two in the midrange of the pyrolysis test regime (r = 0.015 cm/sec; T_S = 472°C). f_S, the corresponding (axi-symmetric) blowing parameter, was calculated via:

$$f_s = -\frac{v_s}{u_e}\sqrt{Re} = \frac{\rho_s v_s}{\sqrt{\rho_s \mu_s a}}$$

for $Re = \dfrac{\rho_s u_E x}{\mu_s}$ and $u_E = ax$ (see Appendix B)

with: $a = 8.7 \times 10^4\ \text{sec}^{-1}$ (Table B-1, Appendix B)

*The numerical factors arise from the necessity of adapting Howe and Mersman's results for wedge flows to the axi-symmetric case of interest here.

$$\dot{m} = r\rho = 0.03 \text{ gm/cm}^2\text{-sec}$$

$$\rho = 1.95 \text{ gm/cm}^3$$

$$\mu_g = 3.5 \times 10^{-4} \text{ gm/cm-sec}$$ (air; Keenan and Kaye (1948); in recognition of low surface concentration of pyrolysis products, see Appendix D)

The calculated value of f_S is -0.22 which is in the range of values for which Howe and Mersman present tabular values of θ. Therefore, the integral in (C-10) was evaluated[+] for $T_E/T_S = 2.0$ and $f_S = 0, -0.577$, and -1.15 and the value corresponding to $f_S = -0.22$ was found by interpolation:

$$\frac{\epsilon \cos\theta}{K_{\lambda,NH_3,S}\, y^*} \mathcal{J}_\lambda = 0.25$$

Then, for:

$$\epsilon = 1.0$$

$$\theta = 65^\circ,$$

$$y^* = 1.5 \times 10^{-3} \text{ cm.}$$

and:

$$K_{\lambda,NH_3,S} = K_{\lambda,NH_3}\, \chi_{NH_3,S}\, \frac{P}{P_{STD}}\, \frac{T_{STD}}{T}$$

with:

$$\chi_{NH_3,S} = 1$$

$$K_{\lambda,NH_3} = 0.17 \text{ cm}^{-1}$$ at 1 atm, 300°K (France and Williams (1964))

$$P = 1.2 \text{ atm}$$ (mean of distribution on surface, see Appendix B, Table B-1)

+In the present nomenclature, Howe and Mersman's results are for $\Theta(\sqrt{3}\eta, T_E/T_S, \sqrt{3}/2\, f_S)$ and integration is with respect to η. Therefore, the values cited are for the integral with respect to $\sqrt{3}\eta$, divided by $\sqrt{3}$.

$$T_S = 745^{\circ}K \qquad \text{(measured)}$$

$$\mathcal{J}_\lambda = o\left[10^{-4}\right] \ll 1$$

The implication is that unreacting NH_3 as a pyrolysis product will not significantly contribute radiometrically to emission from the surface. Even for the conservative assumption that χ_{NH_3} has its maximum possible value (corresponding to equimolar NH_3 and $HClO_4$ at the surface), $\mathcal{J}_\lambda$ is negligibly small.

In the process of the above calculations, predicted thermal boundary-layer thicknesses were also calculated in order to gain physical insight into the boundary-layer scale in the situations of interest. From Howe and Mersman's results, for $T_E/T_S = 2.0$:

f_w *	$(\eta)_{wedge}$ $(\Theta = 0.95)$*	$y(\Theta = 0.95)$** (cm)
0	4.0	3.5×10^{-3}
-0.5	4.7	4.1×10^{-3}
-1.0	6.0	5.2×10^{-3}

*wedge-flow parameters of Howe and Mersman

**$(y)_{axi\text{-}symmetric} = \eta\, y^* = ((\eta)_{wedge} / \sqrt{3}\ )\, y^*$

TABLE C-2 - BOUNDARY-LAYER THICKNESSES VIA HOWE AND MERSMAN (1959)

APPENDIX D - PARTIAL-PRESSURES OF PYROLYZATE AT THE SURFACE AND CORRESPONDING VACUUM SUBLIMATION RATES

Estimation of gas-phase compositions occurring during AP pyrolysis seems to be practical only if gas-phase reactions are neglected. If these reactions cannot be neglected, partial-pressure estimates involve detailed consideration of reaction kinetics, and what reactions are likely to be involved is presently uncertain. The kinetics of the appropriate reactions are even more uncertain.

If gas-phase (and heterogeneous reactions) are neglected, the approach of Spalding (1963) to convective mass transfer is viable in the case of convective heating during pyrolysis. Assuming that all mass transfer coefficients and the heat transfer coefficient are equal, that the gas mixture is ideal and its specific heat uniform, and that the gas state at the surface is uniform, then the surface mass flux may be expressed in terms of a conductance and a driving force (Spalding (1961)):

$$\dot{m} = g B \tag{D-1}$$

The driving force, B, may be expressed, based on the above assumptions, as

$$B = \frac{\Pi_E - \Pi_g}{\Pi_s - \Pi_T} \tag{D-2}$$

where Π is any conserved property, e.g., enthalpy or mass fraction. Considering Π as gas enthalpy (h), g may be expressed from Eq. (D-1) and Eq. (D-2) as: $g = \dot{m} \frac{h_s - h_T}{h_E - h_s}$

or, with the assumption of uniform specific heat, as:

$$q = \dot{m}\,\frac{h_S - h_T}{c(T_E - T_S)}$$

However, $h_S - h_T = q/\dot{m} = c(T_S - T_o) + \Delta h^o_{sub}$, such that:

$$q = \dot{m}\,\frac{(T_E - T_o + \Delta h^o_{sub}/\bar{c})}{T_E - T_S}\left(\frac{\bar{c}}{c}\right) \qquad \text{(D-3)}$$

Also, considering m_i as a conserved property (in an unreactive flow field):

$$q = \frac{\dot{m}_i}{B} = \frac{\dot{m}_i}{\dfrac{m_{i,E} - m_{i,S}}{m_{i,S} - m_{i,T}}} \qquad \text{(D-4)}$$

Assuming further, that the transferred substance is effectively a single species, "i" (AP pyrolyzate), then $m_{i,T} = 1$. Assuming further that $m_{i,E} = 0$, then, equating Eq's. (D-3) and (D-4) yields:

$$m_{i,S} = \frac{1}{1 + \dfrac{T_S - T_o + \Delta h^o_{sub}/\bar{c}}{T_E - T_S}\left(\dfrac{\bar{c}}{c}\right)} \qquad \text{(D-5)}$$

Eq.(D-5) may be expressed in terms of $P_{i,S}$, the partial pressure of species "i" at the surface, via:

$$P_{i,S} = P - \sum_{j \neq i} P_{j,S}$$

$$P_{j,S} = \rho_{j,S}\, R T_S / M_j$$

$$\rho_s = \sum_j \rho_{j,s}$$

$$\bar{M}_J = \sum_{j \neq i} M_j \frac{n_j}{\sum_{j \neq i} n_j}$$

as:

$$\frac{P_{i,s}}{P} = \frac{1}{\frac{M_i}{\bar{M}_J} \frac{T_s - T_o + \Delta h^\circ_{sub}/\bar{c}}{T_E - T_s} + 1} \qquad (D\text{-}5)$$

The maximum, vacuum pyrolysis rate of a subliming material may be related to that rate observed under a non-zero partial-pressure of vapor by the relation (see Eq.(I-5)):

$$r(T_s) = r_{vac}(T_s) \left[1 - P_i / P_{i,eq}(T_s) \right] \qquad (D\text{-}6)$$

Therefore, the vacuum sublimation rate of AP may be deduced from rates measured under non-vacuum conditions by combining Eq.(D-5) and Eq. (D-6) as:

$$r_{vac}(T_s) = \frac{r(T_s)}{1 - \frac{\frac{r(T_s)}{P}}{P_{i,eq}(T_s)\left[\frac{M_i}{\bar{M}_J} \frac{T_s - T_o + \Delta h^\circ_{sub}/\bar{c}}{T_E - T_s} + 1\right]}} \qquad (D\text{-}7)$$

Extrapolations of low-temperature vapor-pressure data (Inami et al. (1963)), along with measured values of T_E and P and with estimated values of $\bar{M}_J$ and c, are sufficient for estimating r_{vac} from convective heating pyrolysis data (r vs. T_S).

APPENDIX E - STATISTICAL ANALYSIS OF PYROLYSIS DATA

E.1 LEAST-SQUARES LINEAR REGRESSIONS

Both the data obtained during this investigation and the published data of others were analyzed to determine kinetic parameters (apparent activation energies, E_S , and pre-exponential factors, A,) by least-squares linear regression. The usual Arrhenius form:

$$r = A \exp(-E_S/RT_S)$$

was transformed to the linear form:

$$Y = a + bX \qquad Y = \ln r$$

$$a = \ln A$$

$$X = 10^3/T_S,$$

and the usual least-squares regression of Y on X was performed. The original range of X $(10^3/T_S)$ for each data "point" was accounted for by considering as X-values the arithmetic means of the maximum and minimum values of $10^3/T_S$ measured for each pyrolysis test. The resulting values for E_S and A are reported in Tables II-1 and IV-1 of the text.

In addition, the data of this investigation only were fitted by least-squares regressions allowing for other typical functional (Arrhenius) forms:

$$r = A_{(\frac{1}{2})} (T_S)^{1/2} \exp(-E_S/RT_S)$$

and:

$$r = A_{(1)} T_S \exp(-E_S/RT_S)$$

This was accomplished by transformations $Y_{\frac{1}{2}} = \ln\left[r/(T_S)^{1/2} \right]$ and

$Y_1 = \ln [r/T_S]$, respectively, followed by the usual least-squares regressions of Y on X ($X = 10^3/T_S$). These results are also reported in Table IV-1.

As was expected, the introduction of pre-exponential powers of T_S had little effect on the results. Graphically, for example, there is no significant difference between the numerical values of the three different functionalities used; for example, the three fitted lines appear as the same line on Fig. IV-1. Parametrically, the pre-exponential factors involving T_S decrease the least-squares regression coefficients, E_S/R, only slightly as the power of T_S in the pre-exponential increases. As can be noted in Table IV-1, the resulting decreases in E_S are too small (< 1 kcal/mole) to be kinetically significant.

Confidence limits on the values of E_S determined from the various least-squares regressions were calculated by using the Student-t test (Goulden (1952), p.107). 90% confidence limits on the regression coefficients were transformed into limits on E_S itself. These confidence limits are also indicated in Table IV-1.

E.2 DISCONTINUITY IN THE PYROLYSIS DATA

A plot of the r *vs.* T_S data in Arrhenius form suggested the possibility of a small discontinuity in the observed trend at about $10^3/T_S = 1.37$ ($T_S = 460^\circ C$). This possibility was tested statistically by calculating least-squares regressions for sub-sets of the data ($\ln r$ *vs.* $10^3/T_S$). One subset consisted of the 9 data points for

$1.487 \leq 10^3/T_S \leq 1.446$ ($^oK^{-1} \times 10^3$), and successive data subsets (based on this subset) included, one-by-one, additional data points down to $10^3/T_S = 1.296$. For each of this first series of subsets, a least-squares linear regression was performed, and for each, a standard error of estimate was calculated. A similar procedure was used at the other end of the pyrolysis-data range in T_S. To a subset composed of the 8 data points for $1.227 \leq 10^3/T_S \leq 1.296$, individual data points for $1.296 \leq 10^3/T_S \leq 1.389$ were successively added, creating a second series of subsets. For each of these subsets a least-squares regression yielded a standard error of estimate. All the standard errors of estimate calculated for both series of subsets are plotted in Fig. E-1 along with an indication of the standard error of estimate for the whole data set (38 points) in the range $1.25 \leq 10^3/T_S \leq 1.475$.

The standard error of estimate for the successive consideration of the data subsets including points at increasing values of $10^3/T_S$ shows a sudden increase in the standard error of estimate in the neighborhood of $10^3/T_S = 1.37$ (see Fig. E-1). This was taken as an indication of a discontinuity in the Arrhenius plot of the data. As the discontinuity is crossed (in considering successively more and more data points), the additional points considered (which lie at $10^3/T_S > 1.37$) are manifest as a sudden increase in scatter about the regression line and hence, as a sudden increase in the calculated standard error of estimate for each successive regression*.

*The absence of such an abrupt change upon considering, successively, data at decreasing values of $10^3/T_S$ is apparently a consequence of the larger number of data involved in this process. As the discontinuity

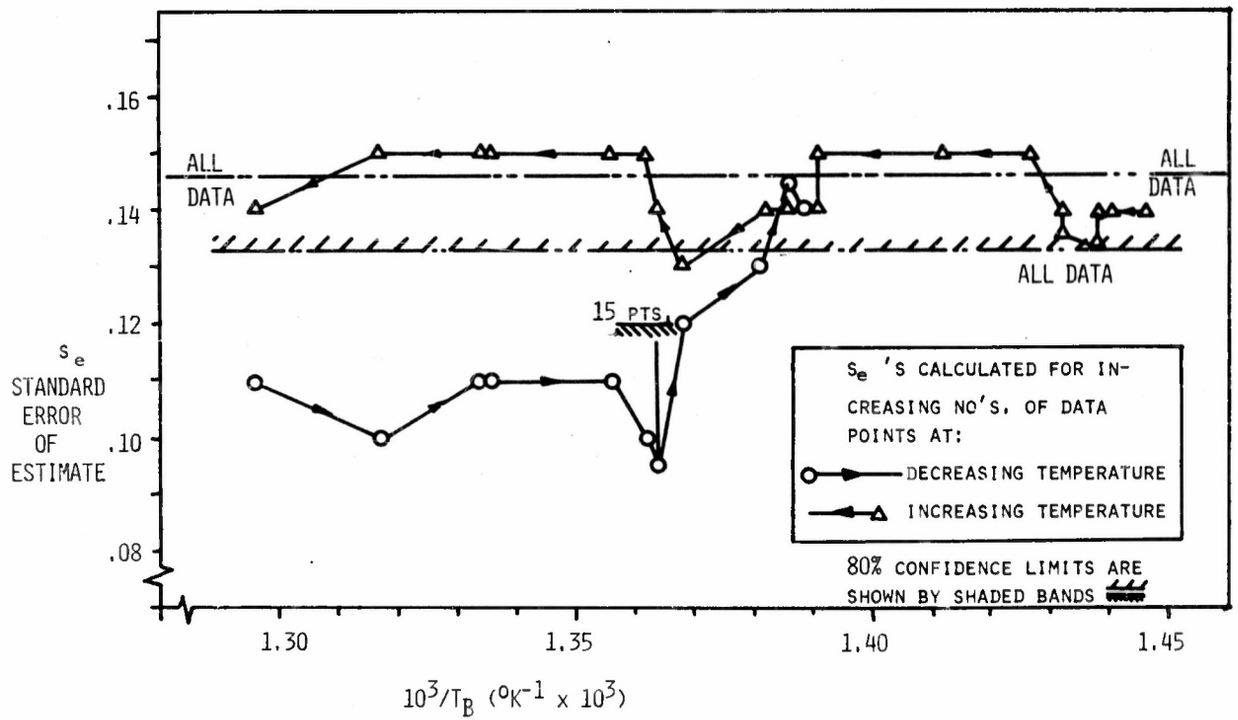

FIGURE E-1: STANDARD ERRORS OF ESTIMATE (S_e) IN $Ln\, r$ FOR SUBSETS OF DATA WITH SUCCESSIVELY INCREASING (AND DECREASING) MAXIMUM (AND MINIMUM) SURFACE (BRIGHTNESS) TEMPERATURES (WITH ONE-SIDED CONFIDENCE LIMITS)

Confidence limits on this hypothesis of a discontinuity may be calculated. These were obtained by considering the standard error of estimates for all the data points as one set and those at $10^3/T_S \leq 1.364$ as another. From these standard errors, corresponding standard deviations and confidence limits (one-sided) were calculated based on the χ^2-test. The confidence limits were then established, by trial and error, for the hypothesis that the two sets of data were exclusive. This confidence limit for the exclusiveness of the two data sets was determined to be about 85%. This fact strongly supports the hypothesis of a discontinuity in the data at $10^3/T_S = 1.36$ to 1.37 ($^oK^{-1} \times 10^3$).

In fact, the possibility of a discontinuity is enhanced when it is realized that strictly the "standard error of estimated y", s_{Ye} (Goulden (1952),p.108), ought to be considered rather than the standard error of estimate, s_e. For the data points considered here, s_{Ye} is approximately 50% smaller than s_e since:

$$s_{Y,e} = s_e \sqrt{\frac{1}{N} + \frac{(X-\bar{X})^2}{(N-1)\,s_X^2}}$$

Standard deviations based on s_{Ye}, rather than s_e, are, therefore, also approximately 50% smaller. Hence, the confidence level of the exclusiveness of the two sets of data is appreciably higher than the 85% value cited above. This aspect of the analysis enhances even farther the hypothesis of a discontinuity in the data. New, higher

---

is crossed in this direction (toward decreased $10^3/T_S$), each additional data point considered has less opportunity to perturb noticeably the previously determined standard error of estimate.

confidence levels were not calculated, however, because of the satisfactorily high value already obtained by the more conservative analysis based on s_e .

While they were not used for confidence-limit calculations, standard errors of estimated y were calculated for the two sets of data referred to above, and the results of these calculations are shown in Figure E-2. These results reinforce the liklihood of the apparent discontinuity at $10^3/T_B \cong 1.36$ being real. The bands around the least-squares regression curves show the limits of the standard errors in estimated y. The results for $1.23 \leq 10^3/T_B \leq 1.36$ and those for the whole test range ($1.23 \leq 10^3/T_B \leq 1.48$) again do not fall within each others error-bands, especially so near $10^3/T_B = 1.36$ where the apparent discontinuity exists. It may, therefore, be inferred that the two sets of data do not come from the same statistical "population", i.e., that a discontinuity does exist which separates two different populations, these having been incorrectly combined in statistical treatment of the data set which covers the whole test range (both populations together).

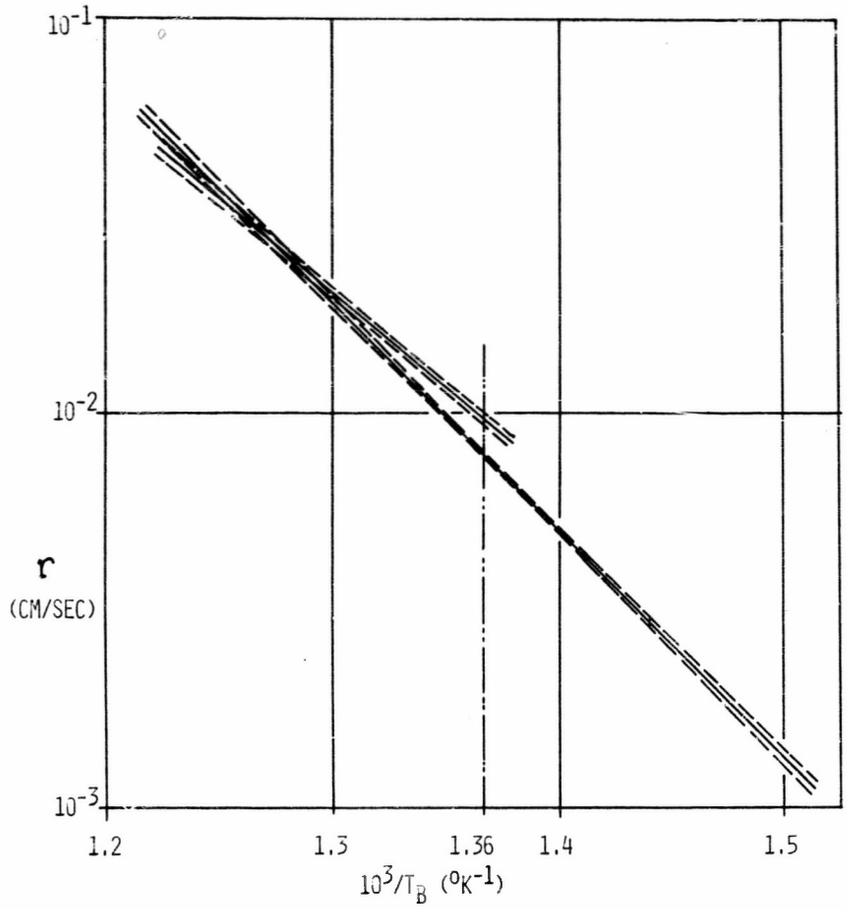

FIGURE E-2: LEAST-SQUARES FITS TO DIFFERENT SETS OF PYROLYSIS-RATE vs. SURFACE BRIGHTNESS TEMPERATURE DATA SHOWING ERROR BANDS FOR "STANDARD ERRORS OF ESTIMATED Y"

APPENDIX F - ESTIMATES OF CONVECTIVE HEAT FLUX DURING PYROLYSIS

F.1 ALTERNATIVE APPROACHES

Several different approaches might serve as a basis for estimating convective heat-flux from an impinging hot-gas jet to a pyrolyzing surface. First, the flux might be determined experimentally by impinging the jet on a calorimeter (see, e.g., Hansel (1964)). In the event that pyrolysis rates are high enough, the heat fluxes during pyrolysis must be deduced from such measured fluxes by accounting for the influences on heat transfer of surface transpiration or "blowing" (see, e.g., Anfimov (1966)). Second, analytical predictions might be made based on the various stagnation-point heating analyses available in the literature. While most of these analyses do allow for the effects of surface transpiration, many are specific to hypersonic flow fields. A few such analyses are, however, either general or have been developed specifically for subsonic flow situations such as that of present interest. Finally, existing empirical correlations for heat transfer from impinging jets (Walz (1964)) might be used for predicting heat fluxes.

A stagnation-point heating model was selected as the most suitable basis for estimating surface heat-fluxes in the present situation. It was felt that the other alternatives were less promising. Calorimetry was not as appealing because of the necessity of either calibration (which was impractical) or use of a "standard" design (which was un-

available). Impinging-jet correlations were judged as impractical owing to the sparse data available, particularly for the relatively small nozzle-distance/nozzle-diameter values used in this study. In this regard, it is noteworthy that impinging jet data have been, in a variety of cases, correlated well with stagnation-point heating analysis (Walz (1964)).

Use of a stagnation-point heating model was supported by experimental measurements of pressure distributions in the jet. Pressure distributions on a flat plate upon which the jet was impinged were of the same functional form as that predicted for semi-infinite stagnation-point flow fields (see Appendix B).

F.2 STAGNATION-POINT HEAT-FLUX ANALYSIS

Estimates of heat fluxes for the present case were based on the analysis and calculations of Reshotko and Cohen (1955), who obtained similarity solutions numerically for the boundary layer equations appropriate to homogeneous, compressible, laminar flow over the forward stagnation point of an axisymmetric blunt body.

Reshotko and Cohen's assumptions were considered critically before using their results. Provision for compressibility in the model was deemed imperative for the present case owing to the relatively large temperature range present in the flow field (T_E/T_S as large as about 2). The laminar flow assumption, which is explicit in the model, appeared justified on the basis of the impinging-jet literature. Studies of impinging jets indicate that boundary-layer transition to

turbulence may be expected to occur at diameters greater than the specimen diameter used in this study (for the Reynolds numbers of this study, Re = 7500 to 21,300); this is primarily a consequence of the strong favorable pressure gradients inherent in jet impingement normal to a flat plate. Further support of the laminar flow assumption is implicit in the apparent success of the model used in estimating heat-fluxes. The assumption of a homogeneous flow-field was judged reasonable in light of the fact that, evaluated in appropriate terms ("blowing parameter", f_w), transpiration rates were low enough ($f_w < 1$) that relatively modest mole fractions of transpired gas (e.g., < 0.1) would be expected within the flow field. The disparate molecular weights and transport properties of the transpired-gas components (NH_3 and $HClO_4$) and the external-flow gas (products of combustion of lean CH_4- 37% O_2/N_2 mixtures), therefore, might reasonably be neglected. To do otherwise would require massive numerical computation (see, e.g., Libby and Sepri (1968)). Such calculations would be of dubious value because of the inavailibility of appropriate basic data for gaseous $HClO_4$ (Pearson (1966), pp.191-199).

Using a well-known procedure, Reshotko and Cohen transformed the two-dimensional boundary-layer equations for compressible, laminar flow into equivalent equations for incompressible flow (Stewartson transformation). A Prandtl number of 0.7 was considered as was a Chapman-Rubesin viscosity law ($\rho\mu$ = constant). Euler number was included parametrically so that the resulting equations might be applied directly to either "wedge" flows or, by way of the Mangler transformation,

to axisymmetric flows. The resulting equations were solved numerically yielding plots of the heat-transfer parameter:

$$\frac{Nu}{\sqrt{Re}} = f\left(\frac{T_s}{T_E}, \frac{v_s}{\sqrt{v_s a}}\right)$$

Additional plots by Reshotko and Cohen show the results of earlier work by them and by others as regards Prandtl number influences (without transpiration). Reshotko and Cohen's earlier results have been verified as a limiting cases of other analyses (e.g., Fay and Riddell (1958)), and therefore, no detailed checks were made on the validity of Reshotko and Cohen's numerical results.

To adopt Reshotko and Cohen's results to the present case, the following values were used to determine values for $Nu/\sqrt{Re_S}$:

μ_s (air (Keenan and Kaye (1948)) at measured surface temperatures*)

ρ_s (air at measured stagnation-point pressures and surface temperatures*)

v_s (measured mass flux from surface + ρ_s)

a (measured, Appendix B)

From the heat-transfer parameter, heat-fluxes were calculated using, additionally:

T_E (measured, Appendix B)

k_S (air (Keenan and Kaye (1948)) at measured surface temperatures*).

*Surface temperatures based on measured brightness temperatures and $\epsilon = 0.72$.

The results of these calculations are shown in Fig. IV-5 of the text.*

In addition to results calculated both with and without transpiration, results are also indicated for the case of transpiration and radiative as well as convective heating of the pyrolysis specimen. Estimates of the surface heat-flux from radiation were based on conservative assumptions, i.e., that the pyrolyzing surface absorbed all radiation transferred to it from a radiator of unity emittance, of diameter equal to the exhaust duct outside diameter, and of a uniform temperature equal to the impinging-jet temperature:

$$q_R = F\epsilon\sigma\,(T_E^4 - T_S^4)$$

Values of q_R are apparent in Fig. IV-5 of the text as differences between the corresponding ordinate values of the lower two curves.

For the sake of comparison with the results described above, estimates were also made for the surface heat-fluxes required to sustain simple sublimation at the pyrolyzing surface:

$$q = r\rho\,[\,c_S(T_S - T_o) + \Delta h^\circ_{sub}]$$

At the various pyrolysis rates, surface temperature data based on $\epsilon = 0.72$ were used, along with appropriate values for ρ (1.95 gm/cm^3), c_S (0.3 cal/gm-$^\circ$K), and Δh°_{sub} (58.2 kcal/mole ÷ 117 gm/mole). The resulting relation between q and r is also shown in Fig. IV-5 of the text.

*Corresponding values based on surface brightness temperatures are approximately 15 to 30% higher at the highest and lowest temperatures, respectively. Trends of the results are essentially unaltered.

APPENDIX G - SURFACE PARTIAL-PRESSURE ESTIMATES FOR POROUS HOT-PLATE PYROLYSIS

Since the boundary conditions for heat and mass transport are dissimilar in the porous hot-plate apparatus, surface partial-pressures may not be deduced from mass and heat transport similarity (as is done in Appendix D for convective heating experiments); surface conditions must be determined by solution of appropriate mass-transport equations. Simplifying assumptions are, however, forced by the uncertainty in transport and other properties and by the lack of knowledge of the appropriate boundary conditions and details of the gas-phase near the pyrolyzing surface. Consequently, order-of-magnitude accuracy is the best that might be expected from attempting to estimate surface partial-pressures in the analytically cumbersome, porous-plate situation.

Defining m_i as the mass fraction of species "i" and considering a binary mixture of species "1" and "2", one-dimensional mass-transport without chemical reaction may be described by:

$$\rho v \frac{dm_i}{dy} = \frac{d}{dy}\left(\rho D_{ij} \frac{dm_i}{dy}\right) \quad (i = 1,2 \; ; \; j = 1,2 \neq i) \qquad (G\text{-}1)$$

Integrating once and applying the boundary conditions:

$$\dot{m}_{1,s} = \dot{m}_s \qquad (G\text{-}2)$$

$$\dot{m}_{2,s} = 0 \qquad (G\text{-}3)$$

(where subscript "1" denotes the vaporizing species and "2" denotes the inert ambient atmosphere), then, at the surface

$$\rho_s v_s m_{1,s} - \rho_s D_{12,s}\left(\frac{dm_1}{dy}\right)_s = \dot{m} \qquad \text{(G-4)}$$

$$\rho_s v_s m_{2,s} - \rho_s D_{12,s}\left(\frac{dm_2}{dy}\right)_s = 0 \qquad \text{(G-5)}$$

Rearranging Eq.(G-5) yields:

$$v_s = \frac{D_{12,s}}{m_{2,s}}\left(\frac{dm_2}{dy}\right)_s \qquad \text{(G-6)}$$

For overall mass conservation:

$$m_2 = 1 - m_1 \qquad \text{or:} \qquad \left(\frac{dm_2}{dy}\right) = -\left(\frac{dm_1}{dy}\right) \qquad \text{(G-7)}$$

Substituting Eq.(G-7) into Eq.(G-6):

$$v_s = -\frac{D_{21,s}}{1 - m_{1,s}}\left(\frac{dm_1}{dy}\right)_s \qquad \text{(G-8)}$$

Combining Eq's.(G-4) and (G-8), then yields:

$$\dot{m} = \rho_s\left[-\frac{D_{21,s}}{1-m_{1,s}}\left(\frac{dm_1}{dy}\right)_s\right]m_{1,s} - \rho_s D_{12,s}\left(\frac{dm_1}{dy}\right)_s \qquad \text{(G-9)}$$

However, for a binary mixture $D_{12,S} = D_{21,S} \equiv D_S$, and therefore, Eq.(G-9) yields:

$$\dot{m} = -\frac{\rho_s D_s}{1 - m_{1,s}}\left(\frac{dm_1}{dy}\right)_s \qquad \text{(G-10)}$$

Defining a characteristic length for diffusion, L, in terms of the derivative in Eq.(G-10):

$$L = \frac{m_{1,s}}{\left(\frac{dm_1}{dy}\right)_s} \qquad \text{(G-11)}$$

Then, from Eq.(G-10) and Eq.(G-11), with the assumption of perfect gases:

$$\dot{m} = \frac{\rho_s D_s}{L} \frac{m_{1,s}}{1 - m_{1,s}} = \rho_s D_s \frac{\frac{M_i}{\rho_s R T_s} P_{i,s}}{1 - \frac{M_i}{\rho_s R T_s} P_{1,s}} \qquad \text{(G-12)}$$

But, from Eq's.(I-5) and (G-12):

$$\frac{\dot{m}}{\dot{m}_{vac}} = 1 - \frac{P_{1,s}}{P_{1,eq}} = \frac{\rho_s D_s}{L \dot{m}_{vac}} \frac{\frac{M_1}{\rho_s R T_s} P_{1,s}}{1 - \frac{M_1}{\rho_s R T_s} P_{1,s}}$$

or:

$$1 - \frac{P_{1,s}}{P_{1,eq}} \quad \frac{\rho_s D_s}{L \dot{m}_{vac}} \frac{\frac{P_{1,s}}{P_{1,eq}}}{\frac{\rho_s R T_s}{M_1 P_{1,eq}} - \frac{P_{1,s}}{P_{1,eq}}} \qquad \text{(G-13)}$$

where $\dot{m}_{vac}$ is the vacuum mass-pyrolysis rate.

Equation (G-13) shows the partial pressure ratio, $P_{i,S}/P_{i,eq}$ ($= \hat{p}$) in terms of two non-dimensional parameters:

$$\frac{\rho_s D_s}{L \dot{m}_{vac}} \equiv \delta \quad ; \quad \frac{\rho_s R T_s}{M_1 P_{1,eq}} = \frac{\rho_s}{\rho_{eq}} \equiv \hat{\rho} \qquad \text{(G-14)}$$

In these terms, then:

$$1 - \hat{p} = \delta \frac{\hat{p}}{\hat{\rho} - \hat{p}}$$

Rearranging Eq.(G-14) then:

$$\hat{p} = \frac{1}{2}\left(1 + \hat{\rho} + \delta - \sqrt{(1 + \hat{\rho} + \delta)^2 - 4\hat{\rho}} \right) \quad \text{(G-15)}$$

which is the basis for determining $P_{i,S}$ from known values of $P_{i,eq}$, ρ_S, D_S, L, $\dot{m}_{vac}$, T_S, and M_1. Strictly speaking, both δ and $\hat{\rho}$ are functions of $P_{i,S}$ since ρ_S, the gas-mixture density at the surface, depends on $P_{i,S}$; rigorous solution of Eq.(G-15) for $P_{i,S}$ requires iteration, therefore. However, in limiting cases, i.e., $P_{i,S} \cong P$ or $P_{i,eq} \ll P$, ρ_S may be well-approximated by the density of either species "1" or "2" at the surface, respectively. For example, for Lieberherr's low-temperature porous hot-plate results, ρ_S was approximated by $\rho_{2,S}$ consistent with the ultimate finding that $P_{i,S} \ll P$.

APPENDIX H - AMBIENT PRESSURE EFFECTS ON SOLID-HOT-PLATE PYROLYSIS EXPERIMENTS

As an aid to interpreting hot-plate pyrolysis data for AP, it is useful to consider the results of the hot-plate pyrolysis experiments on ammonium chloride (NH_4Cl) reported by Chaiken et al. (1962). Unlike reported pyrolysis data for the hot-plate pyrolysis of AP, the data reported for NH_4Cl are for both low and high ambient pressures (surrounding the hot-plate and pyrolyzing specimen).

Figure H-1 shows, as a fitted line, vacuum hot-plate data for $10^3/T_S \leq 2.0$ (P = 1 to 2 mm Hg) and data from isothermal vacuum sublimation data for $10^3/T_S > 2.0$. In addition, data points are shown for tests at 1 atm ambient pressure; at temperatures approaching that for sublimative equilibrium at 1 atm ($10^3/T_S$), these data can be observed to drop to pyrolysis rates less than those in vacuo by an order of magnitude or more.

From Eq. (I-5):

$$r = r_{vac}(T_s)\left[1 - P_i / P_{i,eq}(T_s)\right] \qquad \text{(H-1)}$$

This relation is a consequence of recondensation which opposes sublimation and thereby decreases net pyrolysis rates, r , to below the rates observed in vacuo, r_{vac} , at the same surface temperature. Assuming that ambient pressure, P , equals the partial pressure of pyrolyzate at the surface, then:

$$P_i = P \qquad \text{(H-2)}$$

For the dissociative sublimation of NH_4Cl, the Clausius-Clapeyron relation

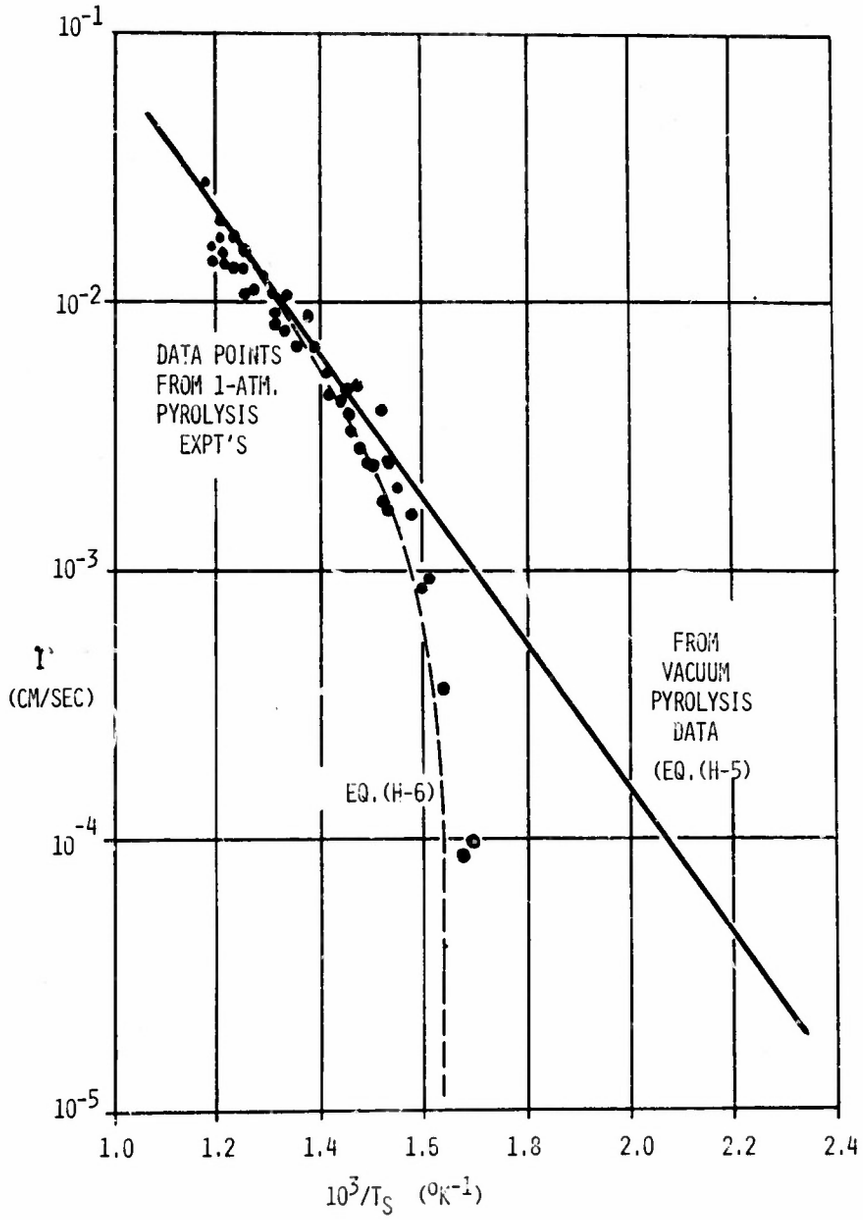

FIGURE H-1: COMPARISON OF MEASURED PYROLYSIS CHARACTERISTICS OF NH_4Cl WITH PREDICTION BASED ON VAPOR PRESSURE OF NH_4Cl

leads to (Eq. (I-2)):

$$P_{i,eq} \sim \exp(-\Delta H_{sub}/2RT_s) \qquad (H-3)$$

and:

$$P_i = P \sim \exp(-\Delta H_{sub}/2RT_{vp})$$

where T_{vp} is the temperature corresponding to an equilibrium vapor-pressure of P.

Therefore:

$$\frac{P_i}{P_{i,eq}} = \exp\left[(-\Delta H_{sub}/2R)\left(\frac{1}{T_s} - \frac{1}{T_{vp}}\right)\right] \qquad (H-4)$$

Assuming from the fitted line of Fig. H-1 that an Arrhenius expression describes $r_{vac}(T_S)$, then:

$$r_{vac} = A \exp(-E_s/RT_s) \qquad (H-5)$$

with $A = 37$ cm/sec and $E_S = 12.3$ kcal/mole*.

Then, for $\Delta H_{sub} = 42.3$ kcal/mole (Chaiken et al. (1962)), Eq's. (H-1), (H-4) and (H-5) yield:

$$r = (37\,\text{cm/sec})\exp(-12.3/RT_s)\left\{1 - \exp\left[(-\Delta H_{sub}/2R)\left(\frac{1}{T_s} - \frac{1}{T_{vp}}\right)\right]\right\} \qquad (H-6)$$

Equation (H-6) was solved for r at various T_S throughout the test range shown in Figure H-1, and the results are shown as the dashed line of Fig. H-1. The fit to the experimental data for 1 atm is seen to be good.

It may be concluded from these data and calculations that, at least for NH_4Cl pyrolysis, Eq.(H-1) is a useful basis for correcting values of r_{vac} to account for recondensation. While such recondensation

---

* The values cited by Chaiken et al. (1962) for these parameters do not appear to fit the data well; the values cited here were fitted anew to the data.

sation effects were proposed qualitatively by Chaiken et al., they apparently have not been checked quantitatively before. Incidently, it is seen (as expected; Williams (1965)) that E_s need not equal ΔH_{sub} since E_s presumably represents the activation energy of some rate-controlling step of the sublimation.

It is useful to note that the success of the above model of recondensation effects depends on the assumption of Eq. (H-2), i.e., that, despite the large loading pressures (ca. 5 atm) pushing the specimen against the hot-plate, sublimation at the specimen surface may be considered as occurring at very nearly the ambient pressure. This observation lends credence to the suggestion that similar tests on AP (with ambient pressures of 1 to 2 mm Hg) represent essentially unopposed sublimation with very little influence by recondensation. Unfortunately, however, the indication that pressure at the surface is near ambient also suggests that various analyses of the effects of a gas film between plate and specimen (e.g., Chaiken et al. (1962)) may be poorly grounded in fact; near-ambient surface pressures would appear most likely to result from "channeling" i.e., irregular erosive effects of the gas film, whereas models of the process typically presume uniform-thickness gas films (Nachbar and Williams (1963)).

APPENDIX J - LINEAR-PYROLYSIS DATA

r (cm/sec)	$10^3/T_S$ ($^oK^{-1} \times 10^3$)	r (cm/sec)	$10^3/T_S$ ($^oK^{-1} \times 10^3$)
LIEBERHERR (1967)		ANDERSEN, ET AL. (1962)	
0.00016	1.520	0.0039	1.332
0.00040	1.495	0.028	1.206
0.00048	1.495	0.029	1.292
0.00060	1.495	0.050	1.161
0.00019	1.485	0.050	1.139
0.00033	1.485	0.057	1.169
0.00033	1.460	0.069	1.195
0.00048	1.442	0.087	1.115'
0.00063	1.400	0.099	1.113
0.0010	1.400	0.133	1.096
0.0020	1.400		
0.0012	1.380	COATES (1965)	
0.0012	1.345		
----- *	-------	0.0019	1.550
0.012	1.355	0.0040	1.325
0.011	1.325	0.0072	1.310
0.015	1.300	0.013	1.296
0.018	1.300	0.015	1.280
0.030	1.225	0.017	1.221
0.030	1.175	0.019	1.210
0.045	1.175	0.021	1.190
0.044	1.120	0.034	1.175
0.040	1.105	0.023	1.170
0.057	1.105	0.026	1.160
0.040	1.040	0.035	1.130
0.031	1.015	0.050	1.115
0.027	1.000		
		* Location of discontinuity in r vs. T_S	

TABLE J-1 - SUMMARY OF PRIOR AP LINEAR-PYROLYSIS DATA

r (cm/sec)	$10^3/T_s$ ($^oK^{-1} \times 10^3$)	r (cm/sec)	$10^3/T_s$ ($^oK^{-1} \times 10^3$)
30-35mm Hg; H_2-N_2 fuel		1 atm.; H_2-N_2 fuel	
0.0026(5)	1.426	0.0065	1.318
0.0028(5)	1.463	0.0066	1.250
0.0030	1.444	0.0068	1.283
0.0031(5)	1.440	0.0089	1.249
0.0032	1.450	0.0091	1.269
0.0034	1.449	0.0095	1.265
0.0035(5)	1.447	0.0095	1.280
0.0038	1.445	0.0095	1.271
0.0047	1.393	0.010	1.305
		0.010	1.260
100-200mm Hg; CH_4-N_2 fuel		0.010	1.277
		0.010	1.273
		0.010	1.270
0.0026(5)	1.410	0.012	1.250
0.0032	1.410	0.012	1.242
0.0038	1.400	0.0132	1.253
0.0040	1.449	0.0139	1.244
0.0040	1.440	0.015	1.244
0.0042	1.439		
0.0042	1.433		
0.0071	1.388		
0.0070	1.359		

TABLE J-2 - SUMMARY OF PRIOR AP PYROLYSIS DATA (POWLING (1967))

Series & Run No's.	$10^3 xT_B^*$ ($^oK^{-1}$)	r (cm/sec)	Series & Run No's.	$10^3 xT_B^*$ ($^oK^{-1}$)	r (cm/sec)
20-2	1.487	0.0021	2-3[a,b]	1.364	0.0099
17-3	1.474	0.0018	2-4[a,b]	1.362	0.010
18-1A	1.468	0.0018	9-1[b]	1.362	0.010
19-5	1.458	0.0024	14-1	1.356	0.010
17-4	1.456	0.0022	18-6	1.336	0.012
19-4	1.455	0.0022	19-13[c]	1.334	0.012
19-6	1.452	0.0028	18-7	1.317	0.019
18-2	1.449	0.0022	2-5[a,b]	1.296	0.021
19-1	1.446	0.0028	2-6[a,b]	1.296	0.022
20-1	1.440	0.0032	9-2[b]	1.260	0.031
19-7[c]	1.438	0.0032	21-4A	1.256	0.027
19-5	1.438	0.0036	21-2	1.256	0.039
19-8A	1.432	0.0030	9-3[b]	1.250	0.032
18-3	1.409	0.0040	12-2	1.248	0.034
19-8B[c]	1.432	0.0040	21-7A	1.236	0.040
17-5	1.427	0.0027	21-8A	1.235	0.056
19-9[c]	1.412	0.0036	21-8B	1.222	0.061
19-12	1.391	0.0052	21-4B	1.241	0.064
13-2	1.391	0.0054	21-7B	1.236	0.080
18-4	1.388	0.0063	21-5	1.251	0.083
19-11[c]	1.386	0.0051	21-6	1.255	0.087
13-3	1.382	0.0058			
18-5	1.368	0.0068			

Notes: *Average of brightness temperature extremes during each run

[a]Specimen from O.N.E.R.A

[b]Radiometric wavelength: 3.14μm

[c]Oxidizer-gas supply pressure: 60 psig

TABLE J-3: SUMMARY OF PRESENT AP LINEAR-PYROLYSIS DATA